FINAL REPORT ~ FHWA-OK-18-05

DEVELOPMENT OF AGGREGATE CHARACTERISTICS-BASED PREVENTIVE MAINTENANCE TREATMENTS USING 3D LASER IMAGING AND AGGREGATE IMAGING TECHNOLOGY FOR OPTIMIZED SKID RESISTANCE OF PAVEMENTS

Joshua Q. Li, Ph.D. P.E.[1]
Dominique Pittenger, Ph.D.[2]
Kelvin Wang, Ph.D., P.E.[1]
Musharraf Zaman, Ph.D., P.E.[2]

[1]School of Civil and Environmental Engineering
College of Engineering, Architecture and Technology
Oklahoma State University
Stillwater, Oklahoma

[2]School of Civil Engineering and Environmental Science
Gallogly College of Engineering
The University of Oklahoma
Norman, Oklahoma

June 2019

Oklahoma Department of Transportation

The Oklahoma Department of Transportation (ODOT) ensures that no person or groups of persons shall, on the grounds of race, color, sex, religion, national origin, age, disability, retaliation or genetic information, be excluded from participation in, be denied the benefits of, or be otherwise subjected to discrimination under any and all programs, services, or activities administered by ODOT, its recipients, sub-recipients, and contractors. To request an accommodation please contact the ADA Coordinator at 405-521-4140 or the Oklahoma Relay Service at 1-800-722-0353. If you have any ADA or Title VI questions email ODOT-ada-titlevi@odot.org.

DEVELOPMENT OF AGGREGATE CHARACTERISTICS-BASED PREVENTIVE MAINTENANCE TREATMENTS USING 3D LASER IMAGING AND AGGREGATE IMAGING TECHNOLOGY FOR OPTIMIZED SKID RESISTANCE OF PAVEMENTS

FINAL REPORT ~ FHWA-OK-18-05

ODOT SP&R ITEM NUMBER 2275

Submitted to:

Dawn R. Sullivan, P.E.
Director of Capital Programs
Oklahoma Department of Transportation

Submitted by:

Joshua Q. Li, Ph.D. P.E.
Dominique Pittenger, Ph.D.
Kelvin Wang, Ph.D., P.E
Musharraf Zaman, Ph.D., P.E

Oklahoma State University
and
The University of Oklahoma

June 2019

TECHNICAL REPORT DOCUMENTATION PAGE

<table>
<tr><td>1. REPORT NO.
FHWA-OK-18-05</td><td>2. GOVERNMENT ACCESSION NO.</td><td>3. RECIPIENT'S CATALOG NO.</td></tr>
<tr><td colspan="2" rowspan="2">4. TITLE AND SUBTITLE
Development of Aggregate Characteristics-Based Preventive Maintenance Treatments Using 3D Laser Imaging and Aggregate Imaging Technology for Optimized Skid Resistance of Pavements</td><td>5. REPORT DATE
Jun 2019</td></tr>
<tr><td>6. PERFORMING ORGANIZATION CODE</td></tr>
<tr><td colspan="2">7. AUTHOR(S)
Joshua Q. Li, Ph.D., P.E.[1]; Dominique Pittenger, Ph.D.[2]; Kelvin Wang, Ph.D., P.E.[1]; Musharraf Zaman, Ph.D., P.E.[2]</td><td>8. PERFORMING ORGANIZATION REPORT</td></tr>
<tr><td colspan="2" rowspan="2">9. PERFORMING ORGANIZATION NAME AND ADDRESS
[1] Oklahoma State University, Stillwater Oklahoma 74078,
[2] The University of Oklahoma, Norman OK 73019</td><td>10. WORK UNIT NO.</td></tr>
<tr><td>11. CONTRACT OR GRANT NO.
ODOT SPR Item Number 2275</td></tr>
<tr><td colspan="2" rowspan="2">12. SPONSORING AGENCY NAME AND ADDRESS

Oklahoma Department of Transportation
Office of Research and Implementation
200 N.E. 21st Street, Room G18
Oklahoma City, OK 73105</td><td>13. TYPE OF REPORT AND PERIOD COVERED
Final Report
Oct 2015 - Sep 2018</td></tr>
<tr><td>14. SPONSORING AGENCY CODE</td></tr>
<tr><td colspan="3">15. SUPPLEMENTARY NOTES
N/A</td></tr>
<tr><td colspan="3">16. ABSTRACT
The objective of this study was to assess the skid resistance performance of pavements in Oklahoma following preventive maintenance treatments. The assessment method employed herein was based on physical aggregate properties and economics in an optimal manner. Several state-of-the-art laboratory and field instruments were used to collect data on aggregate morphology, and 3D surface texture and skid resistance of pavements. The impacts of aggregate characteristics on the skid resistance of pavements were also investigated and used in developing deterioration models and life cycle cost analysis.</td></tr>
<tr><td>17. KEY WORDS
Aggregate Characteristics, Preventive Maintenance, 3D Imaging, Skid Resistance</td><td colspan="2">18. DISTRIBUTION STATEMENT
No restrictions. This publication is available from the Office of Research and Implementation, Oklahoma DOT.</td></tr>
<tr><td>19. SECURITY CLASSIF. (OF THIS REPORT)
Unclassified</td><td>20. SECURITY CLASSIF. (OF THIS PAGE)
Unclassified</td><td>21. NO. OF PAGES
238</td><td>22. PRICE
N/A</td></tr>
</table>

Form DOT F 1700.7 (08/72)

SI* (MODERN METRIC) CONVERSION FACTORS

APPROXIMATE CONVERSIONS TO SI UNITS

SYMBOL	WHEN YOU KNOW	MULTIPLY BY	TO FIND	SYMBOL
		LENGTH		
in	inches	25.4	millimeters	mm
ft	feet	0.305	meters	m
yd	yards	0.914	meters	m
mi	miles	1.61	kilometers	km
		AREA		
in^2	square inches	645.2	square millimeters	mm^2
ft^2	square feet	0.093	square meters	m^2
yd^2	square yard	0.836	square meters	m^2
ac	acres	0.405	hectares	ha
mi^2	square miles	2.59	square kilometers	km^2
		VOLUME		
fl oz	fluid ounces	29.57	milliliters	mL
gal	gallons	3.785	liters	L
ft^3	cubic feet	0.028	cubic meters	m^3
yd^3	cubic yards	0.765	cubic meters	m^3
		NOTE: volumes greater than 1000 L shall be shown in m^3		
		MASS		
oz	ounces	28.35	grams	g
lb	pounds	0.454	kilograms	kg
T	short tons (2000 lb)	0.907	megagrams (or "metric ton")	Mg (or "t")
		TEMPERATURE (exact degrees)		
^oF	Fahrenheit	5 (F-32)/9 or (F-32)/1.8	Celsius	^oC
		ILLUMINATION		
fc	foot-candles	10.76	lux	lx
fl	foot-Lamberts	3.426	candela/m^2	cd/m^2
		FORCE and PRESSURE or STRESS		
lbf	poundforce	4.45	newtons	N
lbf/in^2	poundforce per square inch	6.89	kilopascals	kPa

APPROXIMATE CONVERSIONS FROM SI UNITS

SYMBOL	WHEN YOU KNOW	MULTIPLY BY	TO FIND	SYMBOL
		LENGTH		
mm	millimeters	0.039	inches	in
m	meters	3.28	feet	ft
m	meters	1.09	yards	yd
km	kilometers	0.621	miles	mi
		AREA		
mm^2	square millimeters	0.0016	square inches	in^2
m^2	square meters	10.764	square feet	ft^2
m^2	square meters	1.195	square yards	yd^2
ha	hectares	2.47	acres	ac
km^2	square kilometers	0.386	square miles	mi^2
		VOLUME		
mL	milliliters	0.034	fluid ounces	fl oz
L	liters	0.264	gallons	gal
m^3	cubic meters	35.314	cubic feet	ft^3
m^3	cubic meters	1.307	cubic yards	yd^3
		MASS		
g	grams	0.035	ounces	oz
kg	kilograms	2.202	pounds	lb
Mg (or "t")	megagrams (or "metric ton")	1.103	short tons (2000 lb)	T
		TEMPERATURE (exact degrees)		
^oC	Celsius	1.8C+32	Fahrenheit	^oF
		ILLUMINATION		
lx	lux	0.0929	foot-candles	fc
cd/m^2	candela/m^2	0.2919	foot-Lamberts	fl
		FORCE and PRESSURE or STRESS		
N	newtons	0.225	poundforce	lbf
kPa	kilopascals	0.145	poundforce per square inch	lbf/in^2

*SI is the symbol for the International System of Units. Appropriate rounding should be made to comply with Section 4 of ASTM E380. (Revised March 2003)

Table of Contents

List of Figures

List of Tables

CHAPTER 1 INTRODUCTION

1.1 Background

Skid resistance of pavements plays a significant role in road safety as the friction between tire and pavement surface is a critical contributing factor in reducing potential crashes. Pavement skid resistance has been related to two main surface properties: microtexture and macrotexture (Hall et al., 2009). Microtexture is primarily dependent on aggregate shape, angularity and texture, while macrotexture is a function of asphalt mix properties, compaction method, and aggregate gradation. Several studies in recent years, such as NCHRP 4-30A (Al-Rousan et al., 2007) and NCHRP 4-34 (Wang et al., 2011) projects, have focused on evaluating and developing comprehensive test methods to measure aggregate shape, texture and angularity. However, robust relationships between aggregate properties and the ultimate pavement performance have not been clearly established yet.

Various preventive maintenance treatments are employed by transportation agencies including Oklahoma Department of Transportation (ODOT) to restore pavement condition (skid resistance, in particular, for this project) and retard future deterioration. When using preventive maintenance treatments on pavements in good condition, it is expected that the treatment be cost effective and result in a given extension of life. Aggregate is the main component of many treatments (> 90%). However, aggregate properties in terms of shape, texture, angularity and abrasion resistance have not been integrated into the aggregate selection process for optimal

skid resistance. One of the main causes is the lack of accurate data collection technologies for measurements of both aggregate characteristics and pavement surfaces at highway speed. The most recent developments in optics, 3D laser imaging technology, and computing power have allowed the development of equipment to collect high resolution 3D image data for pavement surfaces. The technological innovations have also made it possible to automatically measure the properties of aggregate shape, texture and angularity with a much higher precision than conventional methods. Recent technological developments have also made it possible to collect pavement performance condition data, including cracking, profiling, and surface texture at highway speed with a much higher resolution. As a result, investigation and quantification of influence of aggregate characteristics on skid resistance of pavements is now possible. Such investigations can adequately account for pertinent properties in the selection of aggregates and pavement maintenance measures.

The objective of this project was to develop an informed aggregate selection process for preventive maintenance treatments of pavements in Oklahoma based on physical aggregate properties such that the skid resistance of pavements is maintained or improved while the economic benefits are optimized. The most recent developments in 3D laser imaging technology is used to collect 3D pavement surface texture data at highway speed at 1 mm accuracy without interfering with the traveling public. This project also used several state-of-the-art laboratory and field data collection instruments to collect ultra-high resolution morphological data for commonly used aggregates in Oklahoma, including index properties pertaining to

shape, angularity, and surface texture. Time series pavement skid resistance data were collected at highway speed using a Grip Tester at selected field sites after various preventive treatments, during the two-year duration of this project. Subsequently the impacts of aggregate characteristics on pavement surface skid resistance properties were investigated and quantified. Also, life cycle cost analysis (LCCA) was conducted to determine an evaluation protocol for pavement preservation treatments. The LCCA results are expected to assist in the selection of aggregate for preventive maintenance treatment purposes. The goal of selecting a treatment method is to maintain or improve pavement performance while minimizing cost.

1.2 Project Tasks

This study includes the following tasks:

- **Task 1 Literature Review**: In this task, a comprehensive review of literature was conducted on the current practices. The literature review was focused on testing of aggregate properties, skid resistance of pavement (pertaining to performance and measurement), and existing relationships between aggregate morphological characteristics and skid resistance.
- **Task 2 Experimental Design**: Working closely with ODOT, the most commonly used aggregate sources and preventive maintenance treatments were identified. A systematic laboratory and field experimental design was developed, which not only considered the influencing factors

pertaining to skid resistance but also leveraged field test sections from existing and previous research projects supported by ODOT.

- **Task 3 Laboratory Testing**: A wide range of physical characteristics of aggregates, such as gradation (size), shape, texture, angularity, durability, and resistance to polishing (under dry and wet conditions), were tested in the laboratory. Both conventional methods and advanced tool, namely, aggregate imaging system (AIMS), were used for this purpose.
- **Task 4 Field Data Collection**: Several state-of-the-art instruments were used to collect 3D surface texture data at 1mm resolution and highway speed, for the entire lane. Skid resistance of the pavement surface was also measured.
- **Task 5 Data Analysis**: The 1mm 3D surface texture data and skid resistance data collected from the selected test sites were acquired and analyzed for cracking, rutting, faulting, texture, and friction. Also, statistical analyses were performed to evaluate the effect of aggregate properties on the skid resistance of pavements.
- **Task 6 Life Cycle Cost Analysis**: This task involved a comprehensive review of literature and implementation of appropriate life cycle cost analysis (LCCA) procedures for pavement preservation. The results were used to develop an evaluation protocol. The LCCA-based protocol can assist in the selection of aggregate for preventive maintenance treatments and for the evaluation of different treatment methods such that pavement performance is maintained or improved at the lowest cost.

- **Task 7 Final Report and Training**: As part of this task, training sessions were organized for ODOT engineers. Also, this task involved submission of a final report documenting outcome of each task conducted in this study and the lessons learned.

1.3 Report Outline

This report consists of seven chapters. An overview of each chapter is given below:

- Chapter 1 provides the overall background and objectives of the project.
- Chapter 2 includes a summary of pertinent literature.
- Chapter 3 presents an overview of the experimental design, focused on the selection of field test sites. The site selection considers the most commonly used aggregates and preventive maintenance treatments in Oklahoma.
- Chapter 4 presents an overview of the comprehensive laboratory test results using traditional instruments and aggregate imaging system (AIMS) to measure morphological characteristics of aggregates used in the test sites.
- Chapter 5 introduces the field data collection instruments, describes the data collection events, and presents the data processing procedures and analysis of results. Statistical models are then developed to evaluate the effects of aggregate properties on skid resistance of pavements.

- Chapter 6 demonstrates the use of life cycle cost analysis procedure and its application to the selection of pavement treatment methods. A performance-based cost sensitivity analysis is performed to analyze the relative differences among annualized cost outputs for different pavement treatments based upon friction performance models developed in Chapter 5.
- Chapter 7 summarizes the conclusions of this study.

CHAPTER 2 LITERATURE REVIEW

Skid resistance of pavement plays a significant role in road safety and has been studied extensively in the last decade. The existing literature on the following five relevant research areas is summarized in this section: (1) aggregate properties and testing; (2) pavement texture and measurement; (3) measurement of skid resistance of pavements; (4) preventive maintenance treatments for restoring skid resistance; and (5) relationships between aggregate characteristics and skid resistance.

2.1 Aggregate Properties and Testing

2.1.1 Aggregate Properties

Mineral aggregates make up 80% to 90% of the total volume and 94% to 95% of the mass of hot mix asphalt (HMA). For this reason, it is important to maximize the quality of the mineral aggregates to ensure proper performance, such as skid resistance of pavement. The quality of mineral aggregates as road paving materials has generally been specified by the toughness, soundness (durability), cleanliness, particle shape, angularity, surface texture, and absorption. Aggregate properties in the Superpave method are grouped into consensus properties, source properties, and gradation limits. Coarse aggregate angularity, flat and elongated particles, fine aggregate angularity, and sand equivalent are consensus properties to ensure

aggregate quality to provide satisfactory performance of HMA for the design life of a pavement at the desired traffic level. Los Angeles (LA) abrasion, sulfate soundness, and deleterious materials are source properties to allow for variances in locally available materials. The gradation limits include nominal maximum aggregate size and control points for various nominal maximum aggregate sizes (Prowell et al., 2005).

Masad (2007) grouped aggregate characteristics based on the following parameters: shape, angularity, and texture. Shape is the first order property reflecting variations in the proportions of a particle, while angularity reflects variations at the corners of a particle. Surface texture is used to describe the surface irregularity at a scale that is too small to affect the overall shape or angularity.

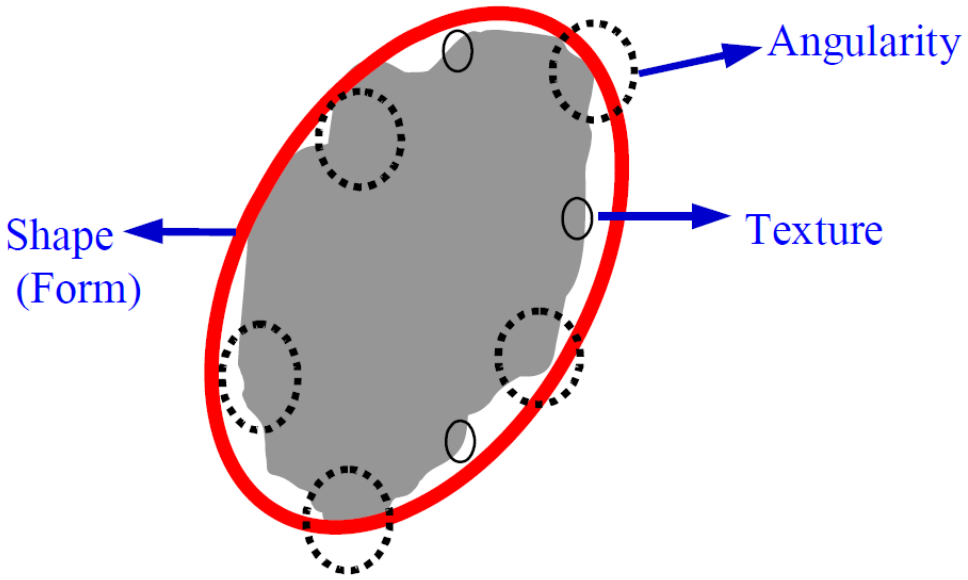

Figure 2.1 Aggregate Shape Properties: Shape, Angularity, and Texture (Masad, 2007)

Based on the study by Hall et al. (2009), the important aggregate properties that influence short- and long-term texture performance are mineralogical and petrographic properties (aggregate composition/structure and mineral hardness), physical and geometrical properties (angularity, shape, and texture), mechanical properties (abrasion/wear resistance and polish characteristics), and durability properties (soundness). The factors that affect pavement surface texture include the following:

- Maximum Aggregate Dimensions - The size of the largest aggregate in an asphalt concrete (AC) pavement or exposed aggregate in Portland cement concrete (PCC) pavement provides the dominant macrotexture wavelength, if closely and evenly spaced.
- Coarse Aggregate Type - The selection of coarse aggregate type should control its angularity, shape factor, and durability, which is particularly critical for AC pavements and PCC pavements with exposed aggregates.
- Fine Aggregate Type - The angularity and durability of fine aggregate is controlled by the material selected and whether it is crushed or not.
- Mix Gradation - Gradation of the mix, particularly for porous pavements, can affect the stability and air voids of pavements.
- Mix Air Voids - Increased air voids provide increased water drainage, which improve friction. Also, increased air voids reduce noise.

2.1.2 Aggregate Properties Testing

ASTM D5821-13 is used to determine the percentage of fractured particles for coarse aggregates. One purpose of such requirements is to maximize shear

strength by increasing inter-particle friction in either bound or unbound aggregate mixtures. Another purpose is to provide stability of aggregates used in surface treatment and to provide increased friction and texture for aggregates used in pavement surface courses. ASTM D5821, or a similar procedure, has been used by 83% of the responding agencies in a survey conducted by Prowell et al. (2005). Table 2.1 lists the ODOT's requirements for crushed faces of aggregates. The Strategic Highway Research Program (SHRP) uses similar requirements.

Table 2.1 Requirements for Crushed Faces of Aggregates

Million ESALs	≤4'' from Surface (ODOT)	>4'' from Surface (ODOT)	≤4'' from Surface (SHRP)	>4'' from Surface (SHRP)
<3	75/75	65/65	75/-	50/-
3 - 10	85/80	75/75	85/80	60/-
10 - 30	95/90	80/75	95/90	80/75
30 -100	100	95/90	100	95/90
>100	100	100	100	100

The Superpave method to measure the angularity of fine aggregates is specified in AASHTO T304, "Uncompacted Void Content in Fine Aggregate, Method A." This method describes the determination of the loose uncompacted void content of a sample of fine aggregate. When measuring any aggregate of known grading, void content provides an indication of the aggregate's angularity, sphericity, and surface texture. This test is performed to ensure that sufficient internal friction resulting from particle shape, angularity, and texture is achieved. Aggregate internal friction is an important component of rut-resistance of asphalt pavements. Most manufactured sands have an uncompacted void content greater than 45%, while most rounded natural sands have an uncompacted void content of 36-40%. Fine

aggregates with an uncompacted void contents in the range of 40-44% are classified as intermediate materials. Such materials typically consist of soft crushed fine aggregates or angular natural sands. Table 2.2 provides ODOT's requirements for fine aggregate angularity.

Table 2.2 Requirements of Fine Aggregate Angularity

Million ESALs	≤4'' from Surface (ODOT)	>4'' from Surface (ODOT)	≤4'' from Surface (SHRP)	>4'' from Surface (SHRP)
<0.3	-	-	-	-
0.3 - 3	40	40	40	40
3 - 30	45	40	45	40
>30	45	45	45	45

Toughness is the percent loss of a material from an aggregate blending during LA Abrasion testing. To evaluate the toughness and soundness of coarse aggregates, ODOT uses the Micro-Deval test. ASTM D6928 and D7428 describe the testing methods for abrasion resistance of coarse and fine aggregates in the Micro-Deval apparatus. The Micro-Deval test measures abrasion resistance and durability of mineral aggregates resulting from grinding with steel balls in the presence of water. For soundness testing, aggregates are subjected to weathering action in ASTM C88-13. ASTM D3744 specifies the test method for determining aggregate durability index, a parameter indicating the relative resistance of aggregate to the production of clay-like fines, when subjected to the prescribed mechanical methods of degradation. To prevent low skid resistance in surface mixes, ODOT requires that the combined coarse aggregates have a minimum percentage of insoluble coarse materials in acid.

Figure 2.2 Micro-Deval Apparatus (Pavement Interactive, 2011)

ASTM D3319 along with ASTM E303 define the laboratory procedure for estimating aggregate polishing in terms of polished stone value (PSV) under vehicular traffic loading, in which the British wheel and pendulum tester is used to determine PSV of selected aggregates. GAPA (2011) concluded that the PSV value should be higher than 43 for roads under normal traffic and 50 for roads with heavy traffic. However, Roe and Hartshorne (1998) reported that aggregates with the same PSV could provide a wide range of skid resistance even at the same traffic level.

Figure 2.3 Accelerated Polishing Machine (Pavement Interactive, 2011)

With the development of laser and computer technology, image analysis has been widely applied to determine aggregate indicators related to pavement performance. For example, Al-Rousan (2004) introduced an improved version of the Aggregate Imaging System (AIMS) to measure the shape characteristics of both fine and coarse aggregates. AIMS' results were compared with those obtained from other test methods in terms of accuracy, repeatability, reproducibility, cost, and operational characteristics (e.g. ease of use and interpretation of results) (Masad et al., 2005; Al-Rousan et al., 2007). These comparisons demonstrated the advantages of AIMS in measuring the shape characteristics of both fine and coarse aggregates.

Masad (2007) concluded that AIMS was capable of distinguishing changes in aggregate shape characteristics before and after Micro-Deval polishing, with repeatable and reproducible results. Mahmoud and Masad (2007) used AIMS to measure aggregate resistance to polishing and degradation. Aggregates from different sources were tested with a wide range of properties. Gransberg et al. (2010) showed that a potential correlation existed between the gradient angularity measured by AIMS and the skid numbers of pavements.

The Laser-based Aggregate Scanning System (LASS) has been applied for the characterization of shape and size parameters of aggregates (Kim et al., 2009). The resulting elongation and flatness ratios, gradation analysis, volume, and particle size distributions exhibited strong correlations with the manual measurements. Maerz and Lusher (2001) developed a new measuring system, called WipShape, that could automatically measure flat and elongated aggregates at ratios of 5:1, 4:1, 3:1, and 2:1. The results were reported in terms of various shape factors including principal axis ratios, roundness, sphericity and angularity. Rao et al. (2002) utilized the University of Illinois Aggregate Image Analyzer (UIAIA) to measure aggregate shape properties. The Multiple Ratio Shape Analysis method (MRA) (Jahn, 2000) was used to measure the shape of coarse aggregates. In addition, many other researchers have applied image analysis to evaluate aggregate characteristics (Fernlund, 1998; Kwan et al., 1999; Mora and Kwan, 2000; Garboczi, 2002; Erdogan et al., 2006; Fernlund, 2005; and Lee et al., 2007).

Lastly, laser detection and ranging (LADAR) systems have also been used to measure aggregate characteristics. Garboczi (2006) applied LADAR along with X-

ray CT to produce raw surfaces of aggregates. When using this method, only one aggregate could be characterized at a time. Wang et al. (2012) developed a prototype Fourier transform interferometry (FTI) system and used this system to characterize aggregate shape, angularity, texture, surface area, and volume of a wide range of aggregate sizes with satisfactory accuracy.

2.2 Pavement Texture and Measurement

2.2.1 Pavement Texture

Two types of surface texture affect wet pavement friction. These are: microtexture (wavelengths of 1μm to 0.5mm) and macrotexture (wavelengths of 0.5mm to 50mm). Microtexture is generally provided in asphalt pavements by the relative roughness of the aggregate particles, while in concrete surfaces microtexture is provided by fine aggregates. Macrotexture is generally provided in asphalt pavement by desired aggregate gradation, and in concrete surfaces by supplemental treatments such as tinning, brooming, diamond grinding or grooving. Currently there is no nation-wide specification on pavement texture in the U.S., while several other countries impose texture requirements for maintaining desired pavement performance. For example, a mean texture depth (MTD) of 1.5 mm (0.06 in.) is required for new AC pavements in U.K. Minnesota requires an MTD greater than 0.8 mm (0.03 in.) on new PCC surfaces (Henry, 2000). The current British specification also requires a minimum sand patch MTD of 0.65mm for new transversely textured PCC surfaces, while 1.0 mm MTD (laser-based) is used to meet the skid resistance requirement (Ahammed and Tighe, 2010). In France, the

specified MTD is from ≥ 0.40 to ≥ 0.70 mm on urban and suburban roads depending on speed level (from < 50 to > 90 km/h), longitudinal slope (≤ 5%), and number of lanes per direction. Special consideration is given for slope greater than 5%. For rural (interurban) roads, the desired MTD is from ≥ 0.60 to ≥ 0.80 mm, depending on speed (from 90 to 130 km/h), longitudinal slope (≤ 5% or > 5%), curve radius (≥ 1000 or ≥ 600 m), and number of lanes per direction (Dupont and Bauduin, 2005). The Chinese specification recommends texture depth (TD) greater than 0.55 mm for AC interstate pavements, but TD varies from 0.77 mm to 1.1 mm on interstate PCC pavements. Larson et al. (2008) recommends a minimum macrotexture for Ohio according to the French specification for intervention at network level, and 1.0 mm as the investigatory (desirable) threshold for network as well as project levels.

Relating pavement texture to crash ratio, pavement texture variation, and texture maintenance level has been studied previously. For example, Roe et al. (1991) used a high-speed texture meter to assess texture depth, and found that surfaces with coarse macrotexture led to less accidents than those with fine texture. In addition, accident risk started to increase when texture depth was less than 0.7 mm. The 0.7 mm texture depth was also identified as the critical factor relative to the loss of friction (Roe et al., 1998). Thresholds of texture depths have been used to maintain good skid resistance. The following classifications have been suggested: > 1.1 mm as ‘Sound’; 0.8 – 1.1 mm as ‘Some Deterioration’; 0.4 – 0.8 mm as ‘Warning Level of Concern’; and < 0.4 mm as ‘Severe Deterioration Requiring Urgent Investigation and Possible Remedial Action’ (Viner et al., 2006). Kanafi et al. (2015) monitored variations of pavement texture and observed that macrotexture decreased

and microtexture increased during the summer time. Early rapid reduction followed by an initial increase, and subsequently gradual decline of macrotexture in laboratory asphalt concrete samples were observed using close range photogrammetry with proprietary photogrammetric software (Millar et al., 2009). Wavelet analysis was applied to interpret macrotexture data collected from a CT meter to determine the wavelength ranges and energy contents that affect the macrotexture properties of pavements (Zelelew et al., 2013; 2014).

2.2.2 Texture Measurement

ASTM has published two standards for pavement macrotexture measurements: E965 “Standard Test Method for Measuring Pavement Macrotexture Depth Using a Volumetric Technique” and E2380/E2380M “Standard Test Method for Measuring Pavement Texture Drainage Using an Outflow Meter.” In E965-15, MTD is calculated by dividing the sample volume by the area covered using the sand patch method. In E2380-15, the outflow meter time is used as an indicator of pavement drainage speed and MTD is used as an indicator of texture. The outflow meter test could relate texture to drainage capacity and serve as an indicator of hydroplaning potential of pavements. The Grease Smear Method is used to evaluate microstructure of airport pavements. Texture depth requirements for runway are documented in the Advisory Circular (AC) 150/5320-12C (FAA, 1997). Doty (1974) compared sand patch and outflow meter methods and found poor to fair repeatability. Pidwerbesky et al. (2006) applied fast Fourier transform (FFT) to analyze the texture image collected from chip sealed pavements and verified the potential to replace sand patch test by a digital image-based method. Sarsam and

Ali (2015) compared sand patch test with close-range photogrammetric method. A high correlation between these two devices was found, which indicates that photogrammetric approach could be an alternative method for texture measurement, with lower cost and comparable accuracy.

Figure 2.4 Sand Patch Method (Pavement Interactive, 2011)

Figure 2.5 Outflow Meter (Pavement Interactive, 2011)

The ASTM E2157 “Standard Test Method for Measuring Pavement Macrotexture Properties Using the Circular Track Meter” introduces the laser-based CT meter method to collect pavement macrotexture profile data. The CT meter data is calculated in terms of MPD in accordance with ASTM E1845, or the root mean square (RMS), or both. Prowell and Hanson (2005) applied a CT meter to collect macrotexture profiles on different asphalt sections. It was concluded that the CT meter produced comparable results with those from the ASTM E965 sand patch test method. Watson et al. (2011) collected CT meter texture data from different locations and found that greater texture numbers were obtained in warmer months than in cooler months.

Figure 2.6 Circular Track Meter

A 3D surface measurement and analysis device, named LS-40 Portable 3D Surface Analyzer (Figure 2.6), scans a 4.25-in by 6-in or 10-in area and produces a high resolution (0.01mm) digital surface based on an intensity image (2D) and a surface depth range image (3D). The LS-40 provides the necessary data to determine MPD by processing thousands of profiles over the entire scanned surface, according to ASTM E1845 specifications, with optional processing modules LS-40 is capable of measuring other surface features, such as aggregate form factor, angularity, and microtexture. A LS-40 can not only be used in the laboratory, but also be placed on a localized pavement surface area in the field at 0.01mm resolution. Liu and Shalaby (2015) used a photometric stereo device to collect and reconstruct pavement 3D surface, calculate simulated MTD, root mean square (RMS), skewness and kurtosis, and correlate texture to noise and friction performance.

Figure 2.7 LS-40 Portable 3D Surface Analyzer

RoboTex is a line laser-based pavement texture profiler engineered by the Transtec Group with the capability of producing 3-D texture images continuously. It measures in three dimensions with sub-millimeter accuracy and produces standard texture metrics such as MPD.

Figure 2.8 RoboTex (Moravec, 2013)

Stationary Laser Profilometer (SLP) is another line laser-based laboratory pavement texture profiler. SLP is capable of capturing the microtexture and macrotexture spectrum of asphalt mixtures and generate corresponding parameter to characterize pavement texture properties (Miller et al., 2012; Chen et al., 2015).

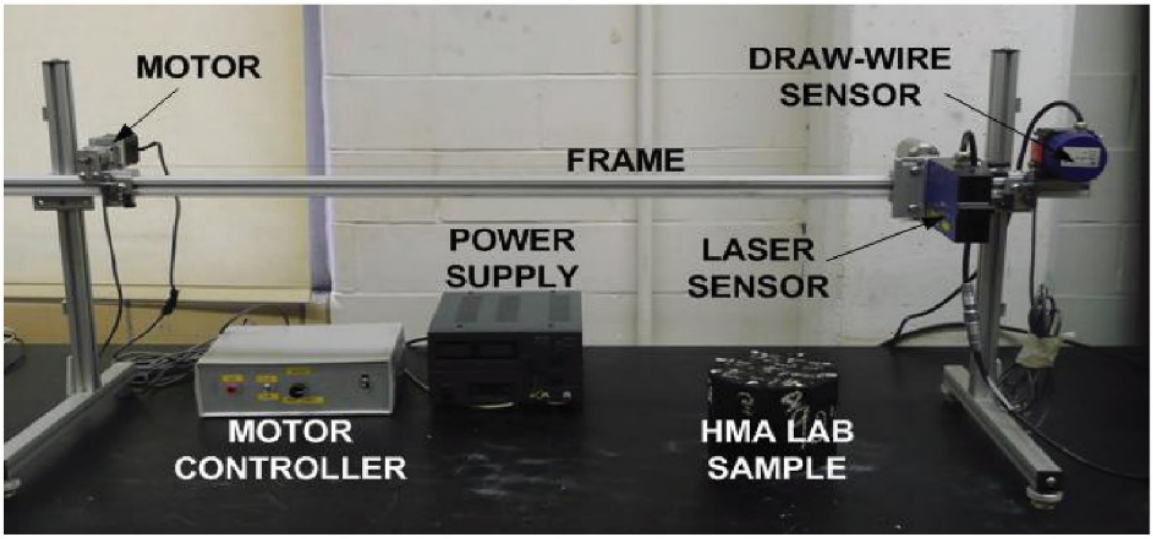

Figure 2.9 Stationary Laser Profilometer (Miller et al., 2012)

Many high-speed profilers have been used to collect pavement texture profiles and calculate MPD for network level evaluations, such as the AMES Engineering high speed texture profiler shown in Figure 2.10. McGhee and Flintsch (2003) conducted validation experiments with high-speed texture measuring equipment and found good correlations with the static texture referencing device. Flintsch (2012) pointed out the need to measure friction and macrotexture concurrently and to determine both low-speed and high-speed friction performance from a single pass. Measurement of pavement microtexture is still not a matured field due to the limited accuracy of laser. Thus, more research in microtexture is needed for better prediction of pavement skid resistance.

Figure 2.10 High Speed Profiler (Courtesy of AMES Engineering)

2.3 Measurement of Skid Resistance of Pavements

2.3.1 Pavement Skid Resistance

Pavement friction resists the relative motion between a vehicular tire and the pavement surface. It results from a complex interplay between two principal frictional force components: adhesion and hysteresis (Hall et al., 2009) (Figure 2.11). The adhesion component of friction results from the small-scale bonding/interlocking of the tire rubber in a vehicle and the pavement surface as they come in contact with each other, which is a function of the shear strength of the interface and the contact area. The hysteresis component of frictional forces results from the energy loss due to bulk deformation of tires in a vehicle. This loss in net frictional force helps stop the forward motion of a vehicle.

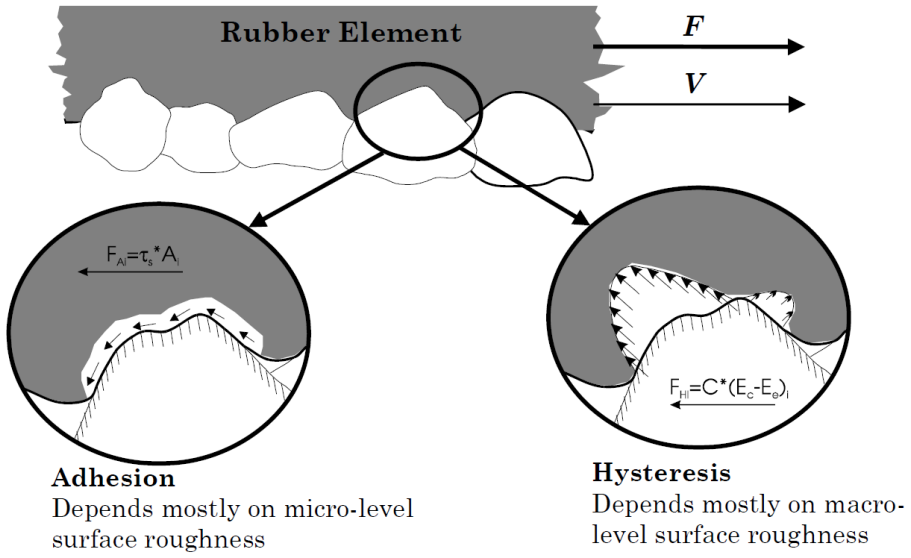

Figure 2.11 Key Mechanisms of Pavement-Tire Friction (Hall et al., 2009)

Because adhesion forces are developed at the pavement–tire interface, they are most responsive to the micro-level asperities (microtexture) of the aggregate particles contained in the pavement surface. In contrast, the hysteresis forces developed within the tire are most responsive to the macro-level asperities (macrotexture) formed in the surface via mix design and/or construction techniques. As a result, adhesion governs the overall friction of smooth-textured and dry pavements, while hysteresis is the dominant component of wet and rough-textured pavements. As depicted in Figure 2.12, microtexture is the degree of roughness imparted by individual aggregate particles, whereas macrotexture is the degree of roughness imparted by the deviation among particles.

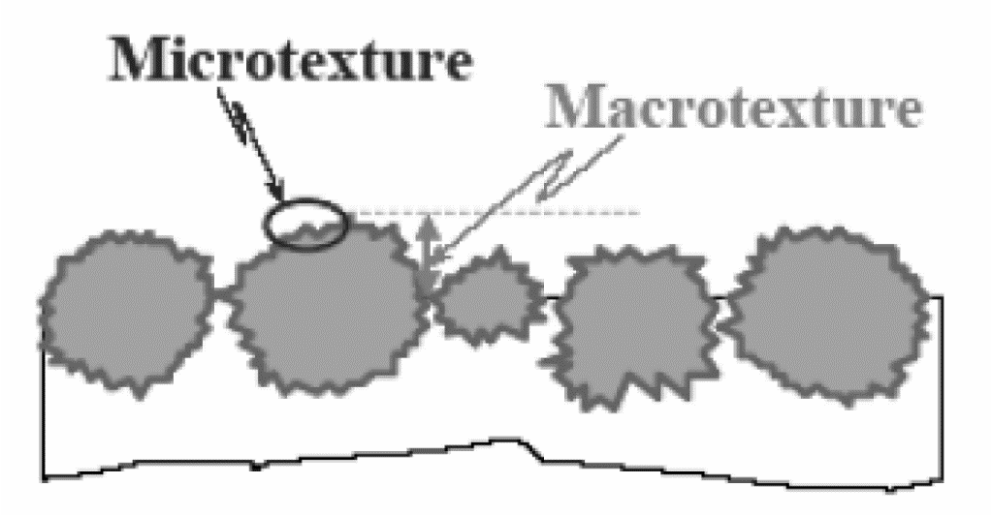

Figure 2.12 Microtexture and Macrotexture (Flintsch et al., 2003)

Hall (2009) grouped the influencing factors of pavement friction forces into four categories: pavement surface characteristics, vehicle operational parameters, tire properties, and environmental factors. Considering various pavement surface conditions (including asphalt type, nominal aggregate size, and texture depth) and contact areas (considering tire loading, inflation pressure and type of tire), Labbate (2001) investigated the skid resistance performance of pavements. The skid resistance showed an initial loss in the early life, followed by an increase in friction, and thereafter a reduction in the equilibrium condition. The rolling resistance increased with reduced contact areas.

The influence of asphalt mixture type and Portland cement concrete surface textures on friction performance of pavements has been studied widely (Asi, 2007; Ahammed and Tighe, 2008). Previous studies have found that air temperature and pavement temperature could affect friction performance of pavements, both in short-term and long-term cycles. At low testing speed, friction tends to decrease with

increasing pavement temperature. An opposite trend is seen at high testing speed (Luo, 2003; Fuents, 2009; Jahromi et al., 2011). Roe et al. (1998) noted that friction reduced with increasing testing speed and reached the minimum level at about 100km/h for smooth tires. The level of high-speed friction depended to a large extent on the low-speed friction. Friction on surfaces with low texture depth dropped more rapidly at high speed. Wilson (2006) identified up to 30% variations in friction performance over a short period of time. The seasonal variation of friction coefficient was neither obvious nor predictable. Kotek and Florkova (2014) conducted long-term friction monitoring on various pavements and concluded that friction coefficients were affected by such characteristics as age, traffic intensity, and climatic conditions of pavements. No definite dependency of friction on traffic intensity was found. Dan et al. (2015) measured friction coefficients of pavement specimens with different age, contamination (water, snow, ice), and temperature conditions. It was found that friction of new pavement exhibited the highest sensitivity to temperature variations.

2.3.2 Skid Resistance Measurement

The Wehner/Schulze machine, developed in Germany, has been widely used to study polishing of aggregate or pavement mix specimens and to measure skid resistance and macro- or microtexture profiles. Kane et al. (2010) utilized the Wehner-Schulze-machine to simulate the polishing process and measure friction of pavement specimens in the laboratory. These data were used to develop models for predicting texture or friction due to polishing of aggregate by traffic. Ueckermann et al. (2015) employed the Wehner/Schulze machine in the laboratory and ViaFriction in the field to collect friction data and validate rubber friction models that are used to

calculate skid resistance based on texture measurements. Do et al. (2007) applied the Webner/Schulze machine to collect skid resistance as well as texture profiles of asphalt mixes under different traffic polishing levels, and compared the results with friction measurements in the field. The results demonstrated that once the surface film of asphalt binder was polished, the pavement friction performance was controlled mainly by the microtexture of aggregates. Other researches have also used the Wehner/Schulze machine to predict skid resistance of pavements or aggregates (Do et al., 2009; Arampamoorthy and Patrick, 2011; Chen and Wang, 2011; Dunford et al., 2012; Dunford, 2013; and Friel et al, 2013).

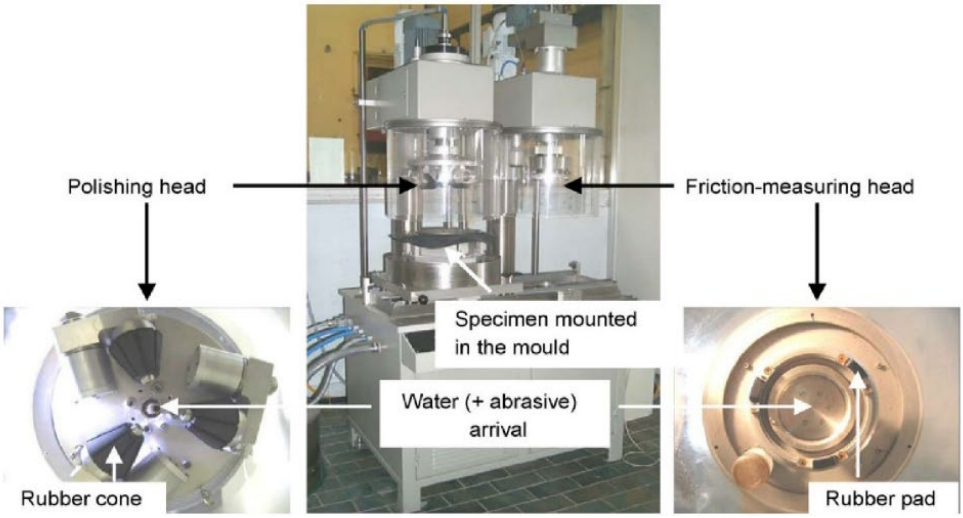

Figure 2.13 Machine Wehner/Schulze (Do et al., 2007)

The British Pendulum Tester (BPT) is a dynamic pendulum impact-type tester. It measures the loss of energy when a rubber slider edge is propelled over the test surface. ASTM E303 illustrates the procedure for measuring surface friction properties using the BPT. Steven (2009) established a temperature correction equation based on the BPT testing. Steven (2009) also evaluated the influences of

different operators, instruments, levels of slider pad wear and temperature variations. Asi (2007) applied the BPT to evaluate skid resistance performance of various pavement mixes considering different binder contents, aggregate types, and mixture design procedures.

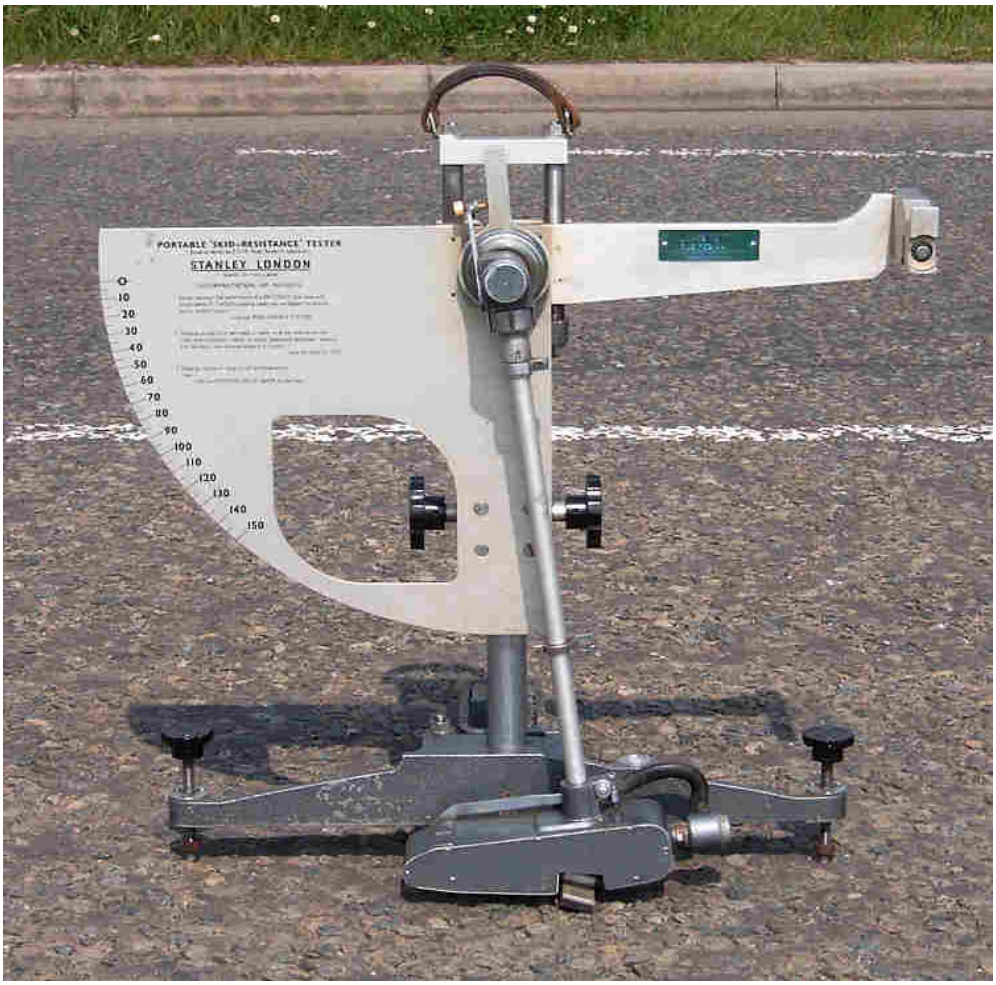

Figure 2.14 British Pendulum Tester

ASTM E1911 provides the specification on measuring surface frictional properties of pavements using a Dynamic Friction Tester (DF Tester). The DF Tester consists of a horizontal spinning disk fitted with three spring loaded rubber sliders which contact the paved surface as the disk rotates. The torque is monitored

continuously as the disk rotational velocity reduces due to the friction between the sliders and the test surface. The torque generated by the slider forces measured during the spin down is then used to calculate the friction at various speeds from 20 to 80 km/h.

Figure 2.15 Dynamic Friction Tester

The Locked-Wheel Skid Trailer (ASTM E274-06) measures the steady-state frictional force on a locked test wheel as it is dragged under a constant load and at a constant speed (typically at 64 km/h [40 mph]) over a wet pavement surface. In this test, water is sprayed on the pavement surface in front of the test tire when the tire reaches test speed. Friction of the pavement surface is determined from the resulting force or torque and is reported as skid number (SN). A higher SN indicates greater frictional resistance. Both ribbed and smooth tires may be incorporated in the test, as standardized by ASTM E501 and ASTM E524, respectively. Kotek and Kovac (2015) measured skid resistance of pavements using different types of tires.

Microtexture had more influence on friction coefficients tested by a tread tire, whose grooves provided much larger channels than those from the macrotexture of pavement surfaces. Macrotexture contributed more variations to the friction performance measured with a smooth tire.

Figure 2.16 Locked-Wheel Skid Trailer

Another widely used method to test side force friction on paved surfaces is pulling a Mu-Meter (ASTM E670) at a constant speed while the test wheels are under a constant static load. This method provides side force friction data along the length of the test surface. A variety of computerized algorithms enables the production of test results, including rolling averages, numeric and graphical representations, friction mapping and reports formatted by a wide variety of national airport regulators.

Figure 2.17 Mu-Meter (Pavement Interactive 2011)

The Grip Tester has been used in recent years by Federal Highway Administration (FHWA) on many demonstration projects in the United States. It is designed to continuously measure the longitudinal friction along the wheel path operating around the critical slip of an anti-braking system (ABS) at highway speed across the entire stretch of a road with much lower water consumption. The Grip tester can provide greater detail about spatial variability for project and network level friction management. The device is capable of testing at highway speeds (50 mph/80 kph) as well as low speeds (20 mph/32 km/h) using a constant water film thickness. The collected data are recorded at 3-ft (0.9 m) intervals by default and can be adjusted by the user. It also follows ASTM E274 "Standard Test Method for Skid Resistance of Paved Surfaces Using a Full-Scale Tire."

Figure 2.18 Grip Tester

ASTM E1960 defines the harmonization procedure to calculate the International Friction Index (IFI) based on pavement macrotexture and wet pavement friction from different devices using smooth tread test tire. Yager (2013) provided a comprehensive summary of pavement friction and texture measuring devices used in airport runway surveys worldwide and in friction rating methods for different equipment. Details on the maintenance procedure and the measuring equipment for airport pavement skid resistance management are given by FAA (1997).

2.4 Skid Resistance of Preventive Maintenance Treatments

Zaniewski and Mamlouk (1996) described the need and benefits, the application procedures and materials for different preventive maintenance (PM)

treatments on asphalt and concrete pavements. The State of California (CalTrans, 2008) developed its own maintenance technical advisory guide for preservation of rigid and flexible pavements. Peshkin et al. (2004) developed an Excel-based methodology to determine the optimal timing for the application of PM treatments on asphalt and concrete pavements. The field data obtained from the long-term pavement performance (LTPP) program have been analyzed by different researchers. The goal was to evaluate the short- and long-term effectiveness of the identified PM treatments on pavement performance, in terms of cracking, rutting and roughness (Hall et al., 2002; Wang, 2013; Gong et al., 2015).

Friction performance of different PM treatments has been investigated by researchers. For example, Kowalski et al. (2009) conducted long-term monitoring of friction and texture properties of pavements involving dense-graded asphalt (DGA), stone matrix asphalt (SMA) and porous friction course (PFC). Comparable frictional performance was observed for SMA and PFC. Both of these pavements exhibited better performance than the DGA. Li et al. (2011) evaluated the long-term friction performance of pavements with different surface treatments using a locked wheel trailer. It was found the friction performance of different PM treatments had a transition phase before forming a stable mosaic.

Watson et al. (2011) found that chip seals had exceptional friction performance measured by a locked wheel trailer using ribbed/smooth tire. Dense graded mixtures displayed the greatest variability of friction between ribbed and smooth testing tires, which were followed by the coarse DGA. Wang et al. (2013) evaluated the initial improvement and long-term variations of friction performance of

pavements (SPS3 sections) with four preservation treatments. It was concluded that slurry seal generated the highest improvement in initial friction. Pierce and Kebede (2015) found a 24-point increase in pavement friction number, on an average, after chip seal applications. The International Slurry Surfacing Association also claimed that slurry seal along with micro surfacing could provide superior macrotexture that greatly enhances surface friction.

Izeppi et al. (2010) carried out a field study on High Friction Surface Treatments (HFST) to evaluate the long-term variations of pavement friction. Through benefit-cost analyses, it was found that HFST significantly increased the surface skid resistance with a positive economic benefit. The effectiveness of HFST in improving pavement skid resistance and reducing crashes at horizontal curves had been demonstrated through several projects (Bledsoe, 2015; Moravec, 2013; SDDOT, 2015; and Bischoff, 2008).

Arambula et al. (2013) conducted four years of performance monitoring of Permeable Friction Course (PFC) sites, including noise, drainability, texture, and skid resistance. The texture of PFC remained practically unchanged over time. Asphalt rubber and performance graded PFC had superior texture and skid resistance performance as compared with the DGA. Aggregates with higher soundness values and polishing resistance exhibited higher friction numbers. Li et al. (2007) compared friction performance of coarse aggregates and conventional Hot-Mix asphalt pavements. Coarse aggregate pavements (such as open-graded friction course, OGFC, and stone mastic asphalt mix, SMA) exhibited consistently better friction performance than regular mixes. Putman (2012) also claimed that

OGFC could provide higher skid resistance than HMA and could result in reduced accident probability.

2.5 Aggregate Characteristics and Skid Resistance

Gardiner (2001) measured friction at sites with Superpave and Marshall Mix designs. It was found that friction related the most to the nominal maximum size of aggregates rather than mix design methods. Li et al. (2007) evaluated the influence of aggregates characteristics on pavement friction performance for different mixture designs. Asi (2007) tested friction over different pavement mixes, and found that harder aggregates produced higher friction values.

Masad et al. (2007, 2009) have been conducting research on aggregate characterization and its relationship to pavement surface skid resistance. They measured the skid resistance of pavements constructed with aggregates from three sources and three different mix gradations. The skid resistance was found to be related to the average aggregate texture and to the texture distributions within the aggregate samples. Analytical models were developed to predict the change of skid resistance as a function of aggregate texture, mixture properties, and environmental conditions. Masad et al. (2009) and Rezaei et al. (2009) developed IFI models to determine the skid resistance of asphalt mixtures based on aggregate characteristics and mixture gradation. The parameters used in the models included the initial and terminal aggregate texture, the rate of change in aggregate texture after different polishing intervals, and the Weibull distribution parameters describing aggregate gradation. Large amounts of aggregate property measurements were

conducted for various surface mixes. Also, field pavement friction and texture measurements were performed on selected sections. Moreover, prediction models and software interface were developed to predict skid resistance of asphalt pavements based on aggregate resistance to polishing, mixture gradation, and traffic levels (Masad et al., 2010; Masad et al., 2011; and Rezaei and Masad, 2013).

Do et al. (2009) proposed a skid resistance predictive model incorporating polishing due to traffic, binder removal and aging effects. Goodman (2009) performed friction and texture measurements on pavements with different asphalt mixtures at various levels of polishing in the laboratory and in the field. A series of friction and texture prediction models was developed for the mix design stage. Kassem et al. (2013) conducted laboratory testing to develop a predictive model for loss of friction on pavement surfaces. It was found that aggregates with higher hardness had higher abrasive resistance. Mixes with coarser gradation maintained larger MPD values than those with finer mixtures. Microtexture decreased with increased polishing and reduced aggregate hardness. Subsequently, an IFI predictive model was developed based on texture, aggregate angularity, and mix gradation. Arambula et al. (2013) also found that aggregates with higher soundness and polishing resistance exhibited higher friction numbers. Ahammed and Tighe (2012) developed an equation to predict skid numbers considering MTD, vehicle speed and aggregate type. The CT meter and DF Tester were generally used simultaneously to obtain pavement texture and friction data for the development of skid resistance models (Rado and Kane, 2014; Kane et al., 2015).

Many other researchers aim to predict pavement skid resistance based on pavement microtexture. For example, Ergun et al. (2004) measured friction and macrotexture on selected pavement sections with different surface characteristics in Belgium. Microtexture measurements were conducted in the laboratory using pavement core samples taken from those sections. Subsequently, a statistical friction prediction model was developed based on micro- and macrotexture properties to predict surface friction. For a given speed, both micro- and macrotexture had strong effects on road surface friction. Serigos (2013) collected pavement texture data using the AMES Laser Texture Scanner (LTS) at 0.015 mm resolution. Skid resistance at low speeds on wet pavement surfaces was significantly affected by both the micro- and macrotexture of pavement surfaces. Incorporating both surface micro- and macrotexture improve the prediction accuracy of skid resistance. In another study, Slop Variance (SV) and Root Mean Square (RMS) were calculated from microtexture profiles. It was found that pavement friction numbers increased with increasing microtexture SV and RMS values (Li et al., 2015). Ueckermann et al. (2015) measured pavement micro- and macrotexture using an optical testing system. A rubber-based friction model was proposed to predict surface skid resistance. It was concluded that non-contact skid resistance measurements could be possible in the future.

2.6 Summary

In this Chapter, a comprehensive literature review was conducted. The literature review was focused on several aspects, including aggregate properties and

testing, pavement skid resistance and measurements, and existing relationships between morphological characteristics of aggregates and skid resistance of pavements. Developments in measuring aggregate shape and texture-related index properties were also reviewed and summarized.

CHAPTER 3 EXPERIMENTAL DESIGN

The commonly used aggregates and preventive maintenance treatments used in Oklahoma were identified in this study, in cooperation with ODOT. A systematic laboratory and field testing plan was established by working closely with ODOT engineers. Effort was made to include ODOT engineering practices and leverage data and field test sections from existing and previous research projects supported by the agency. For each preventive treatment, various aggregate sources were evaluated to determine relationships between aggregate characteristics and skid resistance of associated pavements.

3.1 Pavement Preventive Maintenance Treatments

Various preventive maintenance treatments have been employed by state DOTs, including ODOT, to restore pavement condition (particularly, skid resistance for this project) and retard future deterioration. The following seven different types of preventive treatments used by ODOT were included: High Friction Surface Treatment (HFST), Warm Mix Asphalt (WMA), chip seal, microsurfacing, friction seal, permeable friction course (PFC), thin HMA resurfacing, and Ultra-Thin Bonded Wearing Surface (UTBWC, or Nova chip).

3.1.1 High Friction Surface Treatment (HFST)

In an effort to reduce the fatalities and injuries from crashes that occur at or near horizontal curves, the Federal Highway Administration (FHWA) Office of Pavement Technology has implemented the Surface Enhancements At Horizontal Curves (SEAHC) program and installed HFST at many horizontal curves throughout the U.S. Through various HFST projects, the effectiveness of HFST in improving skid resistance and reducing crashes at horizontal curves has been demonstrated. Tests for friction and texture depth are generally conducted before and after HFST installation to quantify the change in friction and texture depth over time. Pavement friction is measured primarily using the Dynamic Friction Testers (DFT) and agency-owned locked-wheel skid testers, while texture depth and/or profile depth for macrotexture is measured using stationary or low speed devices such as the Circular Track Meter (CTM), ASTM E 965 “Sand Patch” Method, or RoboTex.

3.1.2 Warm Mix Asphalt

The warm mix asphalt (WMA) technology is defined as an asphalt concrete paving material produced and placed at temperatures approximately 50 ºF cooler than those used for conventional hot mix asphalt (HMA). WMA technologies incorporate foaming processes that use water, chemical additives, organic additives, and non-foaming additives (Prowell et al., 2012). The plant foaming and additives technologies account for about 84% and 16% of the WMA market in the U.S., respectively (Hansen and Copeland, 2014). WMA offers significant benefits, notably, lower energy demand during production and construction, extended paving season, reduced emission, improved working conditions, an earlier opening to traffic, and

increased hauling distances (Prowell et al., 2012). As a result, WMA for asphalt pavement construction has dramatically increased over the past decades. WMA in the U.S. had reached about one-third of the total asphalt mixture market, and its usage increased about 577 percent since 2009 (Hansen and Copeland, 2014; Faheem et al., 2018).

3.1.3 Chip Seal

Chip seal is a preventative treatment method to seal existing cracks from weathering effects. Chip seal consists of a binder layer followed by an aggregate layer where there is no mixing of the binder and aggregate before the application. By adding aggregates on top of the binder layer, the surface is initially expected to be rougher than a traditional HMA pavement. On warmer days, it is common for the aggregates to penetrate into the binder layer further, therefore reducing the roughness of the road. The benefits of chip seal include low cost, extended life, elimination of crack sealing, and improvement in skid resistance. Chip seal is typically used on lower traffic routes with less than 2,500 vehicles per day. The types and amounts of binder and aggregate are the major design considerations of chip seal. The binder used in chip seal can vary depending on the types of chip seal used. Chip seal design is heavily dependent of existing surface conditions and the performance can vary due to the application procedures.

3.1.4 Microsurfacing

Also known as modified slurry seal, in microsurfacing treatments emulsions, usually modified with latex and rubber particles, are applied on the pavement surface. The latex and asphalt form a composite structure. Microsurfacing mixtures

contain polymer-modified cationic emulsion, mineral aggregate, mineral filler, water and additives. Microsurfacing mixtures are sprayed with a machine over a prepared surface (Hossain, 2010).

Microsurfacing is a preventative maintenance that preserves the life of the pavement by waterproofing the surface, filling minor cracks, restoring skid resistance and restoring aesthetic appeal with a black surface, at a relatively low cost. The disadvantages of microsurfacing include a longer curing time (2-8 hours). This treatment is not suitable for pavements with severe distresses such as cracking and rutting.

3.1.5 Friction Seal

Friction seal combines the two steps of the chip seal into one by placing emulsified asphalt and aggregates in a single layer. It can help increase the skid resistance of the pavement surface due to the addition of the cover aggregates. This treatment can combat raveling, which can make the pavement slippery and stopping difficult. Friction seal provides good, gripping texture to pavement surfaces. They can be used as a preventive maintenance measure early in the life of a pavement, and can also repair small defects.

3.1.6 Permeable Friction Course (PFC)

Permeable friction course (PFC) is an asphalt overlay that allows rain water to run through the pavement rather than creating runoff. These are bituminous mixtures applied over an impervious base. Road safety could be improved by PFC overlays, with improved driving conditions during rainfall events. The benefits include reduced hydroplaning, increased skid resistance, and improved visibility in wet conditions.

Disadvantages include increased capital cost and maintenance cost as well as reduced service life (Stanard, 2007).

ODOT specifications describe PFC as mixing aggregate, bituminous material, and fibers in a central plant before application. The physical properties of aggregates and binders must meet the standards found in Section 708 of the Oklahoma Department of Transportation Specifications Book (ODOT, 2009).

3.1.7 Thin HMA Resurfacing

According to a 1999 AASHTO survey by the Lead States Team on Pavement Preservation, thin asphalt resurfacing was the most popular preventative maintenance treatment for asphalt and composite pavements (Newcomb, 2009). This popularity has led to a number of studies on the materials, design, and construction of thin overlays in order to optimize pavement preservation strategies. A comprehensive overview of thin-lift asphalt technology has been conducted by Cooley and Brown (2004) and Chou et al. (2008).

Primary advantages of a thin asphalt overlay include long service life and low life cycle cost when placed on structurally sound pavements, and ability to maintain grade and slope with minimal impact to drainage. The relative importance of any of these benefits varies according to the type of project, location, climate, and traffic conditions.

3.1.8 Ultra-Thin Bonded Wearing Surface (UTBWC)

Construction of UTBWC, also named as Nova Chip, involves application of a warm polymer modified emulsion membrane followed immediately with an ultra-thin wearing course for added surface texture (Ahmed, 2010). The membrane layer is

intended to seal the original pavement surface and act as a bond with the wearing course layer. The HMA mixture used in Nova Chip is gap-graded with thickness ranging from 9.5 mm (3/8 inch) to 19 mm (3/4 inch). The gap-graded mix is used to improve stone-to-stone contact while allowing space for the binder to fill in. It is used to extend the life of both HMA and concrete pavements. Advantages of Nova Chip include ease of application, fast construction, increased skid resistance, and strong bond with the original surface. Disadvantages include higher cost than a sprayed seal, specialized equipment and personnel for installation, and low shear resistance (Hossain, 2010).

3.2 Aggregate Types and Sources

As noted earlier, one of the goals of this study was to determine potential relationships between aggregate characteristics and skid resistance of pavement treatments. The most commonly used aggregate sources in Oklahoma include the following (Zaman et al., 2014): (1) Dolese Cooperton (limestone); (2) Hanson Davis (rhyolite); (3) Martin Marietta Mill Creek (granite); (4) Dolese Hartshorne (limestone); (5) Kemp Stone Pryor (limestone) (Zaman et al., 2013). The regionally available aggregate sources with good friction characteristics include mine chat, rhyolite, sandstone, and granite (Heitzman and Vrtis, 2015). In close consultation with ODOT, the following aggregates were identified and collected from the following thirteen sources (Figure 3.1):

- Dolese Co. (limestone): Davis, Oklahoma;
- Dolese Co. (limestone): Hartshorne, Oklahoma;

- Dolese Co. (limestone): Richard Spur, Oklahoma;
- Hanson Aggregates WRP Inc. (rhyolite): Davis, Oklahoma;
- Martin-Marietta (granite): Mill Creek, Oklahoma;
- Martin-Marietta (sandstone): Sawyer, Oklahoma;
- Martin-Marietta (granite): Snyder, Oklahoma;
- APAC Central 66 (limestone): Pawhuska, Oklahoma;
- APAC Central 18 (sandstone): Spiro, Oklahoma;
- APAC Central 14 (sandstone): Jenny Lind, Arkansas;
- Quapaw Co. (dolomite): Drumright, Oklahoma;
- Flint Rock Mine Chat: Picher, Oklahoma;
- Calcined Bauxite: Obtained from DBI Services, which is imported from overseas.

Figure 3.1 Quarry Locations of Aggregates Included in this Study

3.3 Selected Field Testing Sites

To evaluate field performance of skid resistance of pavements with the most commonly preventive maintenance treatments, field testing sites were identified for the experimental design. These sites are listed in Table 3.1 after several rounds of consultation with ODOT. The selection process included the following steps:

(1) Obtaining all ODOT Contract Awards data from 2008 to 2016 from the ODOT website;

(2) Identifying candidate sites that have been treated with preventative maintenance during that time period;

(3) Contacting Construction Division and/or Maintenance Engineers and also the City Engineer of Stillwater for the preliminary selected sites. In general, more sites were recommended initially where the treatment types were known for most cases, but the aggregate types and sources were not traceable.

(4) Acquiring aggregate sources and types for each site from the ODOT SiteManager database;

(5) Delivering an updated list of recommended testing sites (with known aggregate types and sources, and PM treatment types) to ODOT for review and comments;

(6) Holding a face-to-face meeting with the project panel at ODOT discussing the proposed list;

(7) Finalizing the field testing sites for multiple-rounds of data collection.

Forty-five preventive treatment sites, with various PM treatment types, aggregate sources/types, surface ages, and traffic conditions, were selected for field monitoring with the following distributions:

- 8 types of treatments: chip seal, microsurfacing, friction seal, PFC, thin overlay (resurface), Nova Chip (UTBWC), High friction surface treatment (HFST) (6 sites), and SPS-10 Warm-Mix-Asphalt (WMA) overlay (6 sites);
- 7 types of aggregates: granite, limestone, dolomite, rhyolite, sandstone, bauxite, and mine chat;
- Installation age: average 3.6 years, minimum 0.52 years, and maximum 6.10 years;
- Highway function class: 5 on Interstates, 20 on State Highways, 17 on US Highways, 3 City Streets.

The six HFST sections and the six LTPP SPS-10 sites have been actively monitored since November 2015. As a result, these 12 sections had seven data collection events in total. The additional 33 sites have been monitored since September 2016 with 4 data collection events for this project. For each data collection event, approximately 7 daily data trips were required to collect all the data for the 45 testing sites. The testing dates of the testing events are given below:

- 1st testing: the weeks of November 8 and November 22, 2015, only for the HFST and LTPP WMA sites;
- 2nd testing: the week of March 20, 2016, only for the HFST and LTPP WMA sites;

- 3rd testing: the weeks of May 22, and June 19, 2016, only for the HFST and LTPP WMA sites;
- 4th testing: the weeks of September 11, September 18, and September 25, 2016;
- 5th testing: the weeks of January 15, January 22, and January 29, 2017
- 6th testing: the weeks of June 25, July 2, and July 9, 2017,
- 7th testing: the weeks of October 15, October 22, November 5, December 24, 2017.

For the additional 33 sites, a 0.5-mile segment was identified for each site to keep the data consistent and comparable. These segments can be easily located with noticeable physical markers within the right-of-way and have recorded GPS coordinates. The list of the field testing sites, aggregate types and sources, and treatment types is given in Table 3.1.

Table 3.1 Field Testing Sites

ID	Route	Const. Date	Treatment	Aggregate	Quarry
1	SH-1	3/5/2012	Chip Seal	Limestone	Dolese Co (Hartshorne, OK)
2	US-259	9/8/2014	Chip Seal	Limestone	Dolese Co (Hartshorne, OK)
3	SH-39-1	9/2012	Chip Seal	Limestone	Dolese Co (Hartshorne, OK)
4	SH-39-2	9/2012	Chip Seal	Limestone	Dolese Co (Hartshorne, OK)
5	SH-39-3	9/2012	Chip Seal	Limestone	Dolese Co (Hartshorne, OK)
6	US-412	Unknown	Friction Seal	Unknown	Unknown
7	Lakeview Rd. Stillwater	2/9/2015	Microsurfacing	Granite	Martin-Marietta (Snyder, OK)
8	US-64 Perry	2002	Microsurfacing	Mine Chat	Picher OK
9	N Harrah Rd	2012	Microsurfacing	Granite	Martin-Marietta (Mill Creek, OK)
10	SE 29th St	2011	Microsurfacing	Granite	Martin-Marietta (Mill Creek, OK)
11	I-35	6/1/2011	PFC	Unknown	Unknown
12	I-35	6/1/2013	PFC	Unknown	Unknown
13	SH-33	1/20/2011	Resurface	Dolomite	Quapaw Co. (Drumright, OK)
14	SH-33	2/9/2015	Resurface	Dolomite	Quapaw Co. (Drumright, OK)
15	SH-51	7/7/2014	Resurface	Dolomite	Quapaw Co. (Drumright, OK)
16	US-177	7/2/2012	Resurface	Dolomite	Quapaw Co. (Drumright, OK)

ID	Route	Const. Date	Treatment	Aggregate	Quarry
17	SH-77	4/1/2013	Resurface	Granite	Martin-Marietta (Snyder, OK)
18	SH-51	2/4/2013	Resurface	Rhyolite	Hanson Aggregates, WRP Inc (Davis, OK)
19	I-40	8/12/2013	Resurface	Rhyolite	Hanson Aggregates, WRP Inc (Davis, OK)
20	US-77	2/3/2014	Resurface	Rhyolite	Hanson Aggregates, WRP Inc (Davis, OK)
21	SH-9	2/7/2011	Resurface	Granite	Martin-Marietta (Mill Creek, OK)
22	US-64	3/7/2011	Resurface	Limestone	APAC-Central #066 (Pawhuska, OK)
23	SH-15	7/7/2014	Resurface	Limestone	APAC-Central #066 (Pawhuska, OK)
24	US-270	2/6/2012	Resurface	Limestone	Dolese Co (Hartshorne, OK)
25	US-59	2/3/2014	Resurface	Sandstone	APAC-Central #018 (Spiro, OK)
26	US-270	5/19/2011	Resurface	Sandstone	APAC-Central #018 (Spiro, OK)
27	SH-4	2/3/2014	UTBWC	Granite	Martin-Marietta (Snyder, OK)
28	I-35	8/10/2015	UTBWC	Rhyolite	Hanson Aggregates, WRP Inc (Davis, OK)
29	SH-270	3/7/2016	UTBWC	Rhyolite	Hanson Aggregates, WRP Inc (Davis, OK)
30	US-62	8/10/2010	UTBWC	Rhyolite	Hanson Aggregates, WRP Inc (Davis, OK)
31	I-240	3/7/2011	UTBWC	Limestone	Dolese Co. (Richards Spur, OK)
32	US-69	3/5/2012	UTBWC	Sandstone	APAC-Central #018 (Spiro, OK)
33	US-59	5/5/2014	UTBWC	Sandstone	APAC-Central #018 (Spiro, OK)
34	I-40	8/24/2015	HFST	Bauxite	Imported
35	I-40	8/24/2015	HFST	Bauxite	Imported
36	I-44	8/24/2015	HFST	Bauxite	Imported
37	SH-20	8/24/2015	HFST	Mine Chat	Picher OK
38	SH-20	12/17/2013	HFST	Bauxite	Imported
39	SH-20	12/17/2013	HFST	Bauxite	Imported
40	SH-66	6/11/2015	WMA	Rhyolite	Hanson Aggregates, WRP Inc (Davis, OK)
41	SH-66	6/11/2015	WMA	Rhyolite	Hanson Aggregates, WRP Inc (Davis, OK)
42	SH-66	6/11/2015	WMA	Rhyolite	Hanson Aggregates, WRP Inc (Davis, OK)
43	SH-66	6/11/2015	WMA	Rhyolite	Hanson Aggregates, WRP Inc (Davis, OK)
44	SH-66	6/11/2015	WMA	Rhyolite	Hanson Aggregates, WRP Inc (Davis, OK)
45	SH-66	6/11/2015	WMA	Rhyolite	Hanson Aggregates, WRP Inc (Davis, OK)

3.4 Summary

In this Chapter, working closely with ODOT, the most commonly used aggregate sources and preventive maintenance treatments in Oklahoma were identified. A systematic laboratory and field experimental design was developed considering the influencing factors pertaining to skid resistance. These selections also leveraged field test sections from existing and previous research projects supported by ODOT. Forty-five PM sites were selected for field testing, which include 8 treatment types (chip seal, microsurfacing, friction seal, PFC, HMA thin overlay, UTBWC, HFST, and WMA thin overlay), 7 typical aggregate sources/types (granite, limestone, dolomite, rhyolite, sandstone, bauxite, and mine chat), different treatment times, and traffic loading conditions. For each preventive treatment site, aggregate properties and pavement surface performance were tested and measured so that relationships between aggregate characteristics and skid resistance of associated pavements could be determined and evaluated.

CHAPTER 4 LABORATORY AGGREGATE TESTING AND RESULTS

4.1 Background

Pavement surfaces are continuously exposed to conditions related to traffic (i.e. volume, loads, turning motions, decelerating/accelerating motions) and weather (i.e. freeze-thaw, wet-dry cycles) that cause aggregate polishing and degradation. Aggregate polishing and degradation have an adverse impact on these characteristics and result in accelerating the surface deterioration and increasing remediation frequency (Rezaei et al., 2009; Fowler and Rached, 2012; Moaveni et al., 2014). “Although an aggregate might be initially characterized by a high level of angularity or texture and measure good friction values, it may not be suitable for a pavement surface layer if the aggregate cannot maintain a sufficient level of friction due to polishing under traffic” (NCAT, 2017). Essentially, aggregate less prone to texture loss and abrasion will predictively have better skid resistance in the field (Lancieri et al., 2005), and retain higher friction values longer, contributing to adequate pavement safety and longer service life (Neaylon, 2009; Smith et al., 2009).

Most of the state of Oklahoma is comprised of soft aggregates (NSP, 2010; Gransberg, 2012). Table 4.1 shows statewide aggregate quality for Oklahoma, classified with polished stone value (PSV) based upon Neaylons’ 2009 definitions of aggregate quality (Gransberg, 2012). Aggregate PSVs of 55 or above are associated with high resistance to polishing and PSVs less than 45 indicate low

resistance to polishing. To mitigate the polishing issue, limestone is not used in Oklahoma surface course mixtures on medium to high level roadways for asphalt pavements.

Table 4.1 Oklahoma Aggregate Quality (Gransberg, 2012)

Aggregate Quality Level	Percentage Requirement (%)
Good (Average PSV > 55, Min PSV > 45)	21.20%
Marginal (Average PSV < 55, Min PSV > 45)	15.17%
Poor (Average PSV < 45)	63.63%

A wide range of physical characteristics of aggregates such as gradation (size), shape, texture, angularity, durability, and polish resistance (under dry and wet conditions) are tested in the laboratory and analyzed for each aggregate source using conventional methods, aggregate imaging system (AIMS), and high resolution portable 3D surface analyzer. Conventional methods used for aggregate property evaluation include aggregate durability (Micro-Deval AASHTO-T-327) and hardness (LA Abrasion AASHTO-T-96). Three replicates of each test will be conducted. The Micro-Deval apparatus measures the resistance of aggregates to degradation by measuring their abrasion loss in presence of water. A pre-soaked aggregate sample is placed in a jar with a fixed volume of water and a fixed number of steel balls. The unit is then put into rotation for a specified period of time. A Los Angeles Abrasion test is similar in principle to the Micro-Deval test, except abrasion resistance is evaluated under dry conditions and an impact environment. Newly collected data as

well as data from previous projects are used, where applicable, to develop a database on aggregate characteristics.

Technological innovations have made it possible to measure such properties of aggregates as shape, texture and angularity with automated techniques that offer a much higher level of precision and repeatability than conventional methods. One of the most appropriate technologies in this regard is the Aggregate Imaging System (AIMS), available at the University of Oklahoma (OU) Binders Laboratory. This device is used in this task according to the AASHTO TP81-10 (before Micro-Deval) and AASHTO T 327 (after Micro-Deval) test methods. Aggregates are characterized by their shape, angularity, sphericity and texture (Bathina, 2005; FHWA, 2012). AIMS utilizes advanced image processing and analysis techniques in quantifying the shape and texture characteristics of aggregates. It consists of a computer automated unit comprised of an aggregate measurement tray with marked grid points (56 points) at specified distances along the x and y axes. The camera unit consists of an optem zoom 160 video microscope equipped with bottom and top lights to capture images in black and white format as well as in gray format. The camera moves along specified grid locations in the x, y, and z directions. The AIMS setup is controlled by a LabViewTM and IMAQ Vision (version 2.5) software for image acquisition and motion control of the equipment. Newly collected AIMS data as well as AIMS data from previous projects are used, where applicable, to develop a database on aggregate characteristics.

4.2 Aggregate Testing Methods and Characteristics

4.2.1 Aggregate Testing Methods

The Surface Texture for Asphalt and Concrete Pavements (FHWA, 2005b) identifies aggregate properties that influence pavement surface texture, including toughness, polish resistance and angularity. In this study, Micro-Deval and Los Angeles (LA) Abrasion tests are used to indicate aggregate durability. The Micro-Deval test and Acid Insoluble Residue are used to indicate polish resistance (Fowler and Rached, 2012; NCHRP, 2009). The aggregate imaging system (AIMS) is used to indicate angularity, texture, shape and potentially polishing. This section describes each test method.

4.2.1.1 Micro-Deval

Development of Micro-Deval began in France in the 1870's to evaluate road aggregate, and was initially adopted by the American Society for Testing and Materials (ASTM) in 1908 (Amirkhanian et al., 1991). Wu et al. (1998) determined that the only commonly used test that could adequately predict toughness and abrasion resistance was the Micro-Deval. The Micro-Deval test (Figure 4.1) simulates aggregate resistance due to abrasion and weathering. The test evaluates the abrasion resistance and durability of coarse aggregate by evaluating the percentage aggregate weight loss subsequent to rotation in a jar with an abrasion charge (steel balls). A lower Micro-Deval percentage loss indicates aggregate that is more durable and resistant to abrasion.

The wet conditions in the Micro-Deval test are thought to better simulate the field conditions of aggregate abrasion compared to the dry conditions of the LA

Abrasion test (Rogers, 1998). According to the American Association of State Highway and Transportation Officials (AASHTO) (2012), “many aggregates are more susceptible to abrasion when wet than dry, and the use of water in this test incorporates this reduction in resistance in degradation, in contrast to some other tests that are conducted on dry aggregate”. Previous research has also shown there is no correlation in aggregate percentage loss between the Micro-Deval and the LA Abrasion tests (Kandhal and Parker, 1998; Cooley and James, 2003). Essentially, Micro-Deval tends to polish the aggregate, whereas LA Abrasion tends to break it.

Figure 4.1 Micro-Deval Testing Apparatus (Pavement Interactive 2011)

4.2.1.2 Los Angeles Abrasion

The LA Abrasion test (Figure 4.2) is the most widely specified test for evaluating the resistance of coarse aggregate degradation and was originally developed in the mid-1920’s by the Municipal Testing Laboratory of the City of Los Angeles, California (Kandhal and Parker, 1998). According to AASHTO (2010), the LA Abrasion test measures aggregate “degradation of mineral aggregates of standard gradings resulting from a combination of actions including abrasion or

attrition, impact, and grinding". However, other studies have determined that LA Abrasion primarily measures an aggregate's resistance to mechanical breakdown rather than abrasion due to wear (Rogers, 1998; Lane et al., 2000).

The LA Abrasion test simulates and measures degradation that is experienced by coarse aggregate during the construction process. Unlike the Micro-Deval test, the LA Abrasion test is not carried out in the presence of water, and the steel spheres and drum are much larger. Essentially, the LA Abrasion test is used to assess the abrasion and impact resistance of coarse aggregate by evaluating the percentage aggregate weight loss subsequent to rotation in a drum with steel spheres. A lower LA Abrasion percentage loss indicates aggregate that is more resistant to breakage.

LA Abrasion is an empirical test and therefore a poor predictor of field performance (Wu et al., 1998). The test may not be suitable for certain materials, including limestones, as they typically display a high percentage loss, but may exhibit satisfactory field performance (Pavement Interactive, 2011).

Figure 4.2 LA Abrasion Testing Apparatus

4.2.1.3 Acid Insoluble Residue (AIR)

Acid Insoluble Residue (AIR, ASTM D 3042) test results used in this study were provided by ODOT. AIR testing “estimates the percent by weight of insoluble, hard, noncarbonated residue in carbonate aggregates (e.g., limestone, dolomite), using hydrochloric acid solution to react the carbonates. Higher acid insoluble residue (AIR) values indicate larger percentages of siliceous minerals, which are considered more polish resistant than carbonate materials” (NCHRP, 2009).

4.2.1.4 Aggregate Imaging System (AIMS)

Digital vision and the associated motion control software made significant developments in the early 2000’s, which provided the basis of computerized methods for evaluating individual aggregate particle shape characteristics. A number

of techniques were developed for directly measuring aggregate characteristics, including physical measurements of aggregate dimensions, image analysis techniques, and laser scanning (Jahn, 2000; Tutumluer et al., 2000; Kim et al., 2001). These systems are limited as they mostly focus on aggregate form with little consideration towards texture and angularity characteristics.

A study by Masad (2003) addressed these issues, and sought to develop an automated system for analyzing all aggregate shape characteristics, known as AIMS (Masad, 2003). One of the main objectives of the study was to "correlate the aggregate shape characteristics to the aggregate samples with known laboratory performance to demonstrate the system capabilities" (Masad, 2003). The study developed a system that "provides rapid and accurate determination of aggregate shape properties with minimum interference from the operator" (Masad, 2003). Fine and coarse aggregate samples common to asphalt mix designs with known laboratory performance were used to demonstrate the system. The study concluded that:

> "[AIMS] has the ability to analyze the shape of fine and coarse aggregates. It measures the three-dimensions of form through the use of a single camera and autofocus microscope. Aggregate texture is quantified by analyzing gray scale images, and angularity is quantified by analyzing black and white images" (Masad, 2003).

The [first-generation] aggregate imaging system, like the one in the University of Oklahoma (OU) Binder's Laboratory, was developed to capture images and analyze aggregate shape and texture characteristics. The AIMS setup (Figure 4.3)

uses two separate lighting schemes and a camera to capture images of aggregates at varying resolutions, upon which aggregate characteristics can be measured (Masad, 2005). The camera unit has an optem zoom 160 video microscope that operates in the y and z directions over the aggregate measurement tray, which travels in the x direction. The movement of the camera and aggregate tray is controlled by a closed loop direct current servo, which can achieve highly consistent focus.

Figure 4.3 Aggregate Imaging System (AIMS I) (in OU Binders Laboratory

Aggregate particles are placed on the measurement tray at marked locations, and the camera captures black and white, and gray images of the sample using separate lighting schemes. AIMS software analyzes the captured images and produces characteristic measurements (Masad, 2005; Al-Rousan, 2004). The images are stored in a computer, upon which the AIMS software analyzes the images and exports the data to a text file for later use in data analysis. The AIMS aggregate classification chart is shown in Figure 4.4 (FHWA, 2006).

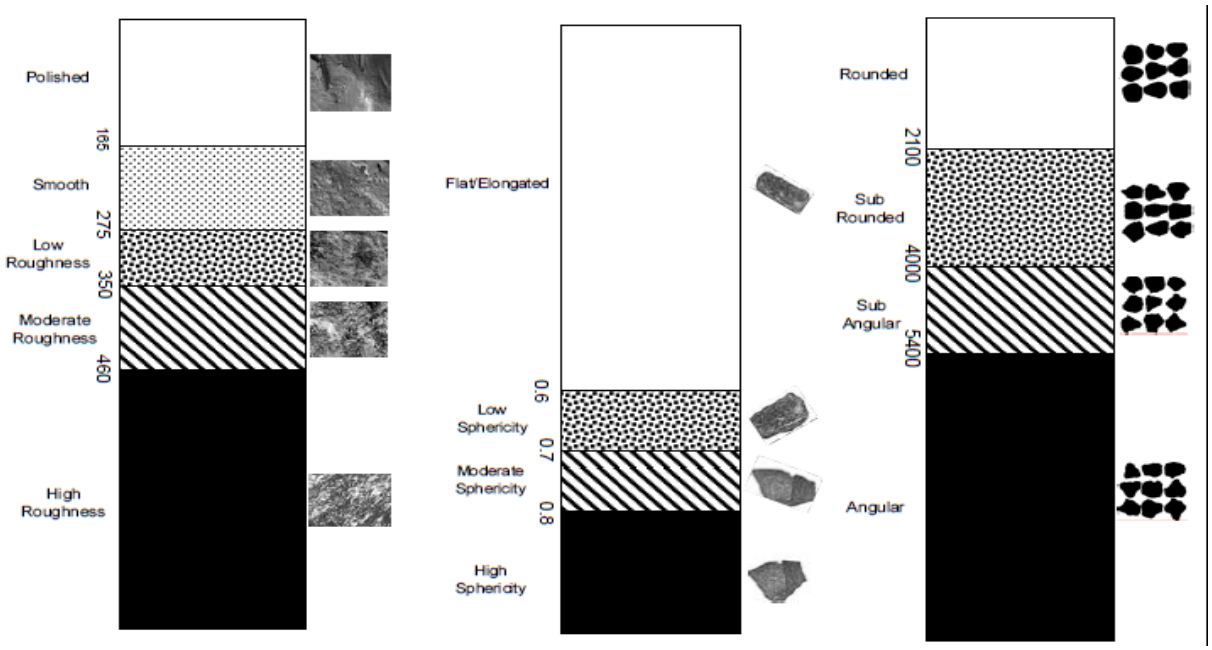

Figure 4.4 AIMS Classification for Texture, Sphericity and Angularity (FHWA, 2006)

A recent study carried out by the Texas Transportation Institute (TTI) sought to develop a predictive model for friction loss of pavement surfaces (Kassem et al., 2013). Specifically, the study demonstrated and validated the use of AIMS to evaluate the change in aggregate characteristics, after Micro-Deval abrasion and polishing (Kassem et al., 2013). Although the main objective of the TTI study was to develop a model for predicting friction loss of pavement surfaces, the study also determined that:

> "[The Micro-Deval test and AIMS] were found to be effective tools for evaluating the abrasion and degradation resistance of aggregates and quantifying the change in the shape characteristics respectively. Aggregates with good resistance to abrasion and polishing demonstrated better skid resistance compared to aggregates with poor resistance to abrasion and polishing. In

addition, mixtures with coarser aggregates gradation exhibited better skid resistance than those with finer aggregate gradation" (Kassem et al., 2013).

Another recent study carried out by Moaveni, Mahmoud, Ortiz, Tutumluer and Beshears (2014) "demonstrated the effectiveness and applicability of implementing advanced image analysis systems for practical and routine testing and quantification of aggregate shape property changes from standard Micro-Deval tests" (Moaveni et al., 2014). AIMS systems were used to capture the changes in shape and size properties of aggregate particles caused by Micro-Deval, simulating field degradation and polishing. Although the image acquisition and processing capabilities of the imaging systems used were different, both of the systems successfully quantified changes in morphological properties of particles from the Micro-Deval tests (Moaveni et al., 2014).

4.2.2 Aggregate Characteristics

Aggregate particles consist of a number of distinguishable geometric aspects, including form, angularity, and surface texture, which due to the difference in size scales, can be used for the purposes of ordering (Masad, 2005). "Any of the properties can vary widely without necessarily affecting the other two properties" (Masad, 2005). Form relates to variations in the proportions of the particle, angularity is associated with the variations at the corners superimposed on shape, and surface texture describes the irregularity of the surface at a "scale that is too small to affect the overall shape" (Masad, 2005). "For the case of coarse aggregate angularity,

there is a distinct difference between angularity and texture, both of which have different effects on performance" (Fletcher et al., 2003).

4.2.2.1 Texture Analysis

The AIMS has the capability to analyze the surface texture of aggregate that is related to friction performance, which is initiated by taking a grayscale image of the surface of the aggregate particle. The Wavelet method, detailed in the NCHRP Report 4-30, is used to determine surface texture (Masad, 2005). The wavelet analysis uses short, high-frequency basis functions and long, low-frequency basis functions to isolate fine and coarse variations in texture. The texture contents in all directions are given equal weight and the texture index is computed as the simple sum of squares of the detail coefficients at that particular resolution. The classifications of texture are shown in Figure 4.4.

4.2.2.2 Angularity Analysis

Aggregate angularity impacts friction performance. The gradient method "is based on the principle that at sharp corners of the image, the direction of the gradient vector changes rapidly, whereas it changes slowly along the outline of rounded particles" (Masad, 2003) and is used to analyze the black and white images (Chandan, 2002). The classifications of gradient angularity are shown in Figure 4.5.

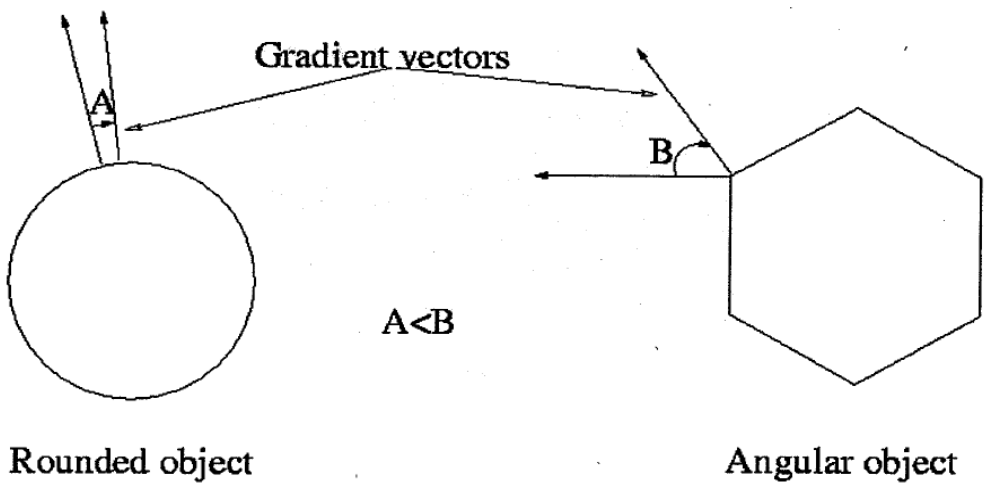

Figure 4.5 Illustration of Difference in Gradient Between Particles (Masad, 2003)

Angularity is calculated based on the values of angle of orientation of the edge points (θ) and the magnitude of the difference of these values (Δθ). The sum of the angularity index values for all the boundary points are accumulated around the edge to get angularity index.

4.2.2.3 Sphericity

Sphericity quantifies an aggregate's form using the three dimensions of the particle, which are the longest dimension (dL), the intermediate dimension (dI), and the shortest dimension (ds) and are used for sphericity and shape factor. A sphericity index of 1.0 denotes that a particle is a perfect sphere or cube while sphericity decreases as a particle becomes more flat and/or elongated. The classifications of sphericity are shown in Figure 4.4.

4.3 Aggregate Laboratory Testing Procedure and Results

4.3.1 Laboratory Testing Procedure

Laboratory testing involved Micro-Deval, LA Abrasion, and AIMS. The goal of the aggregate testing was to gain a better understanding of the impact that aggregate characteristics related to durability, hardness, angularity, shape, texture and polishing have on friction performance. All aggregate samples were washed and oven dried to a constant temperature. Once dry, testing was conducted on the aggregate samples.

4.3.1.1 Micro-Deval Test

Micro-Deval testing was conducted in accordance with the AASHTO T 327 (2012) “Resistance of Coarse Aggregate to Degradation by Abrasion in the Micro-Deval Apparatus”, and conducted on three replicates of each aggregate source, with the exception of the bauxite material, which was too small for the coarse gradation requirements.

A sample (Table 4.2 gradation in test procedure) of 1500 ± 5 g was then immersed in 2.0 ± 0.05 liters of tap water at a temperature of 20 ± 5 °C for a minimum of 1 hour in the Micro-Deval container. 5000 ± 5 g of stainless steel balls were then added to the sample in the Micro-Deval container and then rotated at 100 ± 5 rpm for 12,000 revolutions. The material was then sieved over the 4.75mm superimposed on the 1.18 mm sieve in accordance with AASHTO T 27 (2014) “Sieve Analysis of Fine and Coarse Aggregates”. The retained material was then combined and oven dried to constant mass at 110 ± 5 °C.

The Bauxite material was smaller than the AASHTO T 327 (2012) test gradations. Therefore, a modified Micro Deval procedure was used (MnDOT 2000, Rogers et al 1991). The modifications include preparing samples using sieve sizes from #4 to #200. The samples were saturated in tap water for a 24 ± 4 hours. The excess water was removed and the sample was placed in the Micro-Deval abrasion container with 1250 ± 5g of the stainless steel balls and 750 ± 25ml of tap water. The samples were run in the machine at 100 ± 5 rpm for 15 minutes ± 10 seconds. The samples were then washed over a 6.7mm (0.265”) sieve (to remove stainless steel balls) superimposed over a 75µm (#200) sieve until the washings became clear, being careful not to lose any retained 75µm (#200) material.

The oven-dried samples were then weighed and the Micro-Deval percentage loss was calculated using the test procedure equation of dividing the difference between pre-testing and post-testing mass by the pre-testing mass.

Upon completion of the Micro-Deval testing, the material was then washed, dried, sieved into separate size fractions, and then analyzed using AIMS (Rezaei et al., 2009; Fowler and Rached, 2012; Moaveni et al., 2014; Mahmoud and Masad, 2007). The AIMS methodology performed post Micro-Deval testing is provided in a subsequent section.

4.3.1.2 Los Angeles Abrasion

LA Abrasion testing was conducted in accordance with AASHTO T 96 (2010) “Resistance to Degradation of Small-Size Coarse Aggregate by Abrasion and Impact in the Los Angeles Machine”, and conducted on three replicates of each treated and untreated samples. Material was washed and oven dried at 110 ± 5 °C to

substantially constant mass and separated into individual size fractions. The material was then recombined to meet the “Grading B” requirements.

A sample of 5000 ± 10 g was placed in the Los Angeles testing machine along with 11 steel spheres averaging 46.8 mm. The aggregate and steel spheres were then rotated at a speed of 30 to 33 revolutions/minute for a total 500 revolutions. The material was then sieved on the 1.70 mm sieve in accordance with AASHTO T 27 (2014) “Sieve Analysis of Fine and Coarse Aggregates”. The retained material was then combined and oven dried to constant mass at 110 ± 5 °C. The oven-dried sample was then weighed and the LA Abrasion percentage loss was calculated using Equation 4.5.

4.3.1.3 Aggregate Imaging System

The AIMS system was used to analyze aggregate samples both before Micro-Deval testing and after Micro-Deval testing. Testing was carried out in accordance with AASHTO PP64-11-2013 "Determining Aggregate Source Shape Values from Digital Image Analysis Shape Properties". Post Micro-Deval AIMS analysis was conducted on the samples for different size fractions depending upon what the Micro Deval procedure yielded. However, each Micro-Deval sample yields an adequate AIMS sample size (n=56) for analysis.

Before conducting the image acquisition, the AIMS system was calibrated. Individual aggregate particles were then placed on the locations marked on the aggregate tray. The AIMS software was set to collect black and white images and the computer-automated acquisition ran again. Once images had been collected, the

software analysis was run before beginning the next sample. This process was conducted for each of the different size fraction samples.

4.3.2 Laboratory Testing Results

Current aggregate testing methods provide insightful results that “can be considered as basic guidance in establishing friction performance-related test criteria” (NCHRP, 2009). However, the results must be considered in context and in conjunction. “Just as no single test can distinguish good friction performance from bad, no single test value can be used as a standard for the same purpose. The factors that influence friction performance do so in an interactive manner and on a continuous scale, making it difficult to pinpoint specific discrimination values” (NCHRP, 2009). Additionally, “it is impossible to obtain a 1:1 correlation between friction measuring devices [because] different testers measure different aspects of pavement friction” (Lu and Steven, 2006). Therefore, this section does not attempt to show correlation, but only highlights trends in data resulting from the various methods. Data is provided for the sole purpose of comparative analysis for field pavement treatment results.

4.3.2.1 Micro-Deval, LA Abrasion and AIR Results

Table 4.2 shows the average LA Abrasion and Micro-Deval values for the aggregate sources, but also shows the insoluble residue results provided by ODOT. LA Abrasion test specification in these applications is either less than or equal to 30% or 40% depending on the aggregate’s use. Therefore, all aggregate sources in Table 4.2 would be accepted for use. The acid insoluble residue results show that

the sources are well above the minimum requirement when using a criterion of 60% (Fowler and Rached, 2012).

Table 4.2 Micro-Deval, LA Abrasion, and AIR Results

Source	**Type**	**LA Abrasion** (average %)	**Micro Deval** (average %)	**Insoluble Residue** (average, per ODOT)
Martin Marietta Snyder	Granite	18.3	2.8	99.0
Martin Marietta Mill Creek	Granite	20.7	7.1	99.7
Hanson Davis	Rhyolite	12.0	8.2	96.6
Martin Marietta Sawyer	Sandstone	19.7	7.0	99.9
APAC Spiro	Sandstone	29.4	21.9	97.9
APAC Central 14 (AR)	Sandstone	25.5	11.2	97.0
APAC Pawhuska	Limestone	21.9	16.7	N/A
Dolese Davis	Limestone	24.0	15.1	N/A
Dolese Hartshorne	Limestone	15.7	9.8	N/A
Dolese Richard Spur	Limestone	20.7	14.1	N/A
Quapaw Drumright	Dolomite	17.6	12.1	Not provided
Flint Rock	Mine Chat	Too fine for test procedure	1.7	Not provided
Imported	Bauxite	Too fine for test procedure	4.8	Not provided

Differing mass loss limits have been established for Micro Deval with regard to expected friction performance. Figure 4.6 illustrates the results from this study and the following list describes the mass loss limits:

- 25% Limit: While ODOT does not specify Micro-Deval for preservation treatments, it does use a standard of less than or equal to 25% allowable

percentage loss for other applications (such as Superpave). All of the aggregate types shown in this study meet specification.

- 18% Limit: Wu et al (1998) found that Micro Deval percentage loss of 18% or greater indicates “poor” aggregate quality. Only one sandstone aggregate evaluated in this study would be considered “poor quality” with regard to expected friction performance, as shown in Figure 4.6.
- 15% Limit: NCHRP Report No. 557 sets a limit of 15% for surface course aggregate (White et al., 2006). One sandstone and two limestone aggregates in this study would not be permitted in the pavement treatments using this limit, as shown in Figure 4.6.
- 12% Limit: Good friction performance has also been correlated with aggregates that exhibit Micro-Deval weight loss values of 12% or less (Fowler and Rached, 2012). Therefore, the results indicate that 5 of the 13 sources may not yield the expected friction performance.

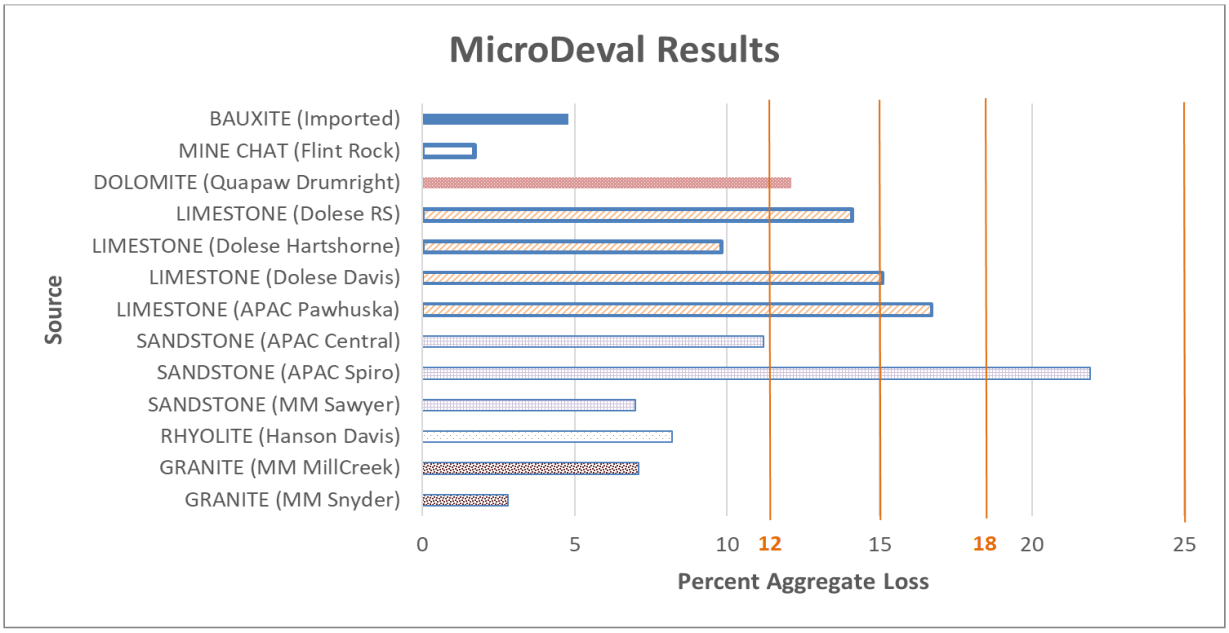

Figure 4.6 Micro Deval Results and Mass Loss Limits

It is important to note that LA Abrasion is an empirical test and therefore a poor predictor of field performance (Wu et al., 1998). Additionally, the Micro-Deval test has been found to better simulate the field conditions of aggregate abrasion compared to the dry conditions of the LA Abrasion test (Rogers, 1998). Previous research has also shown there is no correlation in aggregate percentage loss between the Micro-Deval and the LA Abrasion tests (Kandhal and Parker, 1998; Cooley and James, 2003), which is also the case in this study, demonstrated by the data contained in Table 4.2. Essentially, Micro-Deval tends to polish the aggregate, whereas LA Abrasion tends to break it.

4.3.2.2 AIMS Texture Results

AIMS data can provide insight about an aggregate's ability to enhance a pavement treatment's friction characteristics (FHWA, 2006). This section provides

the preliminary results of the AIMS laboratory testing (i.e. texture, angularity, sphericity) for the aggregates featured in the project's monitored pavement treatments.

Table 4.3 provides the descriptive statistics in tabular form for the AIMS texture of aggregate samples, ordered by percent change in texture due to exposure to Micro Deval testing. The pre- and post-MicroDeval data contained in Table 4.3 are consistent with the nominal maximum aggregate size (NMAS) of the field treatments being investigated in this study. AIMS profiles (pre- and post-Micro Deval) for each aggregate type are provided in subsequent figures and in tabular form in the Appendix A.

Table 4.3 Statistics for AIMS Texture (Pre- and Post-Micro Deval)

Source	Type	Mean (Pre MD)	Std. dev. (Pre MD)	Mean (Post MD)	Std. dev. (Post MD)	% change
APAC Central 14 (AR)	Sandstone	195.1	44.4	225.9	51.3	+7.3
APAC Spiro	Sandstone	154.7	25.6	146.6	25.4	-2.7
Dolese Hartshorne	Limestone	237.2	79.6	215.1	70.3	-4.9
Martin Marietta Sawyer	Sandstone	145.0	54.9	122.2	43.9	-8.5
Hanson Davis	Rhyolite	213.9	72.5	178.9	68.7	-8.9
MM Mill Creek	Granite	246.4	102.7	202.2	70.6	-9.9
Quapaw Drumright	Dolomite	222.2	57.0	179.8	45.3	-10.5
Flint Rock	Mine Chat	102.6	65.6	74.3*	46.4	-16.0
Dolese Richard Spur	Limestone	239.7	108.3	148.6	59.6	-23.5
APAC Pawhuska	Limestone	282.3	128.1	166.3	92.7	-25.9
Martin Marietta Snyder	Granite	461.9	94.1	254.2*	47.9	-29.0
Dolese Davis	Limestone	240.8	76.1	130.6	55.1	-29.7
Imported *	Bauxite	NA	NA	NA	NA	NA

* NA: Too fine for procedure

The sandstone sources in Eastern Oklahoma/Arkansas are positioned at the top of the list with regard to percent change, with APAC Central (AR) material

increasing in texture and APAC Spiro decreasing only slightly in texture. However, the sandstone sources and the mine chat had the least amount of texture initially. The granite samples from Martin Marietta Snyder had the most texture, both pre- and post-Micro Deval (a statistically significant difference), although it exhibited one of the greatest rates of change. There was a statistically significant difference in post-MicroDeval texture for mine chat; it exhibited the least amount of texture of all samples.

Figure 4.7 shows the interval plot of the pre-MicroDeval data. The pooled standard deviation was used to calculate the intervals. The graphs show similar trends in texture, which will be described in further detail in this section.

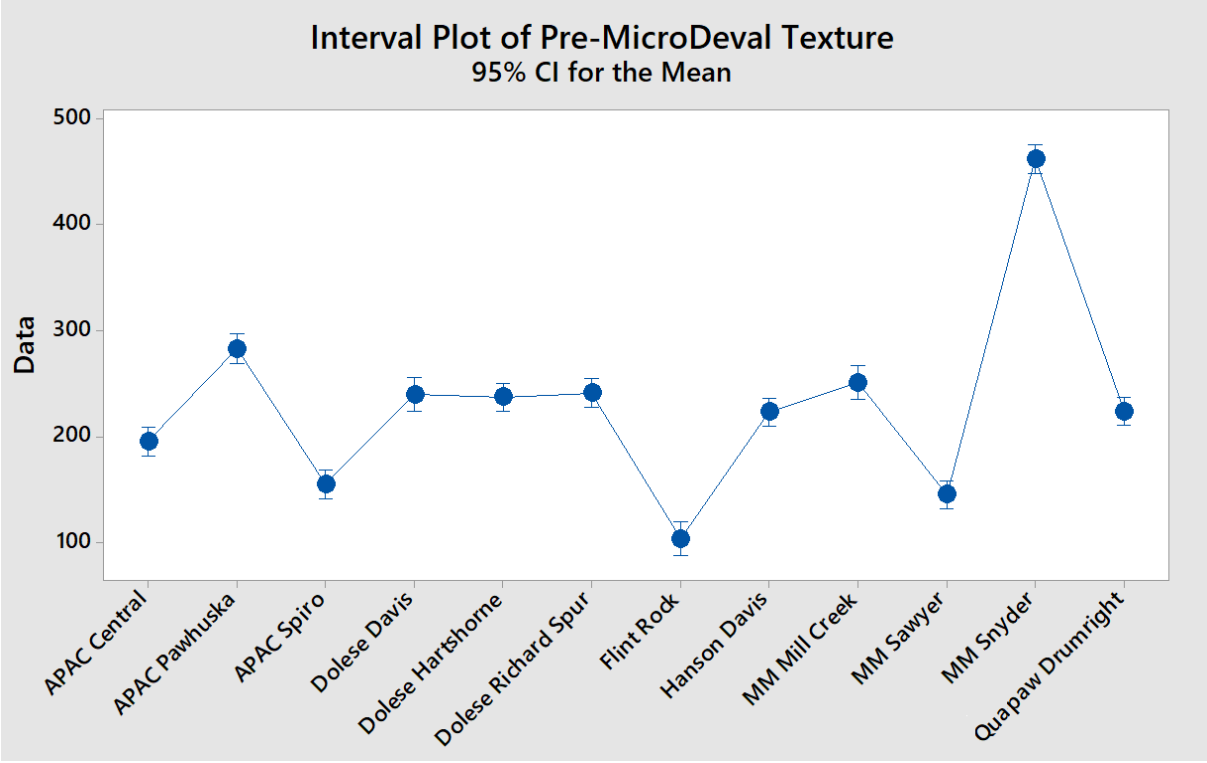

Figure 4.7 Interval Plot of AIMS Texture (Pre-MicroDeval)

Additionally, a comparison of means was conducted to determine the differences between sources regarding pre-MicroDeval texture using Tukey's Pairwise Comparison Method at a 95% confidence level. Means that do not share a letter are significantly different. As noted in the previous paragraph, the MM Snyder material (denoted by the "A" grouping in Table 4.4) and Flint Rock material (denoted by the "F" grouping) exhibit statistically significant differences than all of the other sources.

Table 4.4 Grouping of AIMS Texture using the Tukey Method (95% Confidence) (Pre-MicroDeval)

Source	Type	A	B	C	D	E	F
MM Snyder	Granite	A					
APAC Pawhuska	Limestone		B				
MM Mill Creek	Granite		B	C			
Dolese Richard Spur	Limestone			C			
Dolese Davis	Limestone			C			
Dolese Hartshorne	Limestone			C			
Quapaw Drumright	Dolomite			C	D		
Hanson Davis	Rhyolite			C	D		
APAC Central 14 (AR)	Sandstone				D		
APAC Spiro	Sandstone					E	
MM Sawyer	Sandstone					E	
Flint Rock	Mine Chat						F

Figure 4.8 shows the pre-MicroDeval texture output for the aggregate sources contained in the pavement treatments with 1/2” NMAS material. Research has been conducted regarding the validity of AIMS1 (equipment used in this study) and AIMS2 [“new generation AIMS” (FHWA, 2011)] output and correlation. A recent study showed that AIMS1 and AIMS2 “provided similar ranking of aggregates and comparable results” (FHWA, 2011). However, AIMS1 texture indices have been shown to trend slightly lower (polish values higher) than AIMS2 texture indices based upon results of previous studies by these researchers. Aggregates that have higher polished face values are not as desirable for use in pavement treatments; therefore, the AIMS1 results may appear slightly less favorable than AIMS2 results with regard to texture. Care should be exercised when interpreting the AIMS1 data in this section. The researchers are considering only relative differences and trends in texture for the purpose of comparing field performance of pavement treatments containing the given aggregates, which suits the purpose of this research.

In general, a greater aggregate surface texture should result in better friction performance (Fowler and Rached, 2012). A texture value of 460 or greater indicates high surface texture, whereas a value below 165 indicates a polished particle (FHWA, 2006).

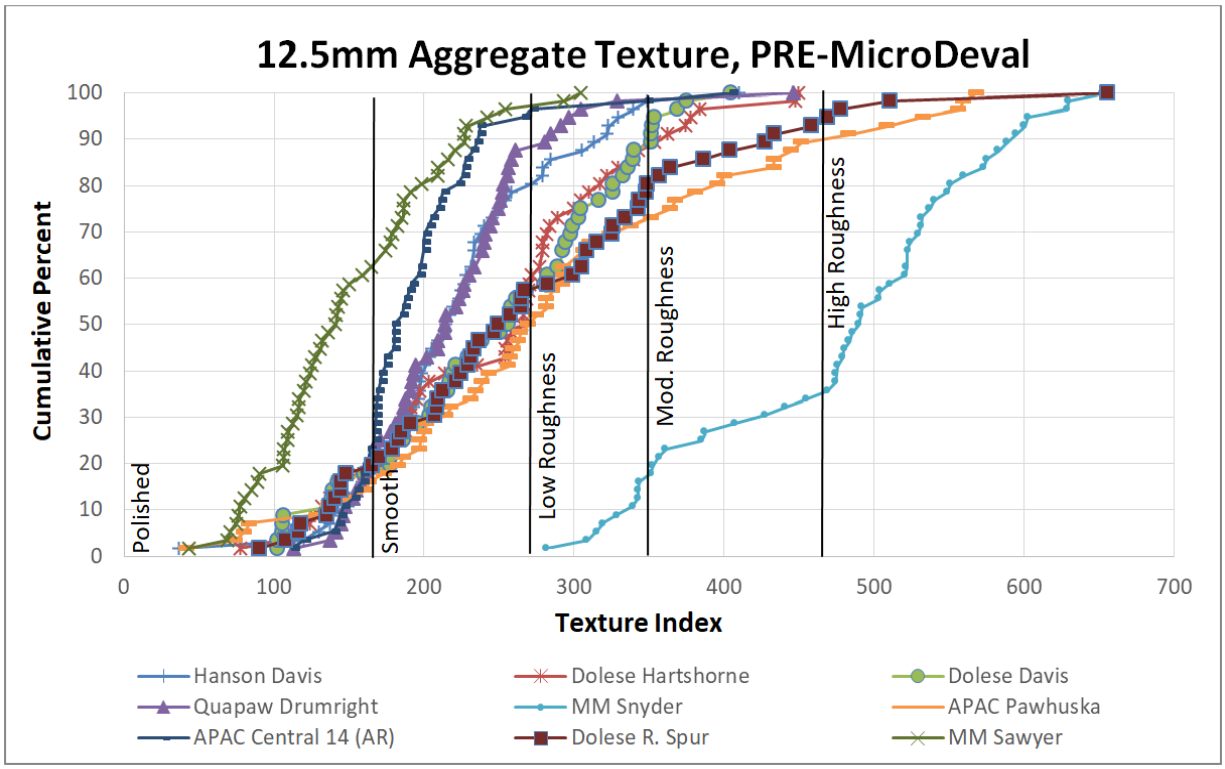

Figure 4.8 AIMS Texture Results for 12.5mm Aggregate(Pre-MicroDeval)

Pre-MicroDeval texture indices for the 12.5-NMAS treatments range from approximately 40 to 650. The sandstone from MM Sawyer exhibits the least amount of texture while the granite from MM Snyder has the most texture (Figure 4.8). Results for aggregate from remaining sources indicate that 20% of surfaces are polished. The dolomite (Quapaw Drumright) and rhyolite (Hanson Davis) trend together. The limestone sources (Dolese and APAC Pawhuska) also share general trends.

Table 4.5 provides the pre-MicroDeval texture results for the aggregates contained in the pavement treatments with NMAS ranging from No.4 to 9.5mm. AIMS cannot capture texture data for fine aggregate, so there is no data for the bauxite material. These data are presented separately because different sizes may

have different characteristics and/or show the limitations of AIMS as aggregate particles decrease. Therefore, one must be judicious about comparing aggregate sources of different NMAS. For example, the 12.5-mm MM Mill Creek material in Table 4.4 exhibits a greater mean than many of the other aggregates and would not trend consistently with the No.4 material shown in Table 4.5. Therefore, for the purposes of this study, the data are provided to evaluate any trending with field pavement treatment performance and are not compared in this section. Related graphs are provided in the Appendix A.

Table 4.5 AIMS Results for Other NMAS Aggregates (Pre-MicroDeval Texture)

Source	**Type**	**NMAS**	**Polished (< 165)** Percent	**Smooth (165 – 275)** Percent	**Low Roughness (275 – 350)** Percent	**Mod. Roughness (350 – 460)** Percent	**High Roughness (> 460)** Percent
APAC Spiro	Sandstone	9.5mm	70	29	1	0	0
Flint Rock	Mine Chat	6.3mm	85	13	2	0	0
MM Mill Creek	Granite	No.4	65	25	6	4	0
Imported *	Bauxite	No.8	NA	NA	NA	NA	NA

* NA – too small for procedure

Figure 4.9 and Table 4.6 show the post-MicroDeval texture using Tukey's Pairwise Comparison Method at a 95% confidence level. Again, the MM Snyder material (denoted by the "A" grouping in Table 4.6) and Flint Rock material (denoted by the "H" grouping) exhibit statistically significant differences than all of the other sources.

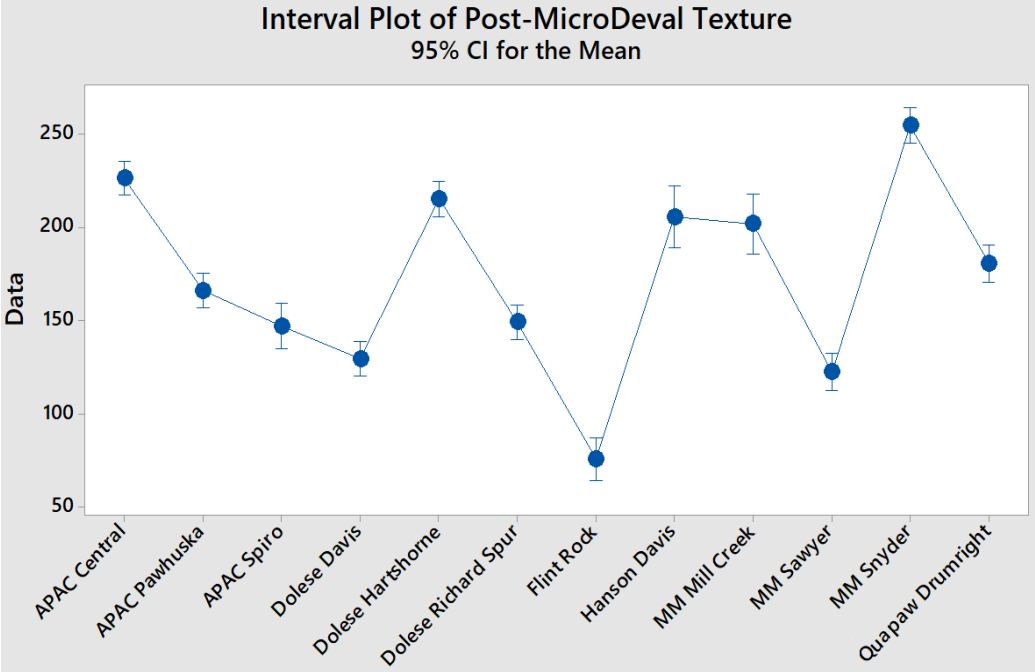

Figure 4.9 Interval Plot of AIMS Texture (Post-MicroDeval)

Figure 4.10 shows the post-MicroDeval texture output for the aggregate sources contained in the pavement treatments with 12.5mm-NMAS material. The results indicate that most of the material becomes classified as polished or smooth after exposure to abrasion. A statistically significant difference exists in data for the granite aggregate sources, the APAC Central (AR) and Dolese Hartshorne material, indicating that these materials may provide an increased level of surface friction and adhesion.

The rhyolite and granite were expected to be more resistant to impact and abrasion than the limestone and sandstone. However, Micro Deval and LA Abrasion results are mixed (Table 4.2). The Micro Deval results show that a limestone source (Dolese Hartshorne) and a sandstone source (APAC Central) was similarly resistant to abrasion as the rhyolite. The AIMS results based upon sphericity in the next

section indicate that the Dolese and APAC material are more cubical in shape and exhibit a lower flat-elongated ratio than did the Hanson rhyolite and MM granite material, which contributes to its impact resistance. Therefore, the shape of the limestone and sandstone particles may compensate for its lower impact resistance.

Table 4.6 Grouping of AIMS Texture using the Tukey Method (95% Confidence) (Post-MicroDeval)

Source	Type	A	B	C	D	E	F	G	H
MM Snyder	Granite	A							
APAC Central 14 (AR)	Sandstone		B						
Dolese Hartshorne	Limestone		B						
Hanson Davis	Rhyolite		B	C					
MM Mill Creek	Granite		B	C					
Quapaw Drumright	Dolomite			C	D				
APAC Pawhuska	Limestone				D	E			
Dolese Richard Spur	Limestone					E	F		
APAC Spiro	Sandstone					E	F	G	
Dolese Davis	Limestone						F	G	
MM Sawyer	Sandstone							G	
Flint Rock	Mine Chat								H

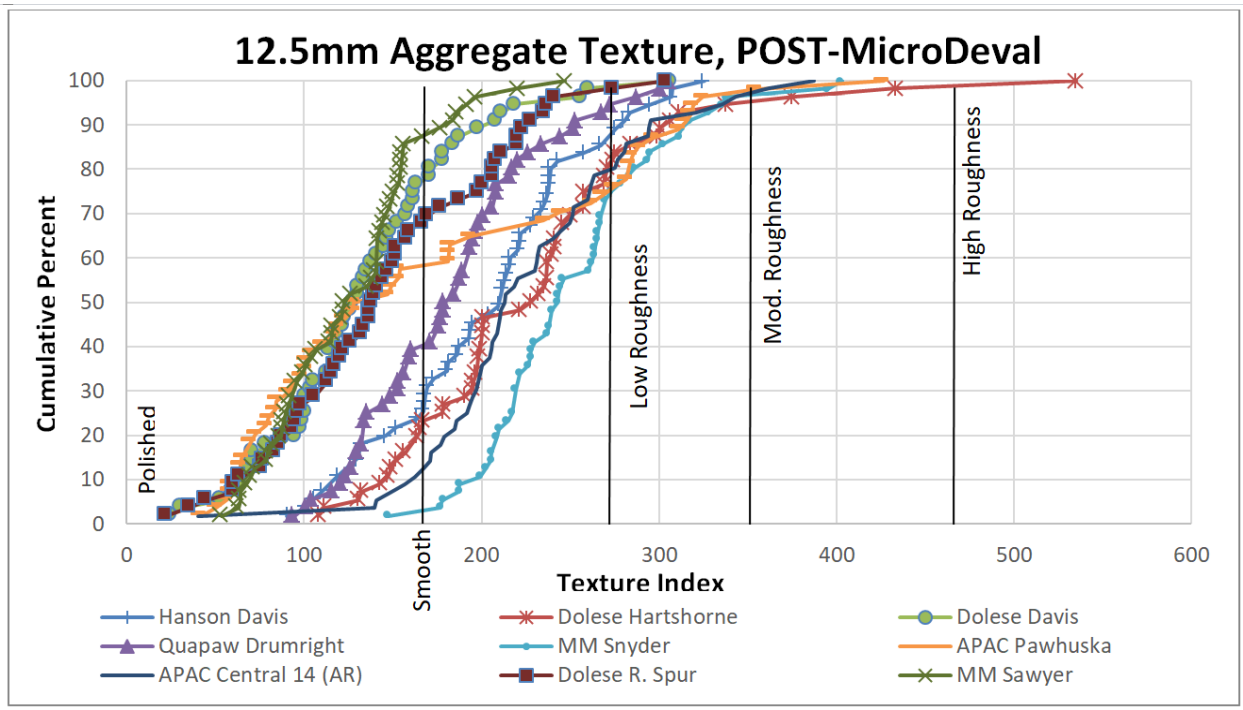

Figure 4.10 AIMS Texture Results for 12.5mm Aggregates (Post-MicroDeval)

Table 4.7 provides the post-MicroDeval texture results for the aggregates contained in the pavement treatments with NMAS ranging from No.4 to 9.5mm. These data show that the material became classified mostly as polished, some as smooth, as a result of exposure to abrasion. Related graphs are provided in the Appendix A.

Table 4.7 AIMS Texture Results for Other NMAS Aggregates (Post-MicroDeval)

Source	Type	NMAS	Polished (< 165)	Smooth (165 – 275)	Low Roug. (275 – 350)	Mod. Roug. (350 – 460)	High Roug. (> 460)
APAC Spiro	Sandstone	9.5mm	73	27	0	0	0
Flint Rock	Mine Chat	6.3mm	93	7	0	0	0
MM Mill Creek	Granite	No.4	90	10	0	0	0
Imported *	Bauxite	No.8	NA	NA	NA	NA	NA

* NA – too small for procedure

4.3.2.3 AIMS Angularity Results

Table 4.8 provides the descriptive statistics in tabular form for the AIMS angularity of aggregate samples, ordered by percent change in angularity due to exposure to Micro Deval testing. The pre- and post-MicroDeval data contained in the table are consistent with the nominal maximum aggregate size of the field treatments being investigated in this study. AIMS profiles (pre- and post-Micro Deval) for each aggregate type are provided in subsequent figures and in tabular form in the Appendix A.

As expected, the granite, bauxite, rhyolite and mine chat materials have the least amount of change in angularity after exposure to abrasion. The sandstones, limestones and dolomite exhibited the most change.

Figure 4.11 and Table 4.9 show the pre-Micro Deval angularity data (gradient method). The pooled standard deviation was used to calculate the intervals. Although the angularity of the bauxite increased after exposure to abrasion, it had the least amount of angularity initially. MM Snyder and Flint Rock Mine Chat exhibited the highest level of angularity post abrasion. The means of all materials are generally closely grouped. The AIMS angularity profiles for the 12.5mm-NMAS materials, shown in Figure 4.12, also show a similar grouping. Even before abrasion, most of the materials exhibit a “sub-rounded” angularity, including the other NMAS materials shown in Table 4.10.

Table 4.8 AIMS Descriptive Statistics for Angularity (Pre- & Post-Micro Deval)

Source	**Type**	**Mean** (Pre MD)	**Std. dev.** (Pre MD)	**Mean** (Post MD)	**Std. dev.** (Post MD)	**% change**
Martin Marietta Snyder	Granite	3189.0	1095.4	3416.6	1888.2	+3.4
Imported	Bauxite	1998.1	514.5	2139.4	544.5	+3.4
Hanson Davis	Rhyolite	3263.1	1085.2	3113.2	1734.1	-2.4
Flint Rock	Mine Chat	3431.1	954.2	3265.4	1197.0	-2.5
Martin Marietta Sawyer	Sandstone	3156.6	1079.7	2635.4	1654.2	-9.0
APAC Pawhuska	Limestone	2777.3	1006.3	2106.2	1290.4	-13.7
APAC Spiro	Sandstone	2946.9	1322.8	2219.9	1794.6	-14.1
Dolese Richard Spur	Limestone	3247.0	906.1	2403.5	1266.0	-14.9
Dolese Davis	Limestone	3509.6	1723.9	2593.5	1479.3	-15.0
Dolese Hartshorne	Limestone	3227.5	1071.5	2361.2	1170.0	-15.5
MM Mill Creek	Granite	3636.5	1481.1	2609.3	678.3	-16.4
APAC Central 14 (AR)	Sandstone	3430.1	1564.8	2383.9	1079.3	-18.0
Quapaw Drumright	Dolomite	3167.2	1428.9	1999.5	962.2	-22.6

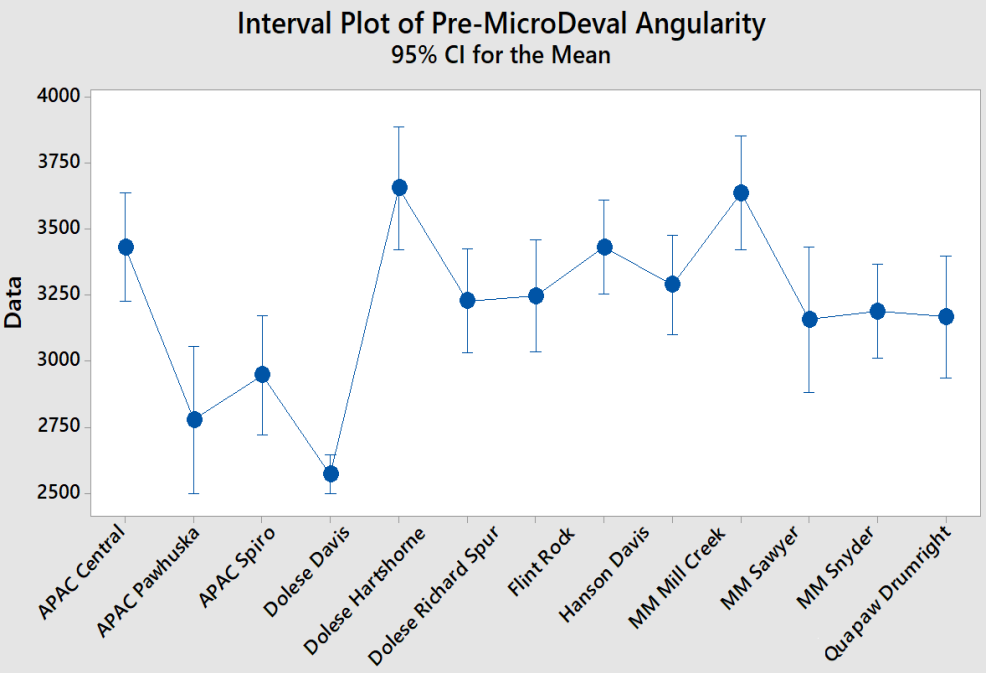

Figure 4.11 Interval Plot of Aggregate Angularity (Pre-MicroDeval)

Table 4.9 Grouping of Aggregate Angularity using the Tukey Method (95% Confidence) (Pre-MicroDeval)

Source	Type	A	B	C	D
Dolese Davis	Limestone	A			
MM Mill Creek	Granite	A			
Flint Rock	Mine Chat	A	B		
APAC Central 14 (AR)	Sandstone	A	B		
Hanson Davis	Rhyolite	A	B	C	
Dolese Richard Spur	Limestone	A	B	C	
Dolese Hartshorne	Limestone	A	B	C	
MM Snyder	Granite	A	B	C	
Quapaw Drumright	Dolomite	A	B	C	
MM Sawyer	Sandstone	A	B	C	
APAC Spiro	Sandstone		B	C	D
APAC Pawhuska	Limestone			C	D
Imported	Bauxite				D

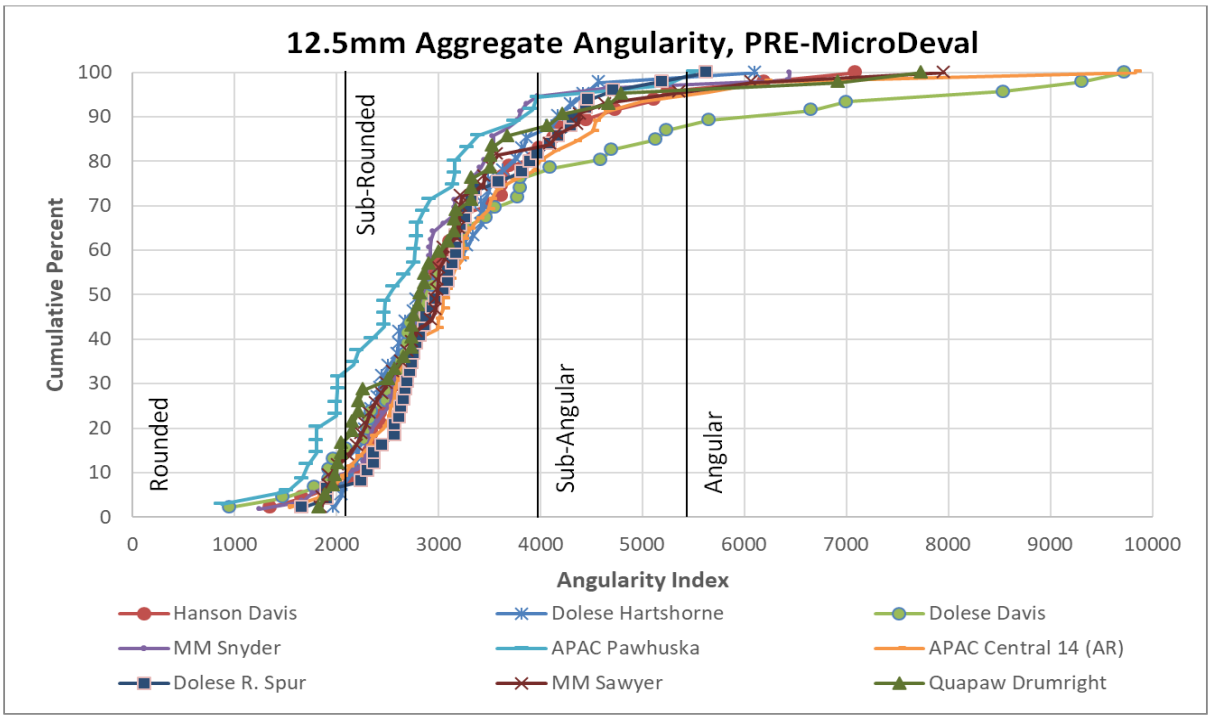

Figure 4.12 AIMS Angularity Results for 12.5mm Aggregate (Pre-MicroDeval)

Table 4.10 AIMS Angularity Results for Other NMAS Aggregates (Pre-MicroDeval)

Source	**Type**	**NMAS**	**Rounded (< 2100)** Percent	**Sub-Rounded (2100 - 4000)** Percent	**Sub-Angular (4000 - 5400)** Percent	**Angular (> 5400)** Percent
APAC Spiro	Sandstone	9.5mm	37	48	2	13
Flint Rock	Mine Chat	6.3mm	5	75	17	3
MM Mill Creek	Granite	No.4	3	65	26	6
Imported	Bauxite	No.8	27	68	4	1

Figure 4.13, Table 4.11 and Table 4.12 show the post-Micro Deval angularity data (gradient method). The pooled standard deviation was used to calculate the intervals for 12.5 NAMS and other aggregates.

Table 4.11 Grouping of AIMS Angularity using the Tukey Method (95% Confidence) (Post-MicroDeval)

Source	Type	A	B	C	D	E
Flint Rock	Mine Chat	A				
MM Snyder	Granite	A	B			
Hanson Davis	Rhyolite	A	B	C		
MM Sawyer	Sandstone		B	C		
MM Mill Creek	Granite		B	C		
Dolese Davis	Limestone		B	C		
Imported	Bauxite			C	D	
Dolese Richard Spur	Limestone			C	D	E
APAC Central 14 (AR)	Sandstone			C	D	E
Dolese Hartshorne	Limestone			C	D	E
APAC Spiro	Sandstone			C	D	E
APAC Pawhuska	Limestone				D	E
Quapaw Drumright	Dolomite					E

Table 4.12 AIMS Angularity Results for Other NMAS Aggregates (Post-MicroDeval)

Source	Type	NMAS	Rounded (< 2100) Percent	Sub-Rounded (2100 - 4000) Percent	Sub-Angular (4000 - 5400) Percent	Angular (> 5400) Percent
APAC Spiro	Sandstone	9.5	70	27	0	3
Flint Rock	Mine Chat	6.3mm	10	72	13	5
MM Mill Creek	Granite	No.4	14	64	9	13
Imported	Bauxite	No.8	34	63	2	1

In general, a more durable aggregate should exhibit lower mass loss, greater retention of angularity, and better friction performance (Fowler and Rached, 2012). There is a correlation between abrasion and polishing resistance, especially for aggregate that is highly susceptible to abrasion (Lancieri, 2005). When aggregate angularity is reduced, the aggregate becomes more susceptible to polishing.

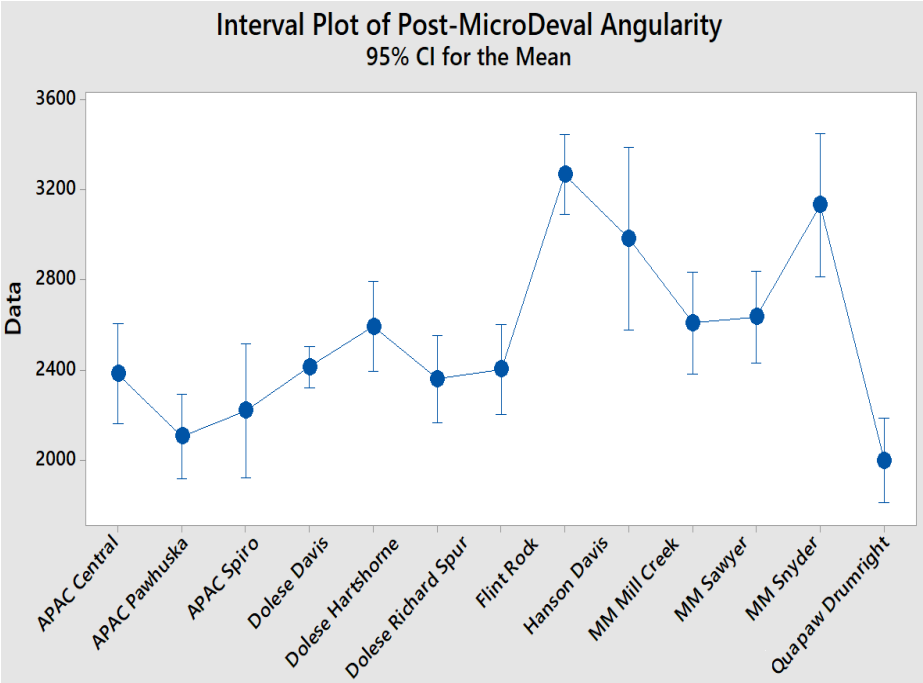

Figure 4.13 Interval Plot of AIMS Angularity (Post-MicroDeval)

An angularity value of 4,000 or above indicates a sub-angular to angular particle, whereas a value below 2,100 indicates a rounded particle (FHWA, 2006). Rounded particles are more susceptible to slide laterally on hot summer days under heavy traffic, which increase the rutting potential certain pavement treatments. The gradient angularity indices can provide insight about the roundedness of particles. Figure 4.14 shows gradient angularity indices output for the 12.5mm-NMAS aggregate. The indices for all of the tested particles in the sample range from 240 to

9000. After exposure to the abrasion, the data is more loosely grouped. About 75% of the Quapaw dolomite material became classified as “rounded”, whereas about 18% of the MM Snyder granite material was classified as “rounded”, indicated by an angularity index of less than 2100. Results did not exhibit a statistically significant difference between the dolomite material and most of the limestones and sandstones, therefore, those materials should contribute the same level of friction performance based on this AIMS parameter.

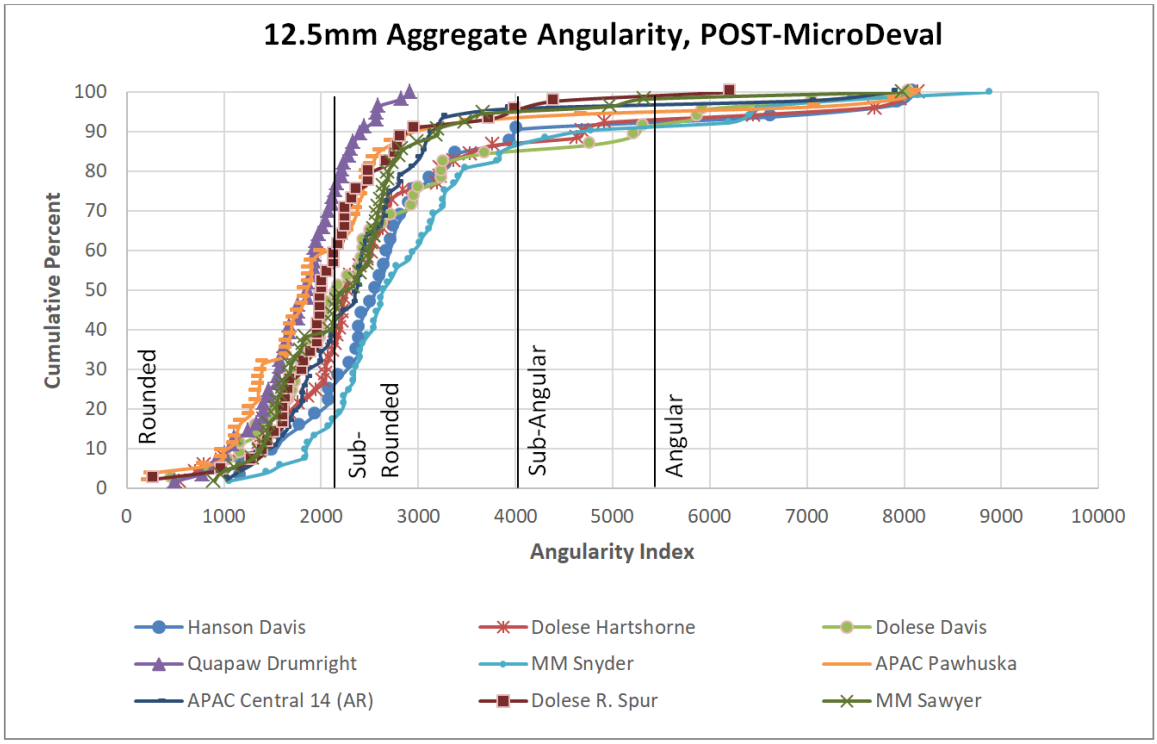

Figure 4.14 AIMS Angularity Results for 12.5mm Aggregate (Post-MicroDeval)

4.3.2.4 AIMS Sphericity

Table 4.13 provides the descriptive statistics in tabular form for the AIMS sphericity of aggregate samples, ordered by percent change in angularity due to exposure to Micro Deval testing. The pre- and post-MicroDeval data contained in the table are consistent with the nominal maximum aggregate size of the field treatments being investigated in this study. AIMS profiles (pre- and post-Micro Deval) for each aggregate type are provided in subsequent figures and in tabular form in the Appendix A.

Table 4.13 Descriptive Statistics of AIMS Sphericity (Pre- and Post-Micro Deval)

Source	**Type**	**Mean** (Pre MD)	**Std. dev.** (Pre MD)	**Mean** (Post MD)	**Std. dev.** (Post MD)	**% change**
Dolese Hartshorne	Limestone	0.646	0.142	0.785	0.087	+9.7
Martin Marietta Snyder	Granite	0.611	0.099	0.669	0.114	+4.5
Martin Marietta Sawyer	Sandstone	0.568	0.098	0.591	0.110	+2.0
Flint Rock	Mine Chat	0.696	0.135	0.714	0.144	+1.3
Dolese Davis	Limestone	0.690	0.112	0.681	0.123	+0.7
Dolese Richard Spur	Limestone	0.592	0.097	0.596	0.102	+0.3
Hanson Davis	Rhyolite	0.635	0.093	0.604	0.102	-2.5
APAC Central 14 (AR)	Sandstone	0.719	0.101	0.654	0.099	-4.7
APAC Spiro	Sandstone	0.711	0.074	0.644	0.100	-4.9
APAC Pawhuska	Limestone	0.697	0.074	0.628	0.112	-5.2
Quapaw Drumright	Dolomite	0.701	0.105	0.595	0.103	-8.2
MM Mill Creek	Granite	0.777	0.081	0.524	0.120	-19.4
Imported	Bauxite	Too fine for procedure				

The Dolese Hartshorne material exhibited the greatest positive change in sphericity and the greatest mean while the MM Mill Creek material exhibited the greatest negative change due to exposure to abrasion. Therefore, the Dolese Hartshorne material, although limestone, may be less prone to breakage under traffic due to its shape than the other materials, which may explain its MicroDeval results as well (Table 4.2).

Sphericity is a relative measure of aggregate shape with the greatest value denoting a cubical particle, the desired aggregate shape. Surface treatment aggregate can protect a pavement treatment from traffic wear, therefore, a high sphericity index is desirable (>0.80). Flat and elongated particles exhibit an index of 0.60 or less. Figure 4.15, Figure 4.16, Table 4.14 and 4.15 show AIMS output for sphericity. The Dolese Hartshorne, Dolese Davis and APAC Central material have the greatest sphericity both pre- and post-MicroDeval exposure. Approximately 80% of the other 12.5mm-NMAS materials are classified as low sphericity and flat/elongated after being exposed to MicroDeval abrasion.

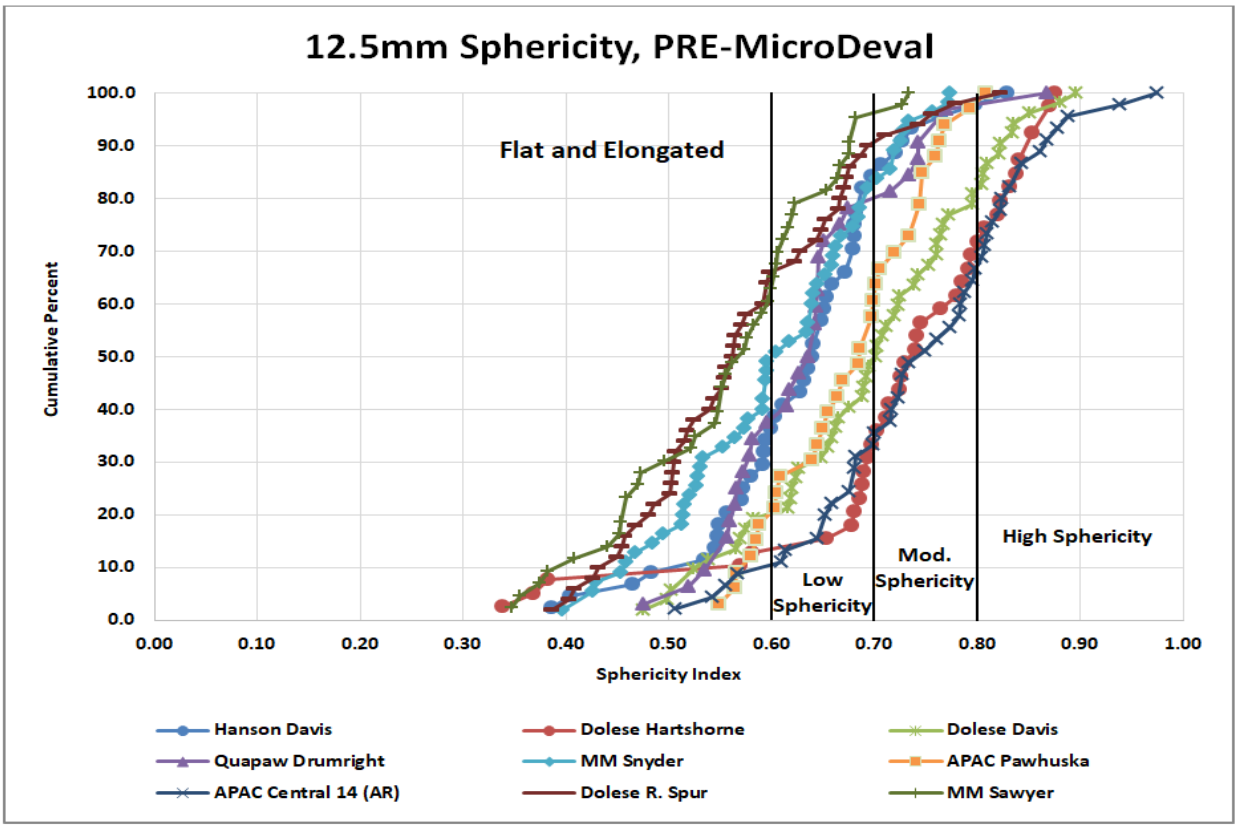

Figure 4.15 AIMS Sphericity Results for 12.5mm Aggregate (Pre-MicroDeval)

More than 70% of the mine chat sample is classified as having sphericity, both pre- and post-MicroDeval exposure (Table 4.14 and Table 4.15). Fifty percent of the APAC Spiro material was considered to be flat and elongated prior to abrasion exposure, which may explain the greater mass loss exhibited.

Table 4.14 AIMS Sphericity Results for Other NMAS Aggregates (Pre-MicroDeval)

Source	Type	NMAS	Flat/Elongated (< 0.6) Percent	Low Sphericity (0.6 – 0.7) Percent	Moderate Sphericity (0.7 – 0.8) Percent	High Sphericity (> 0.8) Percent
APAC Spiro	Sandstone	9.5mm	50	30	17	3
Flint Rock	Mine Chat	6.3mm	27	17	32	24
MM Mill Creek	Granite	No.4	39	35	22	4
Imported	Bauxite	No.8	Too small for procedure			

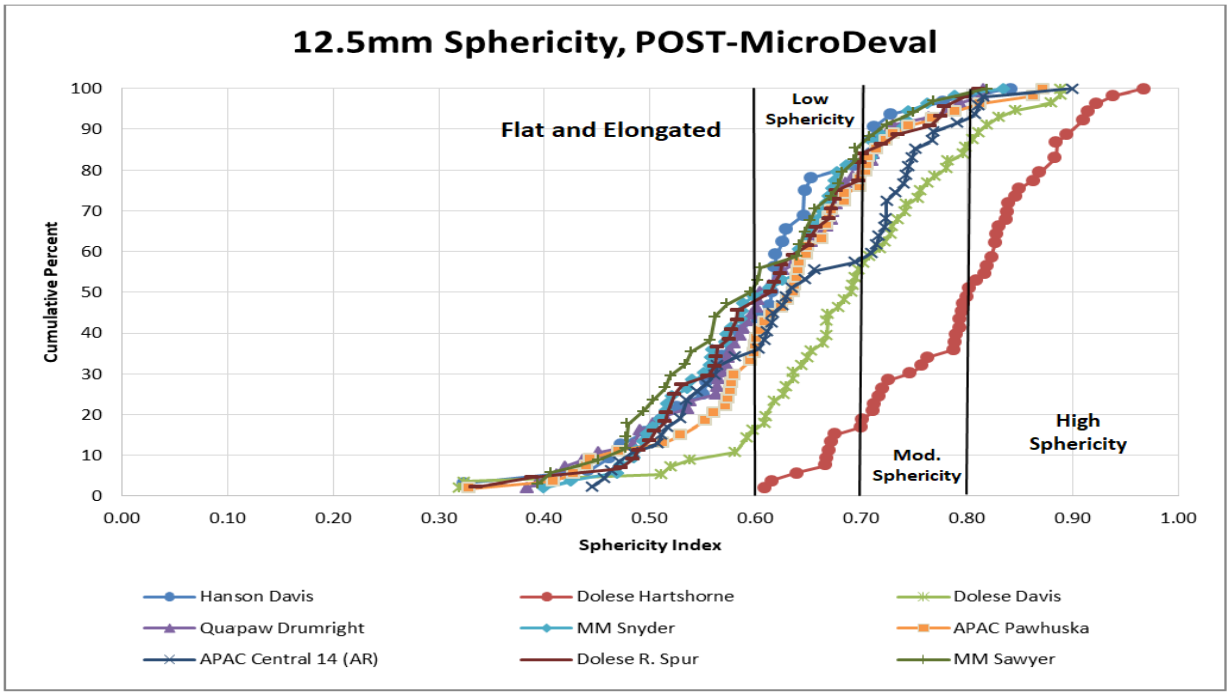

Figure 4.16 AIMS Sphericity Results for 12.5mm Aggregate (Post-MicroDeval)

Table 4.15 AIMS Sphericity Results for Other NMAS Aggregates (Post-MicroDeval)

Source	Type	NMAS	Flat/Elongated (< 0.6) Percent	Low Sphericity (0.6 – 0.7) Percent	Moderate Sphericity (0.7 – 0.8) Percent	High Sphericity (> 0.8) Percent
APAC Spiro	Sandstone	9.5mm	65	29	6	0
Flint Rock	Mine Chat	6.3mm	32	10	26	32
MM Mill Creek	Granite	No.4	11	33	43	13
Imported	Bauxite	No.8	Too small for procedure			

4.3.3 Comparison with NCAT Results

This section provides discussion around the NCAT study results (ODOT, 2015) in context of this study's OU laboratory results for Micro-Deval, LA Abrasion, AIMS. Although current testing methods provide insightful results that "can be considered as basic guidance in establishing friction performance-related test criteria", there may not be direct correlation between methods (NCHRP, 2009), as shown here.

The NCAT study determined that "regionally [Oklahoma] available friction aggregates will not achieve the same level of friction performance when used in place of bauxite as an HFST" (ODOT, 2015). The bauxite material was too small (No.8) for some of the laboratory procedures, and therefore no comparison between materials can be made. However, bauxite's Micro Deval weight loss value of 4.8% (Table 4.2) does support the NCAT finding that bauxite provides good surface friction performance, which has been correlated with aggregates that exhibit Micro-Deval weight loss values of 12% or less (Fowler and Rached, 2012).

NCAT results the Open Graded Friction Coarse (OGFC) mixture contained four types of Oklahoma aggregate that were also evaluated in the OU laboratory: mine chat (Flint Rock), rhyolite (Hanson Davis), sandstone (Martin Marietta Sawyer) and granite (Martin Marietta Snyder) (ODOT, 2015). Table 4.16 shows the LA Abrasion, Micro Deval and Insoluble Residue results for these materials.

Table 4.16 NCAT Laboratory Aggregate Results

Source	**Type**	**LA Abrasion** (average %)	**Micro Deval** (average %)	**Insoluble Residue** (average, per ODOT)
Martin Marietta Snyder	Granite	18.3	2.8	99.0
Hanson Davis	Rhyolite	12.0	8.2	96.6
Martin Marietta Sawyer	Sandstone	19.7	7.0	99.9
Flint Rock	Mine Chat	Too fine for test procedure	1.7	Not provided

These results indicate that these aggregates would facilitate good pavement surface friction. However, if a minimum desirable friction coefficient of 0.4 is considered (Meegoda and Gao, 2015) when evaluating the NCAT results in Table 4.7, then only the MM Sawyer material would exceed the minimum desirable friction. Additionally, the AIMS results (Figure 4.17, Figure 4.18 and Figure 4.19) show that the MM Sawyer material generally has lower indices for texture, angularity and sphericity than the other materials, which indicates less ability to provide friction and reduce wear from traffic.

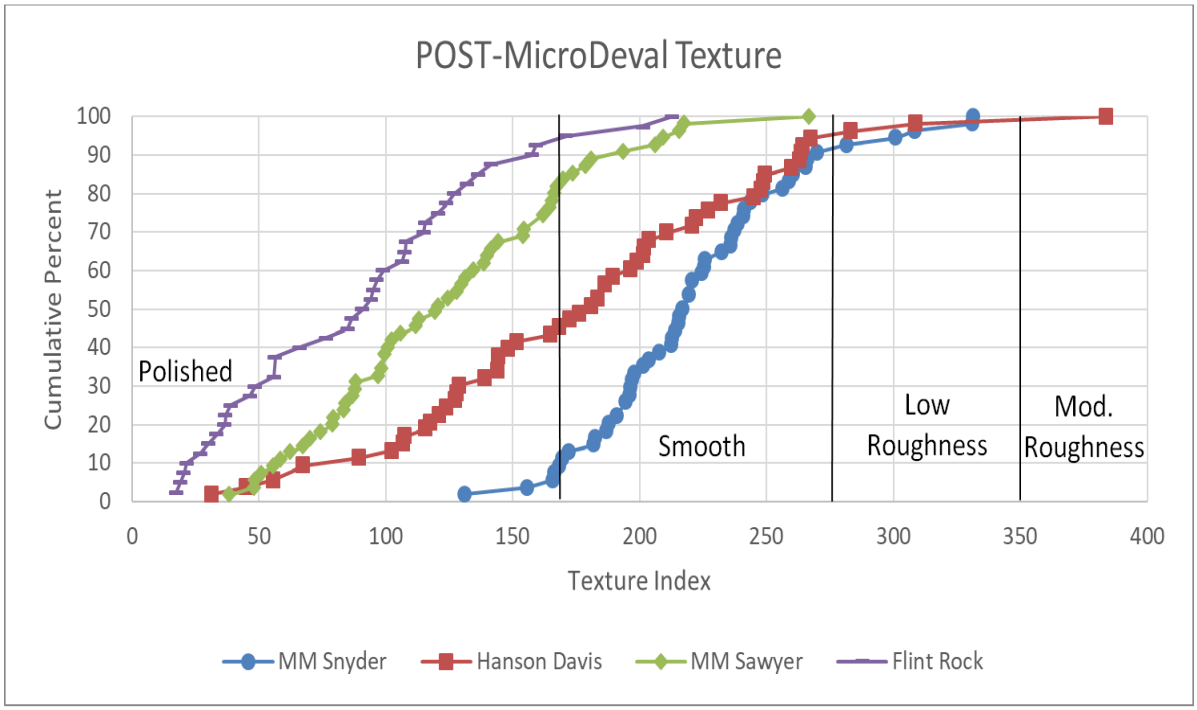

Figure 4.17 NCAT AIMS Texture Results (Post MicroDeval)

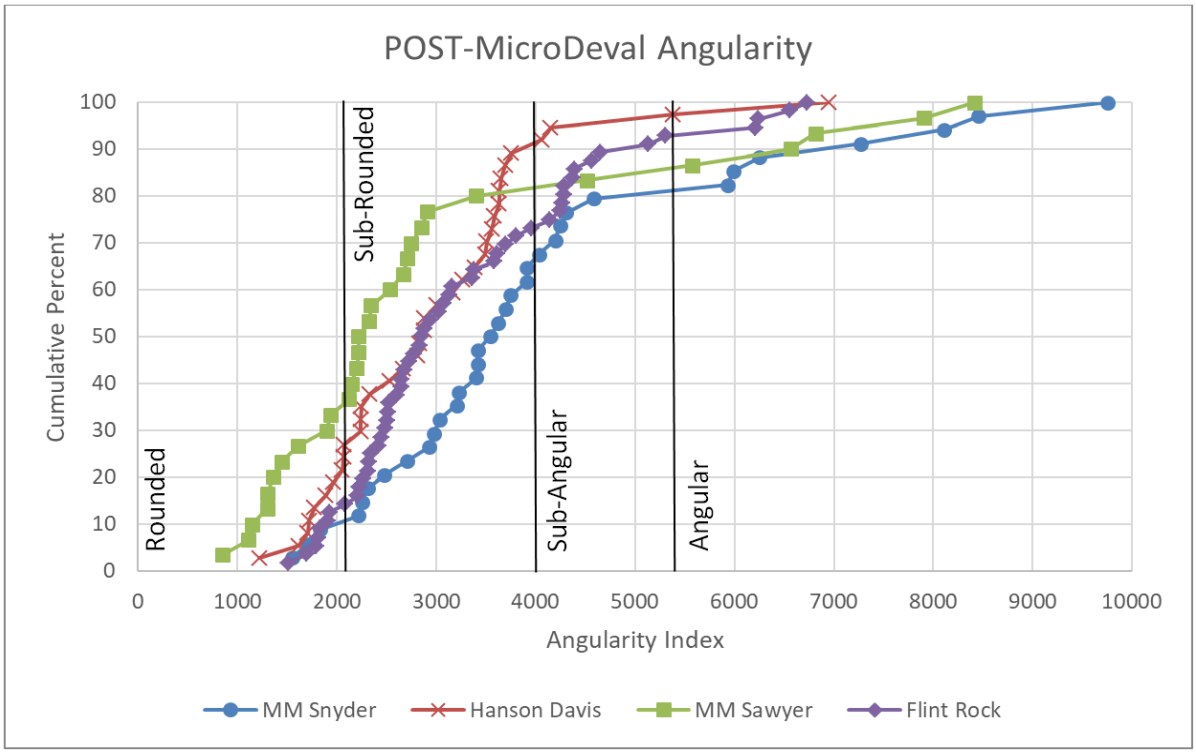

Figure 4.18 NCAT AIMS Angularity Results (Post MicroDeval)

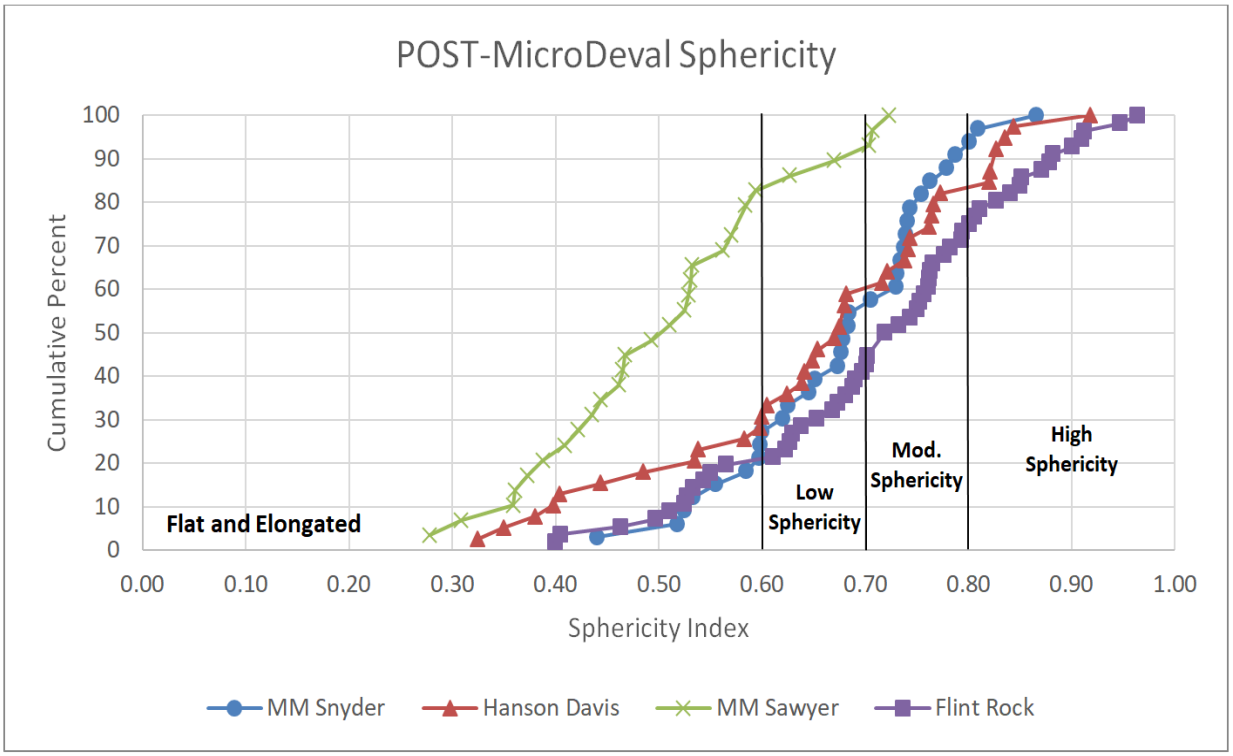

Figure 4.19 NCAT AIMS Sphericity Results (Post MicroDeval)

4.4 Summary

A wide range of physical characteristics of aggregates such as gradation (size), shape, texture, angularity, durability, and polish resistance (under dry and wet conditions) was tested in the laboratory and analyzed for each aggregate source using conventional methods and AIMS. Conventional methods for aggregate property evaluation include aggregate durability (Micro-Deval AASHTO-T-327) and hardness (LA Abrasion AASHTO-T-96). The Micro-Deval apparatus measures the resistance of aggregates to degradation by measuring their abrasion loss in presence of water, using AASHTO TP81-10 (before Micro-Deval) and AASHTO T

327 (after Micro-Deval) test methods to measure such properties of aggregates as shape, texture and angularity with automated techniques that offer a much higher level of precision and repeatability than conventional methods. The laboratory aggregate characteristic data sets are further used in Chapter 5 for the skid resistance model development.

CHAPTER 5 FIELD DATA COLLECTION AND ANALYSIS

5.1 Data Collection Devices

The PaveVision3D System, the AMES high speed texture profiler and the Grip tester were used in the field to collect pavement surface characteristics, macrotexture, and friction data.

The PaveVision3D laser imaging system developed by the OSU research team has evolved into a sophisticated system to conduct full lane data collection on roadways at highway speed up to 60mph (96.5 km/h) with 1mm resolution (Wang and Li, 2017). Figure 5.1 shows the Digital Highway Data Vehicle (DHDV) equipped with PaveVision3D. PaveVision3D is able to acquire both 3D laser imaging intensity and range data from pavement surfaces through two separate sets of sensors. Recently, two 3D high resolution digital accelerometers have been installed on the system. These accelerometers area capable of compensating pavement surface profiles and generating roughness indices. The collected data are saved by image frames that are 2,048 mm in length and 4,096 mm in width. The 1mm 3D pavement surface data can be used for the following:

- Comprehensive evaluation of surface distresses, with automatic and interactive detection of cracks and classifying them based on various protocols;
- Profiling, including transverse profiling for rutting and longitudinal profiling for roughness (Boeing Bump Index and International Roughness Index);

- Safety analysis, including macrotexture in term of mean profile depth (MPD) and mean texture depth (MTD), hydroplaning prediction, and grooving identification and evaluation;
- Roadway geometry, including horizontal curve, longitudinal grade, and cross slope.

Figure 5.1 DHDV with PaveVision3D Ultra

The AMES 8300 Survey Pro High Speed Profiler (Figure 5.2) is designed to collect surface macrotexture data along with standard profile data at highway speeds. Multiple texture indices such as Mean Profile Depth (MPD) can be calculated from the test data. This High Speed Profiler meets or exceeds the following requirements: ASTM E950 Class 1 profiler specifications, AASHTO PP 51-

02 and Texas test method TEX 1001-S. The texture specifications of the Profiler include the following:

- Data collection speed between 25 and 65 mph;
- Laser height sensor with a range of 180 mm and a resolution of 0.045 mm;
- Horizontal distance measured with an optical encoder that has a resolution of 1.2 mm;
- Pavement elevation sampling rate 62,500 samples per second;
- Profile wavelength down to 0.5 mm.

Figure 5.2 AMES 8300 Survey Pro Profiler

Grip Tester (ASTM E274) (Figure 5.3) has been used in recent years by FHWA on many demonstration projects in the United State. It is designed to continuously measure the longitudinal friction along the wheel path operating around the critical slip of an anti-lock braking system (ABS) at highway speed across the entire stretch of a road with much lower water consumption, which can provide greater details about spatial variability for project and network level friction

management. The device is capable of testing at highway speeds (60 mph/100 km/h) as well as at low speeds (20 mph/32 km/h) using a constant water film thickness. The collected data are recorded at 3-ft (0.9 m) intervals by default and can be adjusted by the user. It follows ASTM E274 "Standard Test Method for Skid Resistance of Paved Surfaces Using a Full-Scale Tire".

Figure 5.3 Grip Tester

5.2 Data Collection Events

The six HFST sections and the six LTPP SPS-10 sites have been actively monitored since November 2015 with seven data collection events for this study, while the additional 33 sites have been monitored since September 2016 with 4 data collection events. For each data collection event, approximately 7 daily trips were required to collect all the data for the 45 testing sites. The field testing events for each site are provided in Table 5.1.

Table 5.1 Field Testing Sites

ID	Route	Treatment	Aggregate	Test 1 - 3	Test 4	Test 5	Test 6	Test 7
1	SH-1	Chip Seal	Limestone		X	X	X	X
2	US-259	Chip Seal	Limestone		X	X	X	X
3	SH-39-1	Chip Seal	Limestone		X	X	X	X
4	SH-39-2	Chip Seal	Limestone		X	X	X	X
5	SH-39-3	Chip Seal	Limestone		X	X	X	X
6	US-412	Friction Seal	Unknown		X	X	X	X
7	Lakeview Stillwater	Microsurfacing	Granite		X	X	X	X
8	US-64 Perry	Microsurfacing	Mine Chat				X	X
9	N Harrah Rd	Microsurfacing	Granite				X	X
10	SE 29th St	Microsurfacing	Granite				X	X
11	I-35	PFC	Unknown		X	X	X	X
12	I-35	PFC	Unknown		X	X	X	X
13	SH-33	Resurface	Dolomite		X	X	X	X
14	SH-33	Resurface	Dolomite		X	X	X	X
15	SH-51	Resurface	Dolomite		X	X	X	X
16	US-177	Resurface	Dolomite		X	X	X	X
17	SH-77	Resurface	Granite		X	X	X	X
18	SH-51	Resurface	Rhyolite		X	X	X	X
19	I-40	Resurface	Rhyolite		X	X	X	X
20	US-77	Resurface	Rhyolite		X	X	X	X
21	SH-9	Resurface	Granite		X	X	X	X
22	US-64	Resurface	Limestone		X	X	X	X
23	SH-15	Resurface	Limestone		X	X	X	X
24	US-270	Resurface	Limestone		X	X	X	X
25	US-59	Resurface	Sandstone		X	X	X	X
26	US-270	Resurface	Sandstone		X	X	X	X
27	SH-4	UTBWC	Granite		X	X	X	X
28	I-35	UTBWC	Rhyolite		X	X	X	X
29	SH-270	UTBWC	Rhyolite		X	X	X	X
30	US-62	UTBWC	Rhyolite		X	X	X	X
31	I-240	UTBWC	Limestone		X	X	X	X

ID	Route	Treatment	Aggregate	Test 1 - 3	Test 4	Test 5	Test 6	Test 7
32	US-69	UTBWC	Sandstone		X	X	X	X
33	US-59	UTBWC	Sandstone		X	X	X	X
34	I-40	HFST	Bauxite	X	X	X	X	X
35	I-40	HFST	Bauxite	X	X	X	X	X
36	I-44	HFST	Bauxite	X	X	X	X	X
37	SH-20	HFST	Mine Chat	X	X	X	X	X
38	SH-20	HFST	Bauxite	X	X	X	X	X
39	SH-20	HFST	Bauxite	X	X	X	X	X
40	SH-66	WMA	Rhyolite	X	X	X	X	X
41	SH-66	WMA	Rhyolite	X	X	X	X	X
42	SH-66	WMA	Rhyolite	X	X	X	X	X
43	SH-66	WMA	Rhyolite	X	X	X	X	X
44	SH-66	WMA	Rhyolite	X	X	X	X	X
45	SH-66	WMA	Rhyolite	X	X	X	X	X

5.3 Preliminary Analysis of Field Performance

Analysis of the field data acquired from the HFST sites was conducted to investigate the potential influencing factors of pavement friction. There are six HFST sites in Oklahoma, including two on Interstate 40 (I-40) (eastbound), one on Interstate 44 (I-44) (westbound), and three on State Highway 20 (SH-20) (both directions). Seven data collection visits were made on the HFST sites from November 2015 to December 2017 at approximately three months interval. Figure 5.4 shows the development of pavement skid resistance over time. A decreasing trend of pavement friction is clearly observed for all the HFST sites due to traffic-related polishing (Figure 5.5). The average friction values of the six HFST sites from the seven collection events are 0.97, 0.89, 0.79, 0.73, 0.78, 0.69 and 0.61, with an average deterioration rate of 5.46%. Friction numbers on the HFST sites constructed with bauxite aggregates have decreased by 4.49% in rural areas (SH-20 sites 2 & 3) and 6.56% in metropolitan areas with higher traffic volumes (I-40 and I-44 sites). By contrast, the friction numbers on SH-20 Site 1 constructed with mine chat

aggregates have decreased by 8.45%, which shares the same traffic and environmental conditions as those for SH-20 sites 2 and 3.

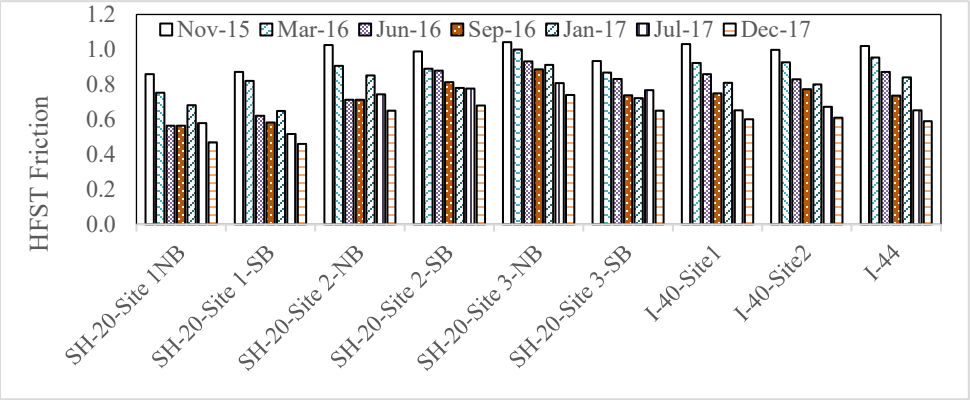

Figure 5.4 Comparison of HFST Average Friction Number

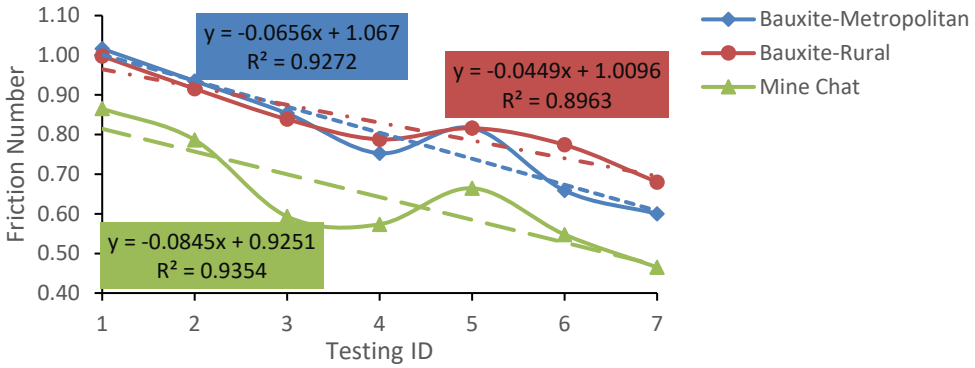

Figure 5.5 Friction Deterioration of HFST

Boxplots are provided in Figure 5.6 to compare the friction performance of different PM treatments and different types of aggregates. The HFST sites exhibit the best friction performance over the testing period. Similar observations have also been reported in previous studies (Moravec, 2013; Bledsoe, 2015, Li et al., 2016). The chip seal sites exhibited a wide variation of friction numbers as compared to the other PM treatments, ranging from the lowest friction number of less than 0.2 to the highest friction number of more than 0.7. Three of the chip seal testing sites are

located on SH-39 built in September 2012 using limestone, while the other two sites on SH-1 and US-259 in southeast Oklahoma were built in March 2012 and September 2014 using limestone but from different sources. The testing sites with the other four treatments showed comparable friction numbers.

For aggregates, the HFST sites using bauxite and mine chat have maintained the highest friction values over the testing period, as shown in Figure 5.7. Testing sites with sandstone as the coarse aggregates exhibited lower friction numbers than those from the bauxite and mine chat sections, but better friction numbers than those using the other four aggregate sources. These results are consistent with the previous studies (Moaveni et al., 2014). Moreover, it was found that the testing sites with limestone showed the highest variation of friction measurements. Limestone is one of the most widely used aggregate types for pavement construction in the U.S. due to its availability and high quality of initial properties (Csathy et al., 1968). However, limestone is generally more prone to polishing under traffic, resulting in poorer long-term skid performance (Smith et al., 2009; Neaylon, 2009; Fowler and Rached, 2012). As a result, the friction performance varies considerably among sites with various treatment ages.

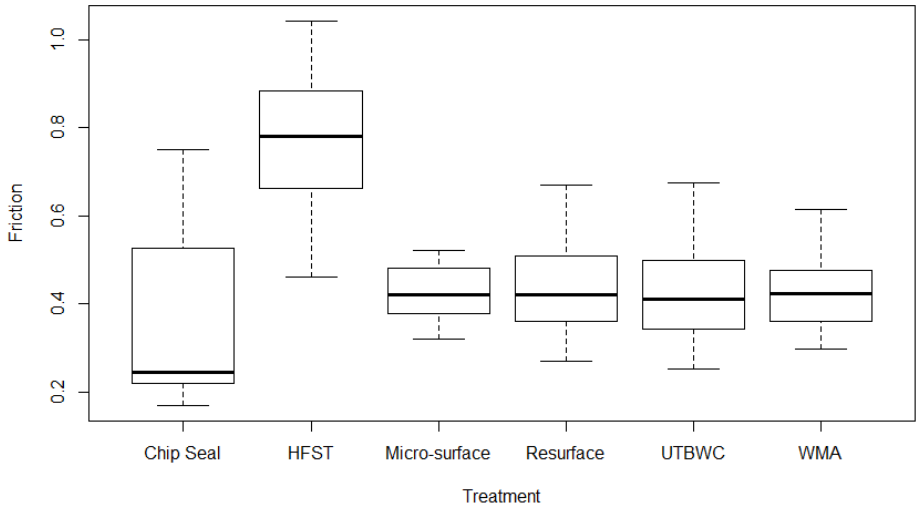

Figure 5.6 Friction for Various Treatments

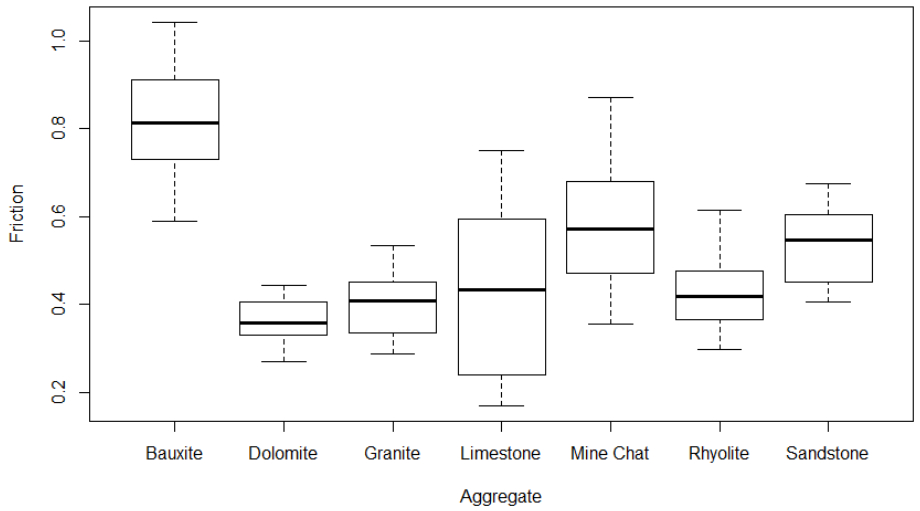

Figure 5.7 Friction of Various Aggregates

Figures 5.8 and 5.9 show the scatterplots of friction numbers by different treatments and aggregate types during the data collection period. Other than sites with HFST and WMA overlay treatments, surface friction did not show a clear decreasing trend for the other PM treatment sites, primarily because of the short

period of field monitoring and possibly the influence of temperature variations during testing. The ambient temperature during data collection in January and December was around 50 ºF, while that in July and September the average temperature was 90 ºF. Generally, the friction number tends to increase with decreased ambient or pavement temperature (Luo, 2003; Fuents, 2009; Jahromi et al., 2011).

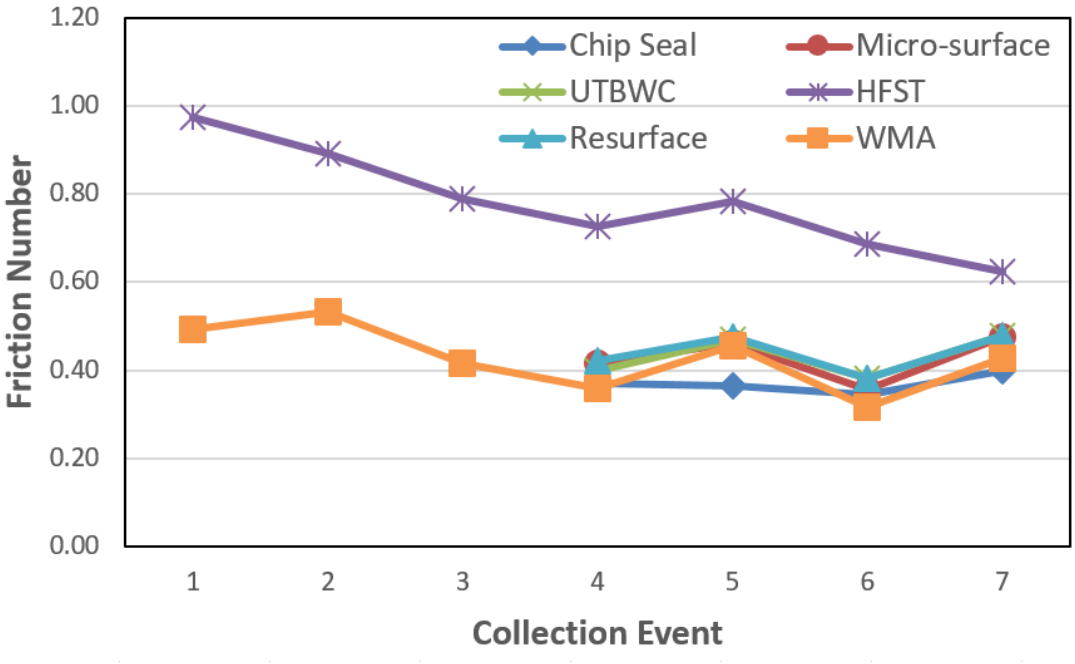

Figure 5.8 Friction Deterioration Trends by Treatment Types

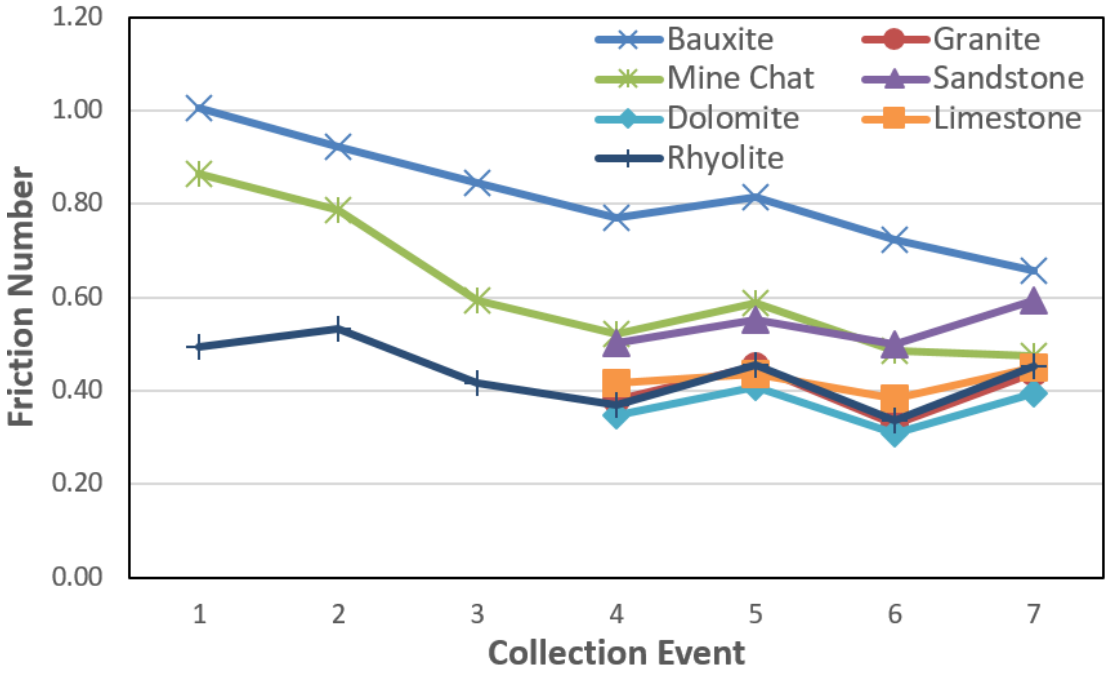

Figure 5.9 Friction Deterioration Trends by Aggregate Types

5.4 Field Performance of HFST Sites

5.4.1 Oklahoma HFST Sites

The field data collection efforts described herein includes testing of the six HFST sites in Salina and Oklahoma City metropolitan area. The locations of the six HFST sites are shown in Figure 5.10, and the detailed information for each site is summarized in Table 5.2. All of the six HFST sites were constructed using fully automated methods.

Sites 1 through 3 are located at three curves on SH-20 with significant number of historical crashes. SH-20 is a curvy two-lane rural highway with various levels of longitudinal grades but without shoulder. Sites 2 and 3 were two standard HFST demonstration sites using bauxite, while Site 1 was constructed with locally

available aggregates (mine chat). The HFST system was installed on both travel lanes for Sites 1 - 3 and field data collection was performed for both lanes.

In September 2015, Sites 4, 4 and 6 were built on urban Interstate Highways (I-40 & I-44) in the Oklahoma City metropolitan area with the purpose of evaluating the durability of HFST system under high traffic volumes. Each location includes three through lanes in one direction, and the HFST system was constructed on all three westbound lanes. The field data collection activities were conducted at highway speed without traffic control in the middle lane of each site.

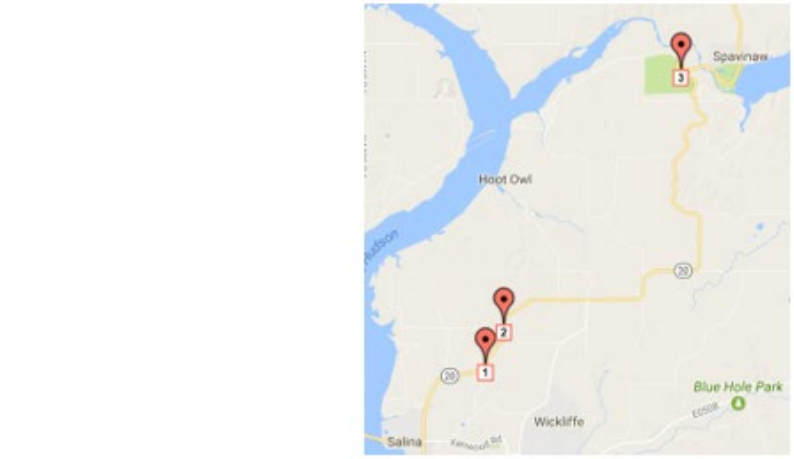

(a) Salina (Rural State Highway)

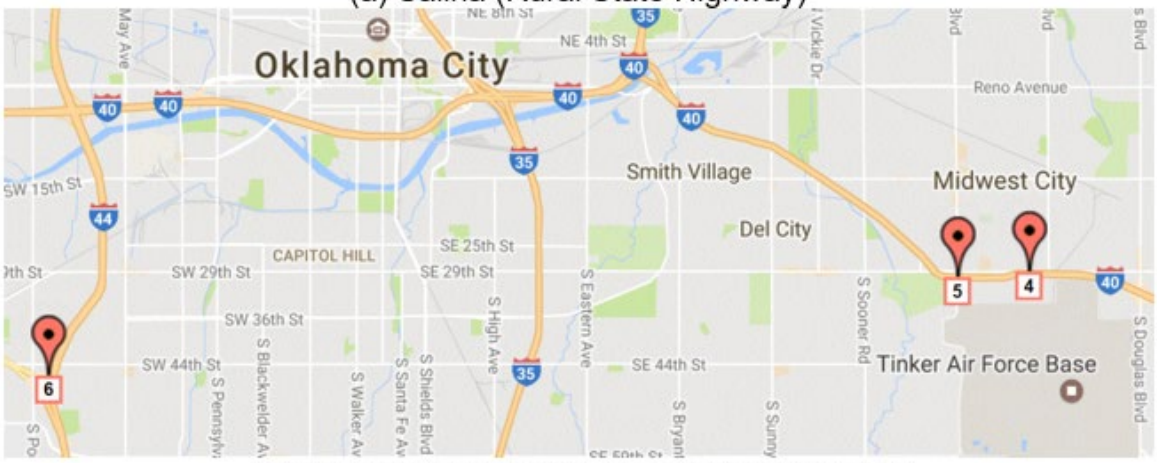

(b) Oklahoma City (Urban Interstate Highways)

Figure 5.10 HFST Sites in Oklahoma

Table 5.2 Detailed Information for HFST Sites in Oklahoma

Site ID	Site Location	2016 AADT	Aggregate	M/Y Treatment	Age (Year)	Radius (ft)	Grade (%)
1	Curve on SH-20 (milepost 2)	3100	Mine Chat	9/11/2015	2.3	2,000	3.5
2	Curve on SH-20 (milepost 3)	3100	Bauxite	12/17/2013	4.0	1,600	5.0
3	Curve on SH-20 (milepost 11.5)	550	Bauxite	3/25/2014	3.7	700	-6.0
4	Curve on west of I-40 (milepost 157)	80,400	Bauxite	9/14/2015	2.3	6,500	-2.5
5	Curve on west of I-40 (milepost 156)	80,400	Bauxite	9/14/2015	2.3	6,500	-1.5
6	Curve on west of I-44 (milepost 116)	121,500	Bauxite	9/14/2015	2.3	6,500	-2.0

5.4.2 Friction and Macrotexture

Pavement friction and macrotexture data on the HFST sections and the abutting pavements were compared to determine the effectiveness of the HFST system in improving pavement surface properties. The average friction numbers and MPD values from the seven data collection events were evaluated to explore the variation of pavement friction and macrotexture characteristics under polishing due to traffic and environmental influences over time. In addition, typical distresses on the HFST surfaces were identified via the 1 mm 3D pavement image data to assess the deterioration of HFST system.

To determine the effectiveness of HFST in improving pavement surface properties, pavement friction data and macrotexture profiles were collected in the left wheel-path with at least 300 ft lead-in and lead-out for each HFST site. The friction number and MPD are summarized at 3 ft interval. Two example data sets are shown in Figure 5.11.

Both HFST sites show clear improvements in friction numbers on HFST sections as compared to those on the abutting non-HFST pavements. Different from friction data, MPD on some HFST sites showed much higher values in contrast to the abutting non-HFST pavements, while others did not show any noticeable differences. HFST Site 6 shows clear improvements in friction number and MPD (Figure 5.11a), whereas minor improvement in MPD on the southbound lane of Site 3 (Figure 5.11b).

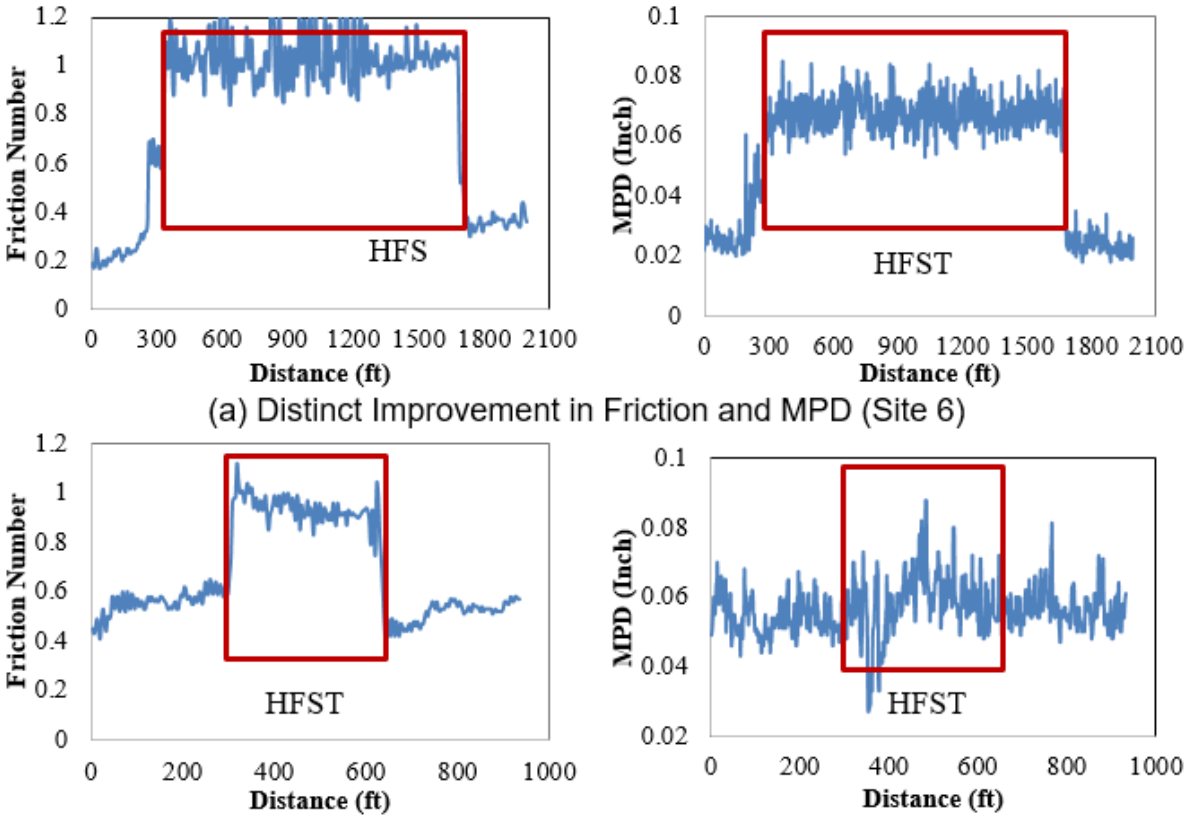

Figure 5.11 Example HFST Friction and MPD Data (Nov 2015)

Paired t-test with equal variance was performed for each HFST site. Since the length of HFST application and non-HFST surfaces (lead-in and lead-out) may not

be the same, the sample sizes for the t-tests were not equal and the missing values were coded as “NA” for the sections with fewer observations. The P-value was used to determine whether the difference between the mean of two groups was likely to be zero. The t-test results for the data sets collected in December 2017 are summarized in Table 5.3. After several years of service, there is still strong evidence that the HFST surfaces have significantly larger friction numbers and surface texture (MPD) values than the abutting untreated pavements (with an average of P-value = 0 for all the HFST sites). The average friction number of the HFST sites is 0.78, while the friction of non-HFST surfaces has an average of 0.32. The average MPD of the HFST sites is 0.062 inches, while the MPD of non-HFST surfaces has an average of 0.051 inches.

Table 5.3 T-Test Results for Friction Number and MPD

Site	Friction Mean - HFST	Friction Mean – Non HFST	Friction P-value	Friction Sig. Diff?	MPD Mean - HFST	MPD Mean – Non HFST	MPD P-value	MPD Sig. Diff?
Site 1-NB	0.47	0.23	0	Yes	0.063	0.057	0	Yes
Site 1-SB	0.46	0.26	0	Yes	0.063	0.059	0	Yes
Site 2-NB	0.65	0.23	0	Yes	0.049	0.064	0	Yes
Site 2-SB	0.68	0.21	0	Yes	0.066	0.053	0	Yes
Site 3-NB	0.74	0.48	0	Yes	0.054	0.053	0	Yes
Site 3-SB	0.65	0.33	0	Yes	0.065	0.062	0	Yes
Site 4	0.60	0.29	0	Yes	0.064	0.034	0	Yes
Site 5	0.61	0.29	0	Yes	0.065	0.054	0	Yes
Site 6	0.59	0.17	0	Yes	0.061	0.036	0	Yes

The deterioration of friction number and macrotexture variation based on the seven field data collection events was investigated to evaluate the long-term performance of HFST. The average friction numbers and MPD values were

compared for each HFST site. In addition, the friction number ratio (FN Ratio) and MPD ratio (MPD Ratio), the friction number or MPD of the HFST surfaces divided by those of the adjacent untreated surfaces were computed to investigate the deterioration of HFST as compared to the adjacent untreated surfaces. The comparison of results for the seven data collection events is plotted in Figure 5.12.

Clear decreasing trends are observed in terms of friction numbers for all the HFST sites (Figure 5.12a). The average friction values of the six HFST sites from the seven collection events are 0.97, 0.89, 0.79, 0.73, 0.66, 0.69, and 0.61. As observed in Figure 5.12b, the FN ratio larger than 1.00 indicates that the HFST surface is still providing higher skid resistance compared to the untreated abutting pavements. After several years of service, the FN ratios remain high for all the HFST sections over time: 2.85, 2.71, 2.77, 2.66, 2.41, 2.63, and 2.32 from November 2015 to December 2017.

On an average, 37.8% of friction reduction has been observed on these HFST sections during the two-year monitoring period. Comparatively, friction numbers on HFST sites with bauxite as the aggregate source have decreased by 31.8% in rural sites (Sites 2 and 3) and 40.9% in the metropolitan area (Sites 4, 5 and 6). Higher traffic volumes seem to slightly increase the friction deterioration rates of HFST. Within the same time range, the friction numbers for Site 1, which uses mine chat as the aggregate source, have decreased by 46.2%, which is 14.4% larger than the average reduction for Sites 2 and 3.

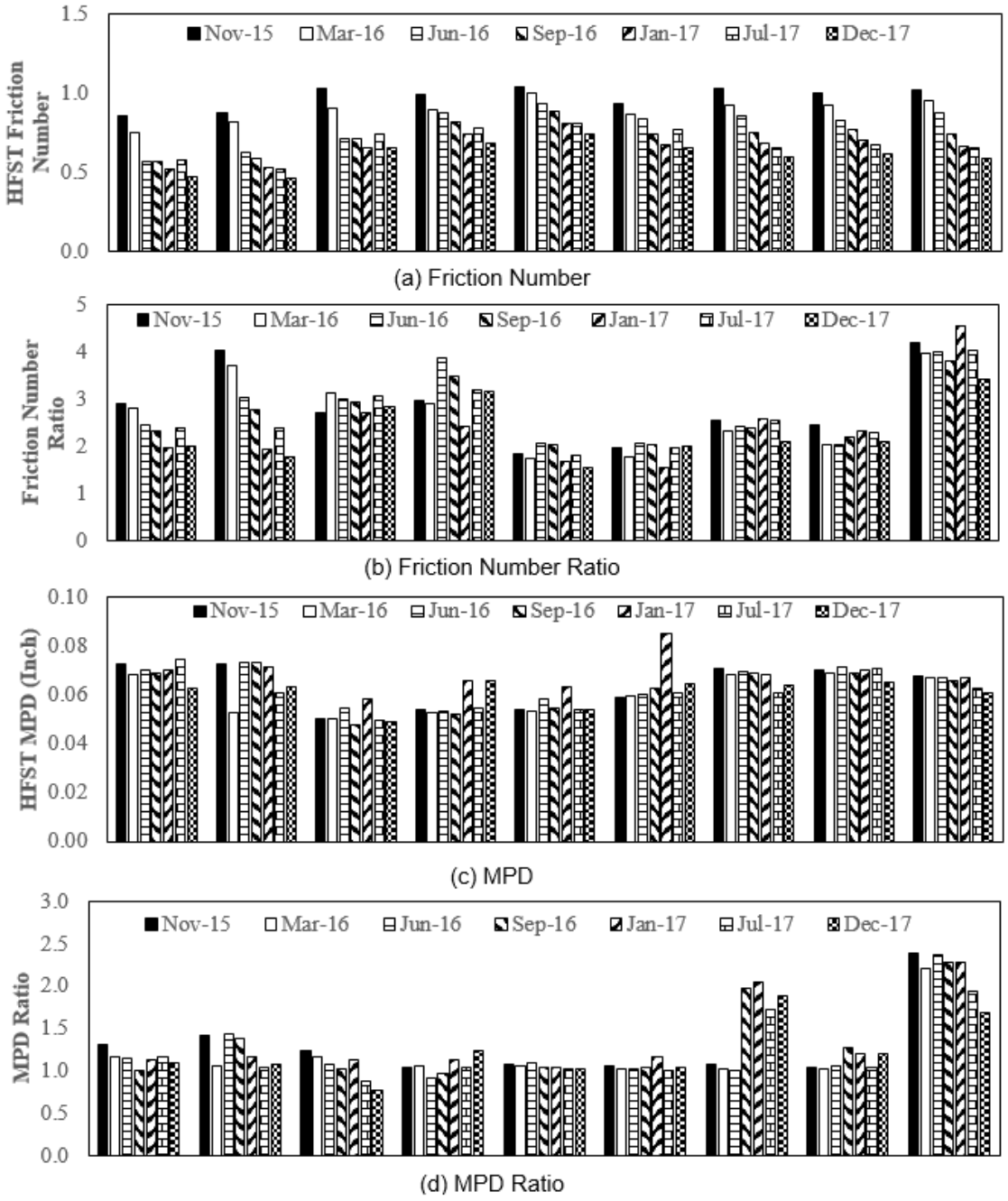

Note: The labels of horizontal axis are: “Site 1-NB”, “Site 1-SB”, ““Site 2-NB”, “Site 2-SB”, “Site 3-NB”, “Site 3-SB”, “Site 4” , “Site 5” , “Site 6”.

Figure 5.12 Field Performance of HFST

As shown in Figure 5.12c, different from the variations of pavement friction numbers displayed in Figure 5.12a, the MPD maintains at a stable state for most

HFST sections over time. In addition, in Figure 5.12d, the MPD Ratios on the HFST sites remained fairly consistent over time: the ratios on Sites 1 through 5 (asphalt section) are close to 1.00 while that of Site 6 (bridge deck) is roughly 2.00. The jump in MPD Ratio observed on Site 4 from September 2016 to December 2017 is primarily due to the new overlay on its abutting untreated pavements.

5.4.3 Surface Distresses

Monitoring the development of surface distresses over time could provide valuable information on the durability of the HFST treatment. HFST system can deteriorate or fail in terms of raveling and delamination, which could result from deficiencies in construction methods, product performance, and environmental conditions during the application and while in service (Izeppi et al., 2010; Waters, 2011; and Li et al., 2016b).

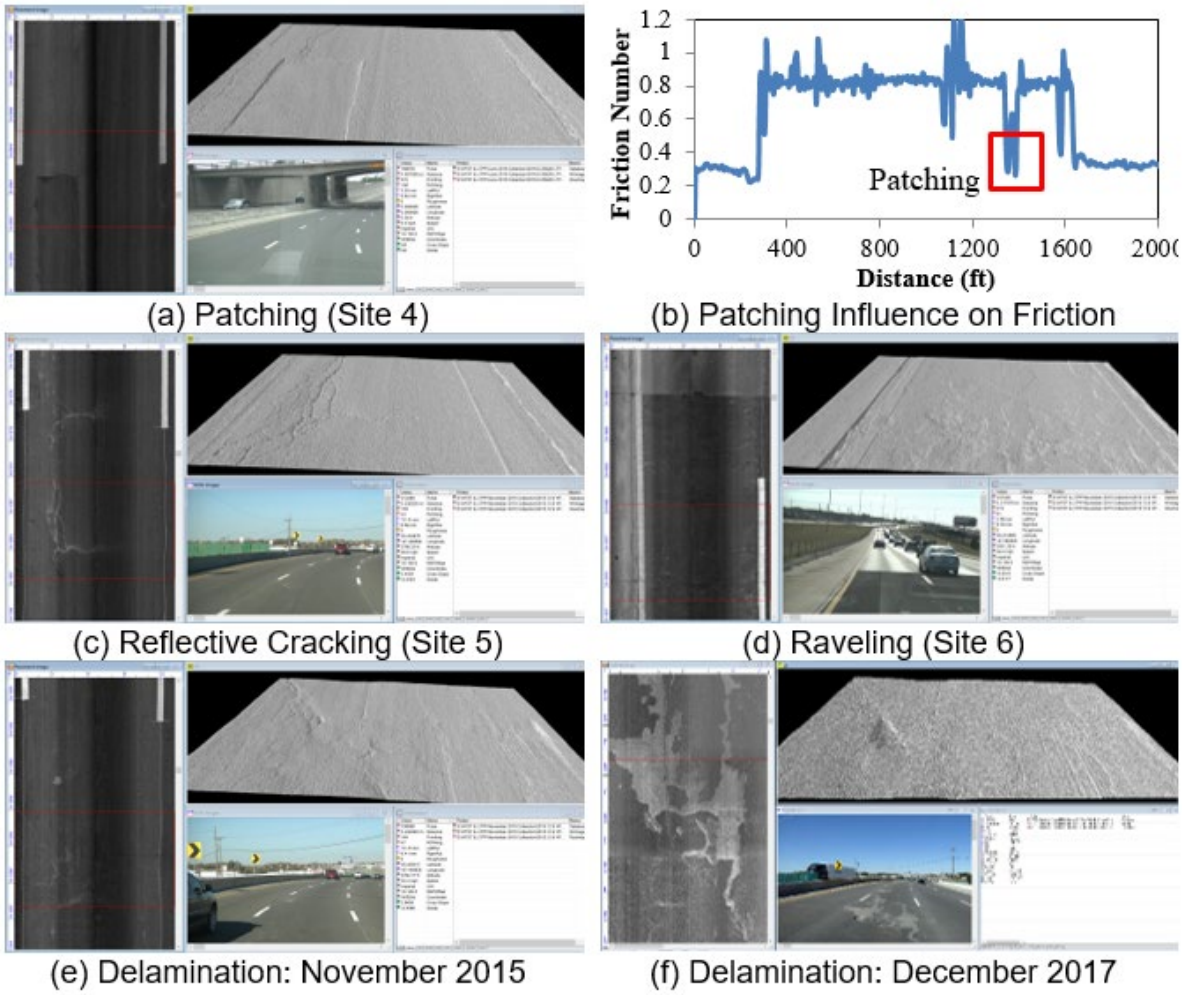

Figure 5.13 Distresses of HFST System

For the six HFST sites in Oklahoma, typical distresses observed on pavements are demonstrated in the 1 mm 3D images in Figure 5.13. The common distress types include patching, reflective cracking, raveling, and delamination. In June 2016, several patches were first observed at Site 4 in the middle lane, as shown in Figure 5.13a. Figure 5.13b demonstrates the influence of patching on the friction measurements. Compared with the adjacent HFST surfaces, distinct lower friction numbers are observed on the pathing area. A similar trend is also observed for the corresponding MPD. In November 2015, reflective cracking was observed at

Site 5 in the middle lane, and raveling occurred in the left lane of Site 6 within three months after the HFST installation, as shown in Figures 5.13c and 5.13d.

With traffic polishing, delamination may occur at locations where the bond strength between HFST and the underlying pavement surface is inadequate. An example is provided in Figures 5.13e and 5.13f to demonstrate how delamination is developed over time using the 1 mm 3D data. In November 2015, no delamination was observed in the middle lane of Site 5, while in December 2017, delamination was noticeable in the 1 mm 3D pavement image at the same location. Approximate 50% of the treatment at that location has been polished due to traffic during the past 25 months.

5.4.4 Crash Reduction Analysis

One of the most important aspects to analyze the performance of HFST systems is to evaluate the crash reduction before and after the installation. ODOT maintains the Statewide Analysis for Engineering & Technology (SAFE-T) database, which is a crash reporting system and includes accident reports received from state and local law enforcement agencies since 1998 (Adams and Warren, 2017). Traffic crashes are reported by the type (rear-end, pedestrian, turning, etc.), time, severity level, vehicle type, roadway, and weather conditions. In this study, the number of property damage crashes and injured crashes on the HFST sites during the five years before the installation and subsequent years after were obtained from the SAFE-T database up to December 2017. The detailed crash information for these HFST sites are summarized in Table 5.4.

The annual crash number and crash reduction for property damage crashes and injured crashes occurred on each site are given in Figure 5.14. Before HFST installation, the average annual number of property damage crashes for Sites 1, 2 and 3 on rural highway SH-20 ranged from 0.4 to 3.2, which is much lower than the range (6.2 to 16.6) for Sites 4, 5 and 6 on urban interstate highways. By contrast, after the HFST installation, the annual number of property damage crashes ranges from 0.0 to 3.5 at these sites. The HFST systems achieve an average crash reduction of 29% to 100% in terms of the annual number of property damage crashes. For example, on average 16.6 annual property damage crashes occurred at Site 5 before the HFST installation, while only 1.3 such damages occurred in the subsequent years afterwards. The HFST system has achieved 92% reduction of property damage-related crashes during the 2.3 years of service. With a combination of sharp and reverse curves, the HFST system at Site 3 has reduced 29% of property damage-related crashes during its 3.7 years of service.

In Figure 5.15, the annual number of injured crashes during the five years before the installation ranges from 0 to 0.8 at these sites, while by December 2017 no crashes were reported in the subsequent years after the installation. For example, at Site 5, on an average 0.8 and 0.0 annual injured crashes occurred before and after the installation. The HFST system has achieved 100% reduction in injured crashes within the 2.3 years of service.

Table 5.4 Crash Reduction Summary of HFST Sites

Crash Type	Period	Crash Data	Site 1	Site 2	Site 3	Site 4	Site 5	Site 6
PDO	Before	# Crashes	2	16	14	31	83	37
		Years	5	5	5	5	5	5
		Crashes/Year	0.4	3.2	2.8	6.2	16.6	7.4
	After	# Crashes	0	3	8	0	3	8
		Years	2.3	3.7	4	2.3	2.3	2.3
		Crashes/Year	0	0.8	2	0	1.3	3.5
		Reduction	100%	75%	29%	100%	92%	53%
Injured	Before	# Crashes	0	2	2	2	4	2
		Years	5	5	5	5	5	5
		Crashes/Year	0	0.4	0.4	0.4	0.8	0.4
	After	# Crashes	0	0	0	0	0	0
		Years	2.3	3.7	4	2.3	2.3	2.3
		Crashes/Year	0	0	0	0	0	0
		Reduction	-	100%	100%	100%	100%	100%

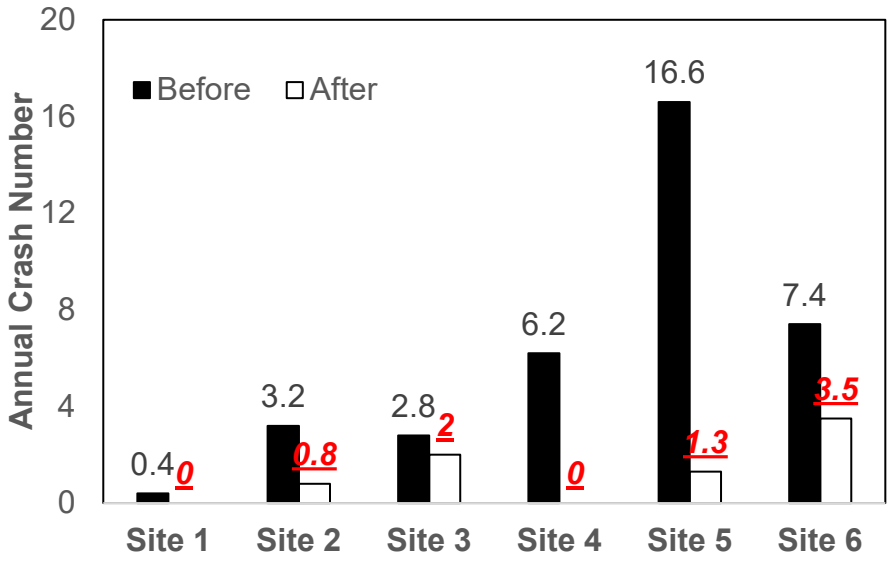

Figure 5.14 Annual Property Damage Crashes Summary of HFST Sites

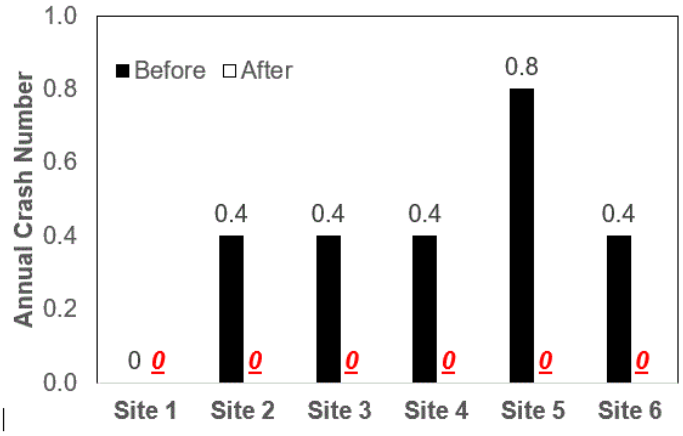

Figure 5.15 Annual Injured Crashes Summary of HFST Sites

5.4.5 Benefit-Cost Analysis

Benefit-cost analysis was performed for the HFST sites in Oklahoma in this study. The unit cost of HFST installation was obtained from ODOT, while the benefits are estimated on the basis reductions in average property damage crashes and injured crashes. The total cost and the HFST benefit are computed for each site, as shown in Equations 5.1 and 5.2.

$$\text{Cost (\$)} = \text{Unit Cost (\$/yd}^2\text{)} \times \text{Section Area (yd}^2\text{)} \quad \text{(Eq. 5.1)}$$

$$\text{Benefit (\$)} = \text{Crash Reduction} \times \text{After Period (Years)} \times \text{Crash Cost (\$)} \quad \text{(Eq. 5.2)}$$

The unit cost is assumed as 50 \$/yd^2 for Sites 2 and 3, but 25 \$/yd^2 for Site 1 and Sites 4, 5 and 6 (ODOT, 2015). The benefits can be estimated through economic and societal impact savings from the reduced crashes (Wilson et al.,

2016). ODOT uses the KABCO scale for evaluating the financial impact of crashes: “K” = fatal injury, “A” = suspected serious injury, “B” = suspected minor injury, “C” = possible injury, and “O” = property damage (Harmon et al., 2018). The unit costs of crashes are provided in Table 5.5, which are used in this analysis. The cost of injured crashes is assumed as the average unit cost of crash types A, B, and C ($2,553,600 + $451,200 + $28,800)/3= $1,011,200). The cost of property damage crashes equals to the cost of crash type “O” ($4,200). The total benefit for each HFST site is the sum of benefits from the reductions in injured crashes and property damage crashes.

Table 5.5 Crash Unit Costs (Harmon et al., 2018)

KABCO	Comprehensive Crash Unit Cost
K	$9,600,000
A	$2,553,600
B	$451,200
C	$28,800
O	$4,200

Accordingly, the benefit-cost ratio can be obtained per Equation 5.3. The detailed cost, benefit, and benefit-cost ratio for each HFST site are summarized in Table 5.6.

Benefit-Cost Ratio = Total Benefit/Cost (Eq. 5.3)

The benefit-cost ratios of these HFST sites range from 6.9 to 27.9. Site 1 only had two property damage crashes during the five-year period before the HFST installation (as shown in Table 3), and no crash has been reported after the installation. As a result, no benefit cost ratio is available for this location. The main

purpose of selecting Site 1 is to test the performance of an affordable local aggregate materials (mine chat herein) for HFST applications. This site is selected not because of its high crash rate, but its adjacency to the two existing rural HFST sites on the same route constructed with bauxite (Sites 2 and 3). It is convenient for ODOT to test, monitor, and compare the performance of the three sites with similar traffic and environmental conditions.

Table 5.6 Benefit-Cost Summary of HFST Sites

Site ID	**2**	**3**	**4**	**5**	**6**
Unit Cost ($/yd^2)	50	50	25	25	25
Length (ft)	450	900	1400	1300	1400
Width (ft)	11	11	12	12	12
# of Lanes	2	2	3	3	3
Cost ($)	*$55,000*	*$110,000*	*$140,000*	*$130,000*	*$140,000*
After Period (Years)	3.7	4	$2	2.3	2.3
PDO Crash Reduction	2.4	0.8	6.2	15.3	3.9
PDO Reduction Benefit ($)	*$37,128*	*$13,440*	*$59,892*	*$147,756*	*$37,884*
Injured Crash Reduction	0.4	0.4	0.4	0.8	0.4
Injured Crash Reduction Benefit ($)	*$1,496,576*	*$1,617,920*	*$930,304*	*$1,860,608*	*$930,304*
Total Benefit ($)	*$3,864*	*$1,533,704*	*$1,631,360*	*$990,196*	*$2,008,364*
Benefit-Cost Ratio	*27.9*	*14.8*	*7.1*	*15.4*	*6.9*

For Sites 2 through 6 with historical crashes, the HFST system is a cost-effective treatment that achieved the benefit-cost ratios between 6.9 and 27.9. The crash reduction in terms of property damage crashes and/or injured crashes is substantial after the installation of the HFST system.

5.4.6 HFST Performance with Local Aggregate

To better understand the performance of Site 1 constructed with local mine chat aggregates, an additional data collection was performed on June 25, 2016 for the three HFST sites on SH-20 (Sites 1, 2 and 3). The three Sites are adjacent to each other with similar traffic and environmental conditions. Friction data was collected by the Grip Tester within the wheel path and also in the middle of the traffic lane. The differences of friction numbers within the wheel-path and in the middle of the lane are primarily caused by traffic polishing. In other words, this data collection can help quantify the polishing resistance of these two aggregate types: mine chat and bauxite.

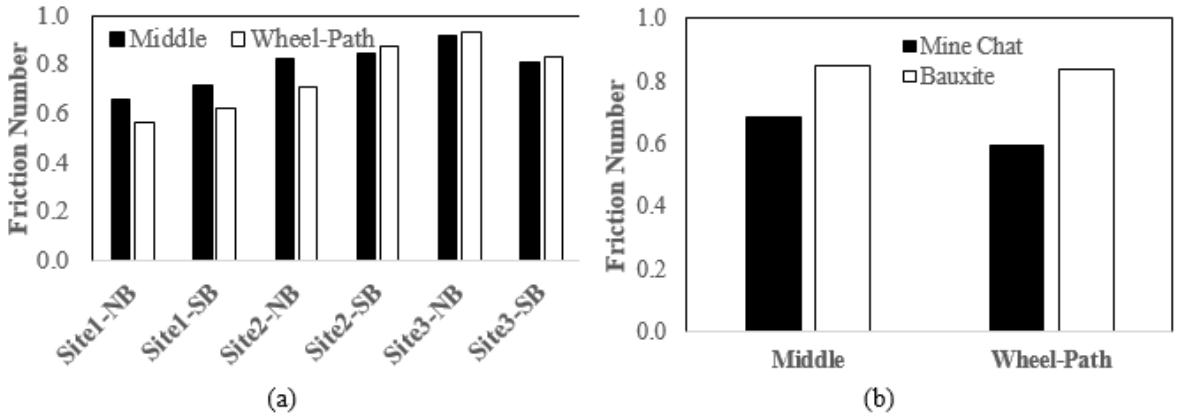

Figure 5.16 Comparison of Friction within Wheel-path and Non-wheel Path

The average friction values in the wheel-path and in the middle of the traffic lane are 0.59 and 0.68 for Site 1, 0.80 and 0.83 for Site 2, and 0.88 and 0.87 for Site 3, respectively, as shown in Figure 5.16a. The corresponding average friction numbers (for HFST treatment) are 0.68 and 0.59 for Site 1 with mine chat, while 0.85 and 0.84 for Sites 2 and 3 with bauxite in the wheel-path and middle of traffic

lane (Figure 5.16b). In addition, it should be noted that Site 1 (with mine chat) was constructed approximately one and a half years later than the construction of Sites 2 and 3 (with bauxite).

It is logical that the friction number in the wheel-path be smaller than that in the center of the lane since traffic polishing mainly occurs within the wheel-path. The larger the difference, the larger the susceptibility of aggregates to traffic polishing. On an average, the HFST with mine chat shows approximately 0.10 decrease in friction in less than a year of service, while no obvious difference is observed for HFST sites with bauxite after more than two and a half year' of traffic polishing.

5.5 Skid Resistance Deterioration Model

5.5.1 Candidate Variables

According to the literature review in Chapter 2, temperature, traffic volume, pavement age, pavement surface characteristics, and aggregate characteristics are considered as the potential influencing factors for the development of friction deterioration model. Temperature data were recorded during the field data collection events. Traffic characteristics, including Annual Average Daily Traffic (AADT) and total traffic volume were acquired from the ODOT SAFE-T database. Pavement ages since the application of PM treatments were obtained from the ODOT's SiteManager database. Pavement surface condition data were acquired using the PaveVision3D laser imaging system. The condition indices for each testing site were computed, including mean profile depth (MPD) for macrotexture, IRI for longitudinal

roughness and rutting for transverse profiling. Aggregate characteristics in terms of angularity, surface texture and sphericity were measured using the AIMS System before and after the Micro-Deval (MD) testing as discussed in Chapter 4. A list of candidate variables is provided in Table 5.7.

Table 5.7. Candidate Variables for the Development of Skid Resistance Model

Variable	Symbol	Description
Friction	FN	Pavement friction number
Treatment	Treatment	Chip seal, microsurfacing, UTBWC, HFST, HMA/WMA thin overlay
Climate	Temp	Ambient temperature
Traffic	AADT	Annual Average Daily Traffic
	TAADT	Total traffic volume, which is AADT multiplied by Age
Pavement	Age	Age in years since PM treatment applied
	MPD	Mean Profile Depth (MPD)
	IRI	International Roughness Index (IRI)
	Rutting	Rutting depth in wheel-path
Aggregate	NMAS	Nominal Maximum Aggregate Size
	MD	Micro Deval loss (%)
	AB	Angularity before MD
	TB	Surface texture before MD
	SB	Sphericity before MD
	AC	Change of angularity after MD
	TC	Change of surface texture after MD
	SC	Change of sphericity after MD

5.5.2 Development of Friction Prediction Model

Multiple linear regression (MLR) analysis was performed to model the deterioration of pavement friction for various PM treatments. MLR is an extension of simple linear regression analysis, which is used to assess the association between

multiple independent variables and a single continuous dependent variable (friction herein). The multiple linear regression can be expressed by Eq. 5.4:

$$Y = b_0 + b_1X_1 + b_2X_2 + \ldots + b_pX_p \qquad \text{(Eq. 5.4)}$$

Where Y is the predicted or expected value of the dependent variable, X_1 through X_p are the p distinct independent or predictor variables, b_0 is the intercept, and b_1 through b_p are the estimated regression coefficients. Each regression coefficient represents the change in Y relative to a one unit change in the respective independent variable, holding all other independent variables constant. Statistical tests can be performed to assess whether each regression coefficient is significantly different from zero.

The ordinary least squares (OLS) statistical analysis results are summarized in Table 5.8. Assessing the p-values suggests that seven independent variables (Temperature, Age, MD, NAMS, AB, TC, SC) are statistically significant at the 95% confidence level. The magnitude of the t statistics provides a means to judge relative importance of the independent variables.

OLS multiple linear model is developed using the statistically significant independent variables. The OLS regress statistics are shown in Table 5.9. It is a widespread notion that statistical models should be interpreted based on the p-value ($p<0.05$). Many researchers have indicated that scientific conclusions should not be based only on whether a p-value passes a specific threshold (Knaub, 1987; Ioannidis, 2007; Ronald et al., 2016), because p-values are sample size dependent and can be misleading in some cases. Instead, standard errors and confidence

intervals are more practically interpretable than a p-value (Knaub, 1987; Ranstam, 2012). Even though the p-value of AADT is 0.1879, many previous studies indicated that traffic volume could affect the deterioration rate of pavement friction (Cenek, 2004; Rezaei et al., 2011; Kotek and Florkova, 2014), and therefore AADT is retained for the model development. The R-squared value of the final MLR model is 0.74 and the p-value of the final model is smaller than 2.2e-16 indicating that the model explains most of the variability of the response data around its mean and the model fits the data well.

Table 5.8. OLS Multiple Linear Model Statistics with All Variables

Coefficients	Estimate	Std. Error	t value	Pr(>|t|)	Sig. Level
(Intercept)	3.7800	0.7874	4.8000	3.77E-06	***
Treatment_HFST	-0.1764	0.0757	-2.3300	2.11E-02	*
Treatment_Microsurfacing	-0.0162	0.0522	-0.3110	7.56E-01	
Treatment_HMA	-0.0337	0.0458	-0.7360	4.63E-01	
Treatment_UTBWC	-0.0263	0.0531	-0.4960	6.21E-01	
Treatment_WMA	-0.0863	0.0544	-1.5860	1.15E-01	
AADT	-3.90E-06	2.98E-06	-1.3060	1.93E-01	
TAADT	4.58E-08	9.59E-07	0.0480	9.62E-01	
Age	-0.0214	0.0060	-3.5920	4.43E-04	***
Temp	-0.0030	0.0004	-8.4340	2.50E-14	***
MPD	-0.6996	0.5813	-1.2030	2.31E-01	
IRI	-0.0003	0.0002	-1.4150	1.59E-01	
Rutting	-0.0238	0.0997	-0.2390	8.12E-01	
MD	-0.0099	0.0032	-3.1040	2.28E-03	**
NMAS	-0.0534	0.0105	-5.0920	1.04E-06	***
TB	-0.0004	0.0002	-2.0470	4.24E-02	*
AB	-0.0005	0.0001	-6.4730	1.27E-09	***
SB	-0.9141	0.8850	-1.0330	3.03E-01	
TC	0.0029	0.0013	2.1900	3.01E-02	*
AC	-0.0040	0.0023	-1.7590	8.06E-02	.
SC	0.0105	0.0035	3.0040	3.12E-03	**

Notes: (1) Significance codes: 0 - '***', 0.001 - '**', 0.01 - '*', 0.05 - '.', 0.1 - ' ';
(2) Residuals: Min (-0.14763), 1Q (-0.03976), Median (-0.00279), 3Q (0.03296), Max (0.18043);
(3) Multiple R-squared: 0.7682, Adjusted R-squared: 0.7375;
(4) F-statistic: 25.02 on 20 and 151 DF, p-value: < 2.2e-16.

AADT, treatment age, ambient temperature, MD loss and NMAS demonstrate negative correlations with friction number, which agrees with the findings from the previous studies (Noyce, 2005; Anupam, 2013; Kassem et al., 2013; Wang and Wang, 2013; Susanna et al., 2017). Unexpectedly, angularity also shows negative correlation to friction, which seems to be against the engineering wisdom. A study by National Center for Asphalt Technology (NCAT, 2017) also found that “although an aggregate might be initially characterized by a high level of angularity and measure good friction values, it may not be suitable for a pavement surface layer if the aggregate cannot maintain a sufficient level of friction due to polishing under traffic.” Another study by Moaveni et al. (2014) found that pavement microtexture could be significantly affected by the angularity of aggregates for certain surfacing types.

Change of texture and sphericity due to MD polishing are positively correlated to friction, which seems plausible. Aggregate polishing and degradation have an adverse impact on aggregate surface texture and sphericity, accelerating the surface deterioration and decreasing friction performance (Rezaei et al., 2009; Fowler and Rached, 2012). A greater negative value of texture (sphericity) loss means higher texture (sphericity) value after MD polishing, indicating the aggregate is more durable and resistant to polishing and abrasion, resulting in longer pavement service life in terms of skid resistance (Neaylon, 2009; Smith et al., 2009).

Table 5.9. OLS Multiple Linear Model Statistics with Significant Variables

Coefficients	Estimate	Std. Error	t value	Pr(>|t|)	Sig. Level
(Intercept)	2.41E+00	1.40E-01	17.167	< 2e-16	***
AADT	-2.02E-06	1.15E-06	-1.757	8.07E-02	.
Age	-0.0122	0.0022	-5.4710	1.66E-07	***
Temp	-0.0029	0.0004	-8.2760	4.34E-14	***
MD	-0.0045	0.0013	-3.5080	5.83E-04	***
NMAS	-0.0354	0.0026	-13.3730	< 2e-16	***
AB	-0.0004	0.0000	-9.6630	< 2e-16	***
TC	0.0050	0.0006	7.8600	4.93E-13	***
SC	0.0110	0.0011	9.7740	< 2e-16	***

Notes: (1) Significance codes: 0 - '***', 0.001 - '**', 0.01 - '*', 0.05 - '.', 0.1 - ' ';
(2) Residuals: Min (-0.142039), 1Q (-0.045609), Median (-0.002986), 3Q (0.037980), Max (0.179431);
(3) Multiple R-squared: 0.7393, Adjusted R-squared: 0.7265;
(4) F-statistic: 57.78 on 8 and 163 DF, p-value: < 2.2e-16.

It is worth stating that aggregate properties have showed a more significant effect on pavement friction than the PM treatment types on skid performance. When both PM treatment type and aggregate property related variables are included as the influencing factors for the friction prediction model development, PM treatment does not show a statistical significance on friction. To demonstrate the impacts of pavement treatments on friction, another prediction model is developed considering PM treatments and several other external parameters as the influencing factors, while excluding aggregate characteristics from the model. Although MPD, IRI, Rutting, NMAS and MD are considered in the initial model development, they do not show significant influence on friction in this model since the p-value is much greater than 0.05. The refined model results are shown in Table 5.10. Total traffic volume, pavement age and temperature are negatively correlated to pavement friction. All the PM treatment types, except for the WMA overlay and chip seal treatments, show

significant influences on pavement friction. In this study, a limited number of testing sites was constructed with WMA and chip seal, which probably interprets its insignificance to the model. The intercepts of the model for the PM treatments shows the following sequence from high to low: HFST > Microsurfacing > UTBWC > Resurface > Chip seal > WMA overlay. Such results are consistent with those from several previous studies (Moravec, 2013; Ji et al., 2015; Li et al., 2016). The R-squared value of this model is 0.51, which is smaller than the model developed in this study based on aggregate characteristics as the influencing variables.

Table 5.10 Regression Model with Treatment Types but not Aggregate Characteristics as the Influencing Factors

Variable	Estimate	Std. Error	t-value	Pr(>|t|)	Sig. level
(Intercept)	0.7118	0.0557	12.768	< 2.2e-	***
HFST	0.3521	0.0581	6.0614	0.0000	***
Microsurfacing	0.2021	0.0708	2.8537	0.0048	**
HMA	0.1117	0.0535	2.0886	0.0379	*
UTBWC	0.1450	0.0642	2.2586	0.0249	*
WMA	-0.0059	0.0633	-0.0931	0.9259	
Chip seal	0	-	-	-	
TAADT	-2.31e-06	0.0000	-3.2463	0.0014	**
Age	-0.0266	0.0064	-4.1755	0.0000	***
Temp	-0.0031	0.0003	-	< 2.2e-	***
				R^2	0.5143
				Adj. R^2	0.5000
				P-value	< 2.2e-16

. Significant level=0.1, * Significant level=0.05, ** Significant level=0.01, ***Significant level=0.001

5.6 Summary

In the field, the PaveVision3D system equipped with the AMES high-speed profiler was used to collect 1mm 3D surface and texture data at highway speed with

full-lane coverage. Grip Tester, a trailer-based continuous surface friction measuring device, was used to measure pavement surface skid resistance. For each preventive treatment testing site, four to seven rounds of field data collection activities were performed. Pavement performance data in terms of cracking, rutting, IRI, texture, and friction number were obtained and analyzed. In particular, the friction and texture characteristics were compared among pavement treatment types and aggregate sources. The effectiveness of HFST in reducing crashes was evaluated and the deterioration of pavement skid resistance was also investigated. Subsequently, statistical analyses were performed to evaluate the effects of various factors, such as the preventive treatment type, aggregate properties, surface age and traffic level, on pavement skid resistance. Seven independent variables, namely ambient temperature, treatment age, Micro-Deval loss, nominal maximum aggregate size, angularity before MD polishing, change of texture and sphericity after MD polishing, were found to be statistically significant at the 95% confidence level for the prediction of pavement friction. It was found that aggregate properties have more significant effect on pavement friction than the PM treatment types. When both PM treatment type and aggregate property variables are included as the influencing factors for the friction prediction model development, PM treatments do not statistically show any significant influence on friction. The skid resistance deterioration model is further used in Chapter 6 for the life cycle cost analysis.

CHAPTER 6 LIFE CYCLE COST ANALYSIS

6.1 Introduction

Preserving infrastructure, such as pavement, has become an issue as transportation agencies are increasingly challenged with “high user demand, stretched budgets, declining staff resources, increasing complexity, more stringent accountability requirements, rapid technological change and a deteriorating infrastructure” (FHWA, 2007). Preservation is especially critical in Oklahoma due to its relatively small transportation budget and correspondingly fragile maintenance budget (Riemer et al., 2010). It is “more cost effective to continuously increase the number of lane-miles of pavements that are candidates for pavement preservation (i.e., good condition)” than to “do nothing” and allow pavements to deteriorate to the point of requiring costly rehabilitation or reconstruction (SCDOT, 2016). Theoretically, this proactive approach could reduce the amount of “costly, time consuming rehabilitation and reconstruction projects” and “provide the traveling public with improved safety and mobility, reduced congestion and smoother, longer lasting pavements” (Geiger, 2005).

Transportation agencies “continue to advocate for the measurement of maintenance expenditures, consideration of such costs in lifecycle evaluations of specific pavement investments, and estimation of the financial needs for maintenance” (Volovski et Al., 2017). “The core of transportation decision making is the evaluation of transportation projects and programs in the context of available

funding" (Sinha, 2007). Tools are available to agencies for "evaluating costs, benefits, timing, longevity and decision-making process to determine an effective pavement preservation program" (MnDOT, 2014). However, relevant literature, historical cost data and treatment timing data are still limited, hampering an agency's ability to use these tools to evaluate investments (Volovski et al., 2017).

Economic analysis is a vital component to *Transportation Asset Management*, and specifically, *Pavement Preservation*, and its application has long been promoted by the FHWA to "highway project planning, design, construction, preservation, and operation" (FHWA, 2005), for cost-effectiveness evaluation and accountability (FHWA, 2007). "Considering the annual magnitude of highway investments, the potential savings from following a cost-effective approach to meeting an agency's performance objectives for pavements are significant" (Peshkin et al., 2004), thus, allowing agencies to stretch the budget to address sustainability needs in infrastructure and enhance stewardship.

To be effective, every programming framework should include a mechanism for assessing the cost effectiveness of alternatives considered for implementation (Sinha, 2007). Life cycle cost analysis (LCCA) is an engineering economic analysis tool that is useful (FHWA, 2002), and some state agencies are required to conduct LCCA for pavement construction and rehabilitation decision making (MnDOT, 2017), although it is not commonly being used by frontline pavement managers to determine the most cost-effective pavement preservation treatment alternative for a given project (Gransberg et al., 2010; Bilal et al., 2009; J. Hall et al., 2009; Monsere et al., 2009; Cambridge et al., 2005). It has also been noted that the level of

complexity associated with developed tools and data collection effort should be commiserate with the impact of the decision-making process that is facilitated ("funding is to [be used to] improve road infrastructure, not to make decisions") (MnDOT, 2014). LCCA can become quite complex, so an analyst should be judicious about the level of detail included (FHWA, 1998). The analysis can be simplified by including only differential costs, i.e. omitting those that cancel out, as well as disregarding those costs that contribute minimal or no impact on the results (FHWA, 1998). The goal is to implement costing tools that are "simple, effective, and relevant" (MnDOT, 2014).

LCCA can facilitate a pavement preservation strategy and can benefit the "user (reduced travel time, vehicle operating, accidents), agency (timely and appropriate maintenance and rehabilitation), and public (objective, consistent, transparent, and repeatable decision making)" (Falls and Tighe, 2004). The FHWA states the following purpose for LCCA use:

> "LCCA is an analysis technique that builds on the well-founded principles of economic analysis to evaluate the over-all-long-term economic efficiency between [mutually exclusive] competing alternative investment options. It does not address equity issues. It incorporates initial and discounted future agency, user, and other relevant costs over the life of alternative investments. It attempts to identify the best value (the lowest long-term cost that satisfies the performance objective being sought) for investment expenditures." (FHWA, 1998)

The FHWA offers “LCCA Principles of Good Practice” in its *Life Cycle Cost Analysis in Pavement Design, Interim Technical Bulletin* released in 1998. “Good Practice” is that *constant dollars* and *real discount* rate be used for the purposes of discounting future costs (i.e. omit inflation and effects). FHWA recommends a rate between 3-5% be used in analyses, which is consistent with the OMB Circular A-94. Other “LCCA Principles of Good Practice” are integrated with the LCCA procedures/methodology.

6.2 Life Cycle Cost Analysis Procedures

The following are LCCA procedures, as excerpted from the FHWA *Life Cycle Cost Analysis Primer* (FHWA 2002) and the *Interim Technical Bulletin* (FHWA 1998):

1) Establish design alternatives [and analysis period];
2) Determine [performance period and] activity timing;
3) Estimate costs [agency and user];
4) Compute [net present value] life cycle costs;
5) Analyze results;
6) Reevaluate design strategies (FHWA, 2002; FHWA, 1998).

6.2.1 Design Alternatives and Analysis Period

The first step in the procedure involves establishing strategies, i.e. associated rehabilitation and maintenance activities of each alternative expected over the analysis period (FHWA, 1998). The analysis period can be selected by various

methods when alternatives have differing performance periods for the purposes of comparing all alternatives over a “common period of time”, which is an engineering economic analysis principle (White et al., 2010). The general suggestion when using the net present value (NPV) method is that the analysis period be a standard length, such as 35-40 years, and long enough to allow “at least one major rehabilitation activity” for each design alternative (FHWA, 2002). When using the equivalent uniform annual cost (EUAC) method, the analysis period can vary with the caveat that any service life truncations will be addressed (Pittenger et al., 2011, Bilal et al., 2009). To avoid the common “mistake” associated with employing the EUAC method, the analyst must consider any encroachment for engineering economic principles adherence (White et al., 2010; Lee, 2002). For example, if a treatment has a typical five-year service life, but the next pavement intervention is planned in three years, then the anticipated service life value used in the LCCA must be three years to get a more accurate estimate for life cycle cost.

6.2.2 Performance Period and Activity Timing

The second step involves determining the performance period (i.e. cash flow diagram) for an alternative, which is the period that covers one life cycle of that alternative. It is generally determined by the analyst’s judgment based on experience and historical data (FHWA, 1998). Activity timing includes the determination of maintenance and other activity frequency associated with a specific alternative strategy.

6.2.3 Agency and User Costs Estimation

The third step involves determining or estimating agency and user costs for each of the competing alternatives. Agency and user costs are determined for each of the competing alternatives and future costs are "discounted" to determine the NPV. Agency costs are those costs directly incurred by the agency, such as costs for project supervision and administration, materials, labor and traffic control for the initial installation, as well as any associated rehabilitation and maintenance costs required over the life cycle of the alternative. These costs are generally based on current and/or historical costs.

According to the FHWA, *salvage value* is the value associated with each alternative determined at the point of analysis terminal and involves any *residual value* (value attributed to the reclaimed materials) or any *serviceable life* (value attributed to alternative "life" that exists after analysis terminal) and should be attributed to alternatives appropriately for the purposes of analysis (FHWA, 1998). *Sunk costs*, which are costs occurring pre-analysis, should not be included in the analysis unless they specifically apply to the alternatives that are to be compared (FHWA, 1998).

User costs relate to costs incurred by the traveling public in both *work-zone* and *non-work-zone* phases for a given extent of road for which alternatives are being compared (FHWA, 1998). Generally, the user costs incurred during *non-work-zone* phases are disregarded in LCCA due to a lower likelihood of difference among alternatives (FHWA, 2002). Differing [work zone] user costs among alternatives are

pertinent to the analyses, and generally include “[time] delay, vehicle operating, and crash costs incurred by the users of a facility” (FHWA, 1998).

> “User costs are heavily influenced by current and future roadway operating characteristics. They are directly related to the current and future traffic demand, facility capacity, and the timing, duration, and frequency of work zone-induced capacity restrictions, as well as any circuitous mileage caused by detours. Directional hourly traffic demand forecasts for the analysis year in question are essential for determining work zone user costs.” (FHWA, 1998)

It is suggested that “different vehicle classes have different operating characteristics and associated operating costs, and as a result, user costs should be analyzed for at least three broad vehicle classes: Passenger Vehicles, Single-Unit Trucks, and Combination Trucks” (FHWA, 1998). Unit costs are generally translated into monetary terms (for the purposes of analysis) and can be ascertained from various sources, and those costs escalated with the use of the transportation component of the *Consumer Price Index (CPI)* (FHWA, 1998). *Delay* costs are calculated by multiplying the unit of “wait” time attributed to each alternative’s work-zone timings by the monetary unit (FHWA, 1998). *Vehicle operating costs* (VOC) are calculated by multiplying the vehicle-related cost factors attributable to each alternative’s work-zone timings by the monetary unit (FHWA, 1998). Crash costs are calculated by multiplying the number of specific types of crashes by their respective monetary unit (FHWA, 1998). User costs as a result of detours are typically assigned a cents-per-mile rate, such as that used by the Internal Revenue Service for mileage allowance (FHWA, 1998).

6.2.4 Compute Life-Cycle Costs (NPV)

As excerpted from FHWA's LCCA Interim Technical Bulletin:

> "Economic analysis focuses on the relationship between costs, timings of costs, and discount rates employed. Once all costs and their timing have been developed, future costs must be discounted to the base year and added to the initial cost to determine the NPV for the LCCA alternative.

6.2.5 Analyze Results

LCCA has two possible computational approaches: *deterministic* and *probabilistic* (FHWA, 1998). The deterministic approach involves using discrete input values and a single output value and has been the traditional LCCA type used in transportation decision making (FHWA, 2002). A *sensitivity analysis* should be conducted so that the analyst may determine the level of variability of a given input value relative to the output (FHWA, 1998). For example, an analyst chooses a 4% discount rate to do the LCCA, which results in output (a preferred alternative). The sensitivity analysis will allow the analyst to conduct a *What if* scenario to determine if choosing a 5% discount rate would result in different output (different preferred alternative). The sensitivity analysis is limited in application because it is unable to analyze simultaneous variability (FHWA, 2002).

A deterministic-type LCCA is less complex than a probabilistic type and can be adequate, and therefore appropriate, when uncertainty is not expected to have a material effect on the outcome of the economic analysis (FHWA, 2003). However, if uncertainty could materially alter the outcome, the deterministic approach is not

recommended because of its inability to effectively analyze simultaneous variability (FHWA, 2003). The stochastic approach using probabilistic methods involves analyzing input value probability based on the full range of *What if* scenarios allowed by sensitivity analysis by providing a distribution of NPV results (FHWA, 2002). It is generally accompanied with a *risk analysis,* which unlike sensitivity analysis, does allow the analyst to determine the level of certainty about simultaneous variability in all input parameters (FHWA, 1998). Stochastic LCCA specifically addresses and quantifies the *uncertainty* associated with a transportation project decision and contributes to decision validation (FHWA, 1998).

The normal distribution is commonly assumed to be the appropriate distribution for data in stochastic analysis and is further justified by the central limit theorem (Montgomery, 2009). The central limit theorem states that most data are "approximately normal" (or approximately symmetric in nature) and grow more normalized as sample size increases (Montgomery, 2009). It also states that it should be applicable in most cases where possible values of a given input are identically distributed and do not "depart radically from the normal" (or are not extremely skewed) (Montgomery, 2009). There is no standard rule for sample size and the central limit theorem. Some smaller samples can be approximately normal, while other cases may need larger sample sizes to fit the normal distribution.

A triangular distribution is a continuous distribution that contains user-defined values for (a) the minimum value, (b) the maximum value and (c) the most likely value for an input variable. It is commonly used for variables that have limited sample data but can be reasonably estimated. This type of distribution may be

appropriate for service life input values. No significant research has been done to quantify the actual service lives of PPTs; therefore, service life data is limited. This type of distribution has also been suggested for discount rate input values of 3, 4 and 5%, the discount range suggested by the FHWA (1998).

FHWA provides guidance for conducting stochastic LCCA (FHWA, 1998), which includes three steps. First, the analyst must decide whether to treat the input values deterministically or probabilistically. Secondly, the input data must be *fitted* to the appropriate probability distribution. Lastly, risk analysis should be conducted. The stochastic LCCA calculation for NPV is illustrated in Figure 6.1.

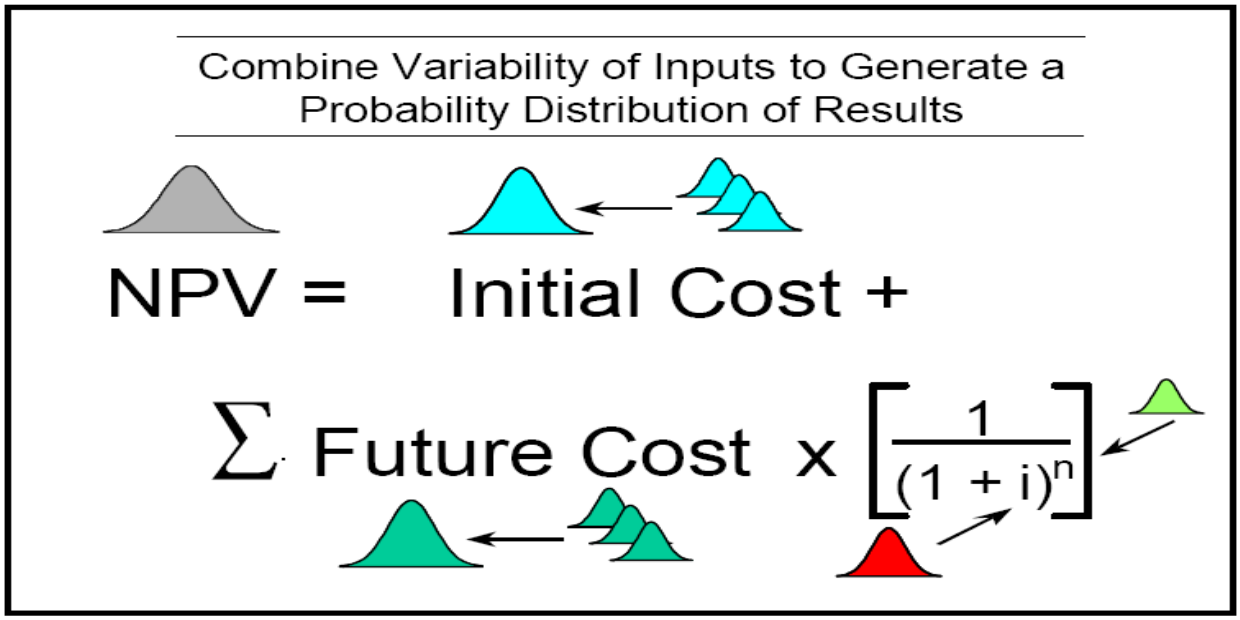

Figure 6.1 Computation of NPV using probability and simulation (FHWA, 1998)

Step 1: Deterministic and Probabilistic Input Value Determination

Step one of stochastic LCCA requires the analyst to identify which input values have associated uncertainty and will have a material effect on the outcome

(FHWA, 2004). Only those values should be treated probabilistically to simplify the analysis (FHWA, 2004). The deterministic approach does not allow probabilistic values, but the probabilistic approach allows deterministic values. If a pavement manager expected service life to contribute uncertainty that would affect outcome, then it should be incorporated into the analysis in a probabilistic manner (represented as a probability distribution). If material cost was not expected to have an impact, then it could be treated deterministically (represented as a point estimate). If the pavement treatment was expected to incur maintenance costs comparable to those of other alternatives and would not have a material effect on the output, those costs could be ignored altogether (FHWA, 1998). Input value distributions can be subjectively defined based on the pavement manager's judgment or objectively defined based on historical or current data from sources like bid tabulations and pavement management systems. Ultimately, the analyst must use judgment to properly assess and address uncertainty in analyses.

Step 2: Selecting Appropriate Probability Distributions

The second step of a stochastic analysis is to "fit" a given data set to the "best" theoretical probability distribution (FHWA, 1998). This is commonly accomplished with statistically-based *goodness-of-fit* tests, such as Anderson-Darling (A-D) and chi-squared (χ^2) tests (Lomax, 2007). Software is available that can execute the task in seconds (Pallisade, 2011). Determining the appropriate probability distribution for given data is a critical step to ensure output validity,

because the LCCA is based upon the theoretical probability distribution, *not* the actual data (Lomax, 2007; Tighe, 2001).

Step 3: Risk Analysis

The third step of a stochastic approach is *risk analysis* (FHWA, 1998), which is based on probability theory. It can be defined as a "systematic use of available information to determine how often specified events may occur and the magnitude of their consequences" (Palisade, 2011). Like sensitivity analysis, risk analysis seeks to expose uncertainty associated with input parameters. Risk analysis differentiates itself from sensitivity analysis because it combines "probabilistic descriptions of uncertain input parameters with computer simulation to characterize the risk associated with future outcomes" (FHWA, 1998). It also allows the analyst to assess variability in all input parameters simultaneously (FHWA, 1998). Risk analysis can be conducted on a deterministic basis or a stochastic basis, although employing deterministic risk analysis (like triangular distribution) results in oversimplification and reduced accuracy (Palisade, 2011). A Monte Carlo simulation satisfies the conditions of a probabilistic, quantitative risk analysis and is the type used in this research. Monte Carlo simulation is a "computerized mathematical technique that allows people to account for risk in quantitative analysis and decision making" (Palisade, 2011).

6.2.6 Reevaluate Design Strategies

LCCA results should be coupled with other decision-support factors such as "risk, available budgets, and political and environmental concerns" (FHWA, 2002). The output from an LCCA should not be considered the answer, but merely an indication of the cost effectiveness of alternatives (FHWA, 1998). Considering cost effectiveness without also considering treatment effectiveness (and vice versa), or the *economic efficiency* of a treatment, may not provide the whole picture either and may result in not selecting the "best" alternative (Bilal et al., 2009).

6.3 Performance-Based LCCA of Pavement Treatments

This research aims to develop, complete and report economic and life cycle cost analysis using deterministic and stochastic engineering economic analysis so that a friction-based cost model may be created that can produce standardized results relevant to pavement managers when comparing pavement preservation alternatives. As pavement preservation becomes increasingly vital to sustainability in infrastructure, it has become apparent that economic analysis, specifically LCCA, could be an essential tool in assisting ODOT pavement managers in the selection of cost-effective alternatives that may yield extended service lives of Oklahoma pavements. This LCCA research is the synthesis of a comprehensive literature review and inclusion of pavement preservation treatment field trial data via pavement performance (friction) models, which is becoming common practice (Volovski et al., 2017; Choi et al., 2016; MnDOT, 2014).

Surveys of ODOT staff were conducted in a previous study to determine status and inputs to LCCA for pavement preservation treatment evaluation (Zaman et al., 2012). The responses indicated that initial cost plays a primary role when deciding which pavement treatment to employ and that long-term cost or cost-effectiveness of a treatment selection is not considered, i.e. performance-based LCCA is not conducted. The survey also yielded information about other decision-making factors, as well as the types of preservation and maintenance treatments typically applied in Oklahoma, and each treatment's cost range, productivity range and typical service life range based on factors such as average annual daily traffic (AADT), percent truck traffic and pavement condition. This information will be used to provide context for this study's results.

LCCA Equivalent Uniform Annual Cost (EUAC) Method

Maintenance funding is authorized on an annual basis making comparing alternatives on an annual cost basis more closely fit the funding model than using NPV which would assume availability of funds across the treatment's entire service life (Pittenger et al., 2011). Equivalent Uniform Annual Cost Method (EUAC) has been deemed appropriate for this application (MnDOT, 2014; Thoreson et al., 2012; Gransberg and Scheepbouwer, 2010; Bilal et al., 2009; Sinha and Labi, 2007). Therefore, it was selected for the model used in this research. EUAC can provide an annualized cost for a pavement treatment. Figure 6.2 shows an example illustration of EUAC LCCA based upon pavement condition.

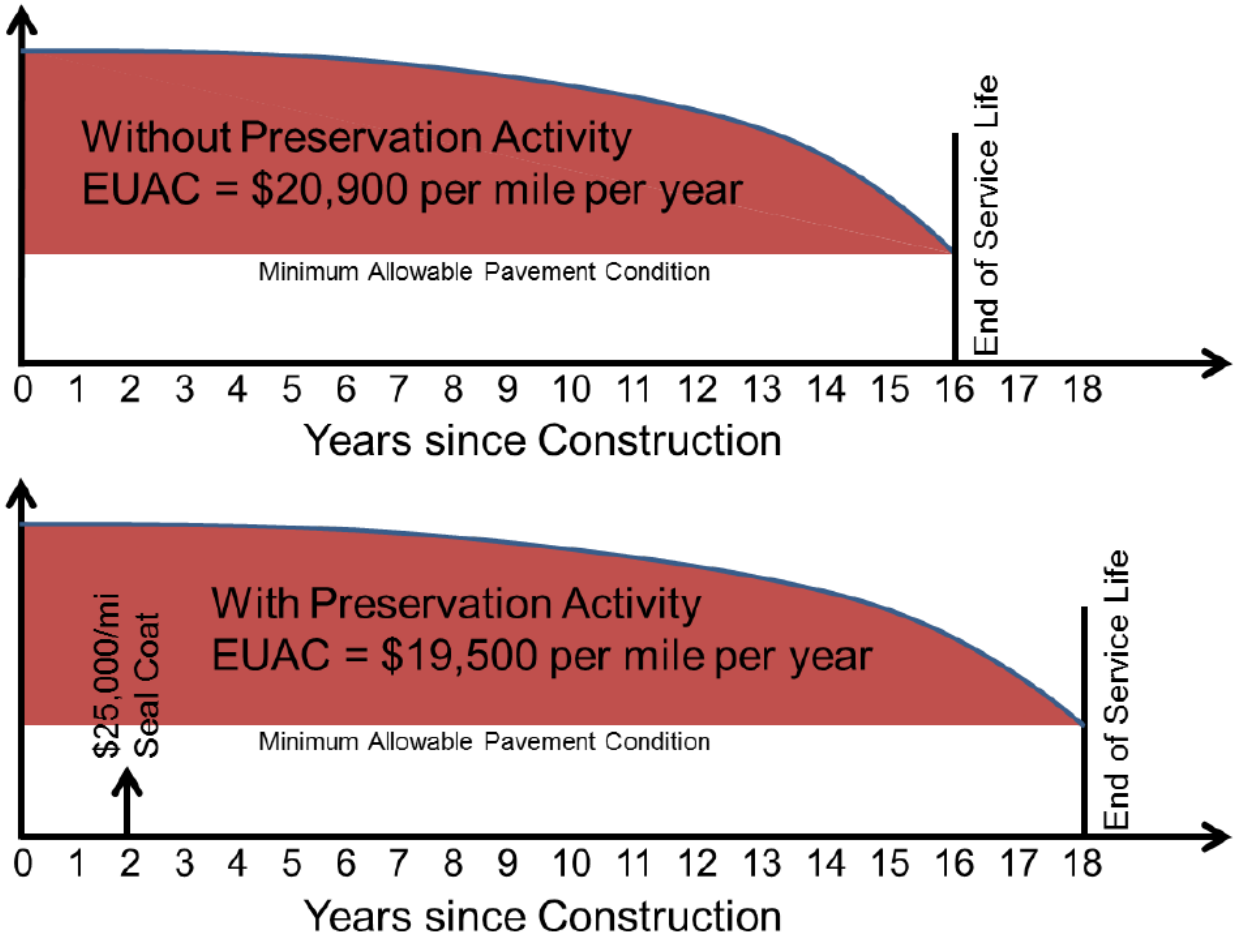

Figure 6.2 Example LCCA using EUAC Method (MnDOT 2014)

The application of the EUAC LCCA model used in this research is informed by the OLS friction prediction model created for this project. Input values are based upon field trial, vendor and ODOT survey data, literature review results and bid tabulations. The model's logic is shown graphically in the flow chart found in Figure 6.3. The LCCA procedures, as excerpted from the FHWA *Life Cycle Cost Analysis Primer* (FHWA, 2002) and the *Interim Technical Bulletin* (FHWA, 1998) and discussed in the previous section of this writing, serve as the basis for the EUAC model.

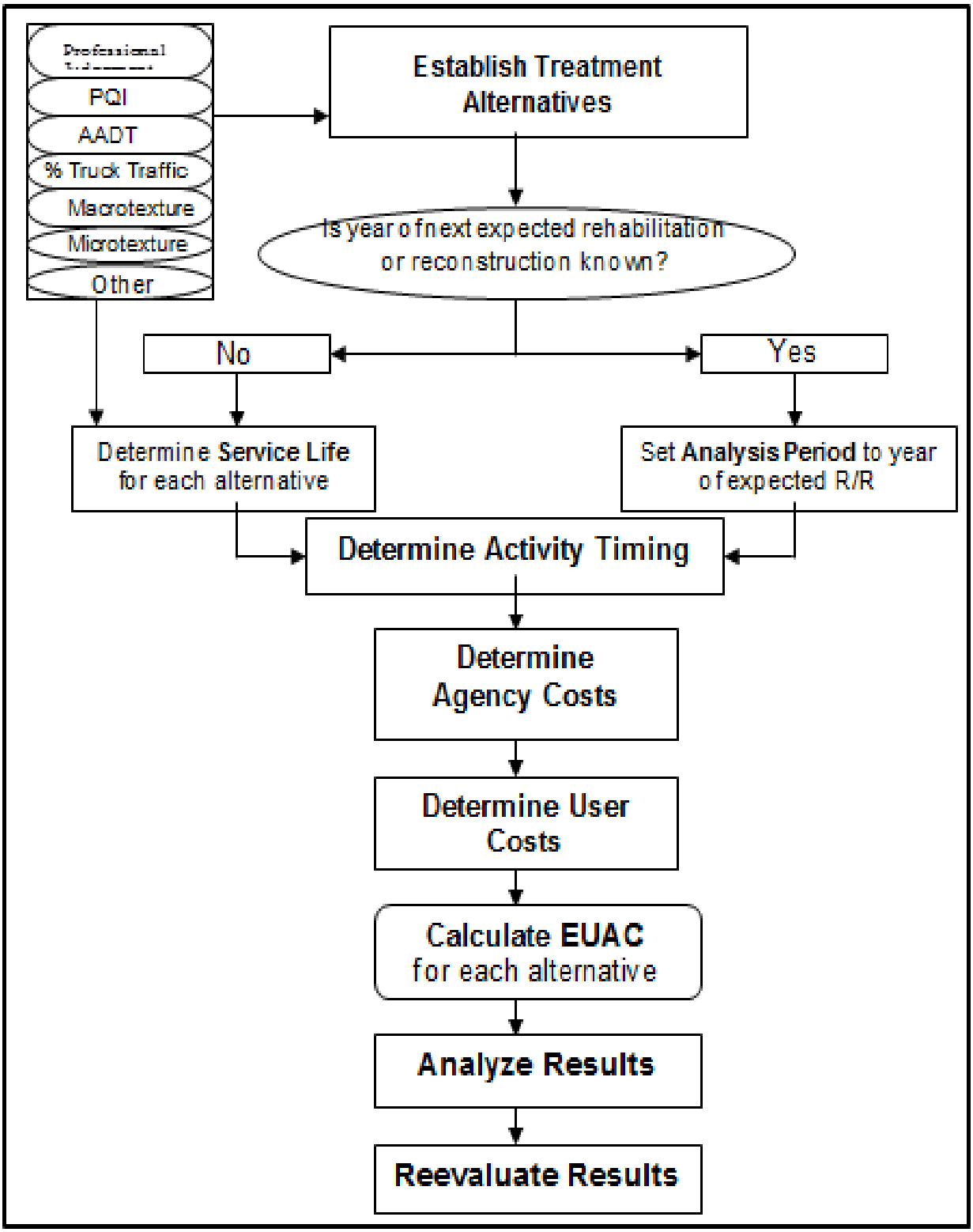

Figure 6.3 Pavement Preservation EUAC LCCA Model Logic

LCCA Step 1: Establish [pavement treatment] alternatives [and analysis period]

Each alternative's service life is selected consistent with the EUAC method. The AP for each treatment alternative is equal to its own *anticipated service life* ($ASL_{alt} = AP_{alt}$) (Pittenger et al., 2011).

LCCA Step 2: Determine [service life and] activity timing

The next step is to enter service-life length for each alternative. This step should be exercised with care due to the sensitivity of the parameter (FHWA, 1998). Friction is an indicator of treatment performance that can be used "to maintain an appropriate level of pavement friction for all pavement sections within the highway network, based on each section's friction demand" (Hall et al., 2003). Friction data can also be used to evaluate economic performance of a treatment (Zaman et al., 2012). Specifically, friction data can be used to determine service life values based upon actual local performance, which can yield superior results to empirical values (Volovski et al., 2017; Choi et al., 2016; MnDOT, 2014; Bilal et al., 2009; Reigle and Zaniewski, 2002). Table 6.1 provides the information used in EUAC evaluation. Service life input for each treatment is provided as a value range and is informed by ODOT survey results, literature review and performance data (Zaman et al., 2012; Bilal et al., 2009; Stroup-Gardiner and Shatnawi, 2008; FHWA, 2005; Reigle and Zaniewski, 2002).

Table 6.1 Pavement Treatment Service Life Estimation

Pavement Preservation Treatment	Service Life (range, years)
Thin-Lift Hot Mix Asphalt (HMA)	8 – 12
Thin-Lift Warm Mix Asphalt (WMA)	8 – 12
Permeable Friction Course (PFC)	8 – 12
Chip Seal	3 – 5
Ultra-Thin Bonded Wearing Course	8 – 10
High Friction Surface Treatment	7 – 12
Microsurfacing	7 – 10

After determining service life, Step 2 of the LCCA process requires determining maintenance activity timing. For this demonstration, maintenance includes crack seal and 2%-of-total-area patching with a three-year frequency for all asphalt treatments (Zaman et al., 2012).

LCCA Step 3: Estimate Agency & User Costs

The next step is to estimate agency and user costs associated with the pavement treatments being evaluated. Due to the lack of robust historical cost data, agencies have been using average values for cost data “that typically have large standard deviations or cost ranges that are too large to assist in any meaningful prediction of maintenance costs for specific highway segments” (Volovski et al., 2017). Therefore, costs should be scrutinized and carefully selected. The average cost for treatments used in this study are shown in Table 6.2. These values are informed by the ODOT survey and verified by field trial data, literature review (Stroup-Gardiner and Shatnawi, 2008; FHWA, 2005; Bausano et al., 2004) and ODOT bid tabulations.

Table 6.2 Average Pavement Treatment Cost

Pavement Treatment	Average Cost per Square Yard
Thin-Lift Hot Mix Asphalt (HMA)	3.25
Thin-Lift Warm Mix Asphalt (WMA)	3.25
Chip Seal	1.77
Permeable Friction Course	3.75
Ultra-Thin Bonded Wearing Course	4.00
High Friction Surface Treatment	19.00
Microsurfacing	2.50

User costs do not need to be included in LCCA if installation time and frequency for the pavement preservation treatments being considered differ greatly (Bilal et al., 2009). Therefore, user costs were not calculated for this demonstration.

LCCA Step 4: Compute Life Cycle Costs

The EUAC model used in this research calculates life cycle cost for each alternative based on the EUAC method (Pittenger et al., 2012). All incurred costs expected throughout the service life of an alternative are brought to a base year, summed, and then annualized according to the *treatment's service life* as proposed in this research, determined by field data and pavement manager professional judgment.

The discount rate selected for the demonstration of the model was 4%. Project length input was one lane-mile. The life cycle cost calculations were conducted to determine the EUAC of each alternative. LCCA input values and output

results for this scenario are shown in Table 6.3. The results were manually verified (Zaman et al., 2012).

Table 6.3 Life Cycle Cost and Service Life Input for EUAC Calculation

Treatment	Cost (Average, $ per SY)	Service Life (Range, in Years)	EUAC (mean, $ per lane mile)
Thin-Lift Hot Mix Asphalt (HMA)	3.25	8 – 12	3,500
Thin-Lift Warm Mix Asphalt (WMA)	3.25	8 – 12	3,500
Chip Seal	1.77	4 – 6	3,700
Permeable Friction Course	3.75	8 – 12	3,800
Ultra-Thin Bonded Wearing Course	4.00	8 – 10	4,400
High Friction Surface Treatment	19.00	7 – 12	17,700
Microsurfacing	2.50	7 – 10	3,100

In this scenario, the chip seal has the lowest initial cost, but the microsurfacing and asphalt (HMA/WMA) treatments have lower life cycle costs. However, inherent variability in LCCA parameters (e.g. service life) can provide different outcomes, so results should be analyzed for sensitivity (Zaman et al., 2012).

LCCA Step 5: Analyze the Results

Deterministic (empirical and performance-based) and stochastic methods are used to expose sensitivity in LCCA and support decision making. Essentially, the variability (uncertainty) of critical LCCA parameters are evaluated to determine when output rankings change in a manner that would materially alter the decision-making information. Service life and discount rate values are generally sensitive parameters

(FHWA, 1998), so both are analyzed for sensitivity. Additionally, the EUAC output is analyzed for sensitivity by using the OLS performance prediction model created for this study.

Analyze LCCA Results – Deterministic Methods

The deterministic, performance-based analysis is a relatively new concept that can be used to assess pavement preservation treatment's *economic efficiency* that derives cost as a function of service life (Pittenger et al., 2011; Bilal et al., 2009; Reigle and Zaniewski, 2002). The service life value is based upon *actual* performance data rather than assumption. Incorporating performance data into analyses may contribute to determining the optimal preservation timing (Peshkin et al., 2004) so that a pavement manager can install the "right treatment to the right road at the right time" (Galehouse et al., 2003). Friction values (deterministic, performance-based) are routinely collected by ODOT and can be extrapolated to estimate service life duration based upon *localized* performance (Pittenger et al., 2011). These parameters were used to verify the sensitivity of the service life value in the LCCA.

The discount rate used in the LCCA is generally a sensitive parameter and the sensitivity should be analyzed on a case-by-case basis (FHWA, 1998). For example, when selecting a *discount rate less than 4%,* the HMA could have a lower EUAC ($4,580) than chip seal ($4,643). When *using a discount rate higher than 4%*, the HMA could have a higher EUAC ($4,814) than chip seal ($4,749). This means

that the selection of a discount rate could effectively drive the pavement preservation design decision between these three alternatives.

Sensitivity analysis can also be based upon critical, performance-driven factors (Volovski et al., 2017; Choi et al., 2016), such as those factors captured in the OLS performance prediction model. The analyst can compare the performance-based output to the empirical data-based output to assess sensitivity (Volovski et al., 2017; Choi et al., 2016). For example, the impact of traffic level (AADT) on chip seal service life can be considered and quantified in terms of dollars and can indicate the sensitivity of the chip seal EUAC.

A performance-based cost sensitivity model was created in this study to analyze the sensitivity of EUAC output for pavement treatments based upon performance parameters (Equation 6.2). Internal validation of the model was conducted to verify model output. Because the model operates on the function of cost and because it assumes linearity, validation methods used interpolation and extrapolation values to manually verify the model algorithm. The mean values of performance parameters and cost data can be used to compute a baseline EUAC for sensitivity analysis of the cost for pavement maintenance treatments (Volokski et al., 2017; Choi et al., 2016).

EUAC=(2.41+(-2.02E-06*AADT)+(-0.0122*Age)+(-0.0029*Temp)+(-0.0045*MD)+(-0.0354*NMAS)+(-0.0004*AB)+(0.005*TC)+(0.011*SC))^-(EXP LCCA) (Eq. 6.2)

Where EUAC is the value of the treatment cost based upon friction performance parameters and the exponent (EXP_{LCCA}) is calculated when solving with the "base case" using the mean EUAC LCCA output. The response variable, EUAC, was transformed as EXP_{LCCA} of the expenditure to satisfy the OLS linearity assumption (Volokski et al., 2017). Other equation terms were previously defined in Equation 6.1 section. The "base case" equation is calculated using the mean values for each variable in the multivariate regression equation (Table 6.4).

Table 6.4 Descriptive Statistics of Critical Performance (Friction) Factors

Statistics	AADT	Age	Temp	MD	NMAS	AB	TC	SC
Min	30.00	0.25	35.00	1.70	4.75	1998.10	-29.70	-19.40
Max	25155.00	15.47	96.00	21.90	12.50	3636.50	-1.50	9.70
Range	25125.00	15.22	61.00	20.20	7.75	1638.40	28.20	29.10
Median	2684.50	2.61	74.00	8.20	12.50	3227.50	-8.90	-2.50
Mean	4410.59	3.19	73.15	8.73	11.21	2969.54	-12.13	-2.14
Variance	37086440.0	5.75	229.18	28.13	6.03	297434.10	81.93	33.46
Std Dev.	6089.86	2.40	15.14	5.30	2.46	545.38	9.05	5.78
Coef Var.	1.38	0.75	0.21	0.61	0.22	0.18	-0.75	-2.70

A useful application for this equation is in predicting overall annual expenditures for system-level management (Volokski et al., 2017). Using the equation and baseline EXP_{LCCA}, sensitivity analysis can be conducted on costs based upon performance (friction) parameters (Volokski et al., 2017; Choi et al., 2016). However, the estimates from this type of equation "may not be appropriate for a specific pavement segment due to the large variability associated with this data" (Volokski et al., 2017). For example, pavement age is averaged across all treatment types although treatment service life lengths vary considerably. "This variability may be relatively inconsequential for state-level forecasting, but could lead to unreliable

predictions of maintenance expenditures for specific pavement sections" (Volokski et al., 2017). Because pavement age and condition are highly correlated, it is "often not possible to include both as separate terms in a model with intuitive and statistically significant parameter estimates. Modeling pavement maintenance expenditures as a function of both cost and condition would yield multicollinearity, resulting in inconsistent parameter estimates" (Volokski et al., 2017). Therefore, the cost and condition factors in this study have been dynamically modeled separately and the static performance model output will serve only as a sensitivity analysis for the static LCCA model output.

Linear regression using OLS (performance model) estimation was used to evaluate the effect of performance (friction) variables on pavement treatment cost (Volokski et al., 2017). Table 6.5 provides linear regression equations created from calculated LCCA output cost values that were used to determine the treatment-specific EXP_{LCCA}. Beyond the baseline value, the model can provide EXP_{LCCA} (y) for a specific treatment with a given value for service life (x) to determine sensitivity for the EUAC distribution of a given treatment based upon performance parameters. The R-squared value is 1 because each equation was created by interpolating linearly between the range of given LCCA output values for each treatment.

Table 6.5 Treatment-specific EXP_{LCCA} - Exponent Relationships

Treatment, Exponent Relationship	
Hot Mix/Warm Mix Asphalt	y = 0.3348x - 11.324
Chip Seal	y = 0.5323x - 12.152
Permeable Friction Course	y = 0.3366x - 11.463
Ultra-Thin Bonded Wearing Course	y = 0.3833x - 11.926
High Friction Surface Treatment	y = 0.412x - 13.704
Microsurface	y = 0.3622x - 11.331

Table 6.6 provides performance-based cost sensitivity model (static) inputs, which will be used to evaluate sensitivity of individual performance parameters on cost. Results for various scenarios are demonstrated in this section and provided in Appendix B.

This type of sensitivity analysis will reveal how sensitive an EUAC is to a specified performance factor. Sensitivity analysis of a treatment's EUAC is conducted by changing one variable within the performance model while holding all other variables constant.

Table 6.6 LCCA Output Values and Corresponding EXP_{LCCA} Values

Pavement Treatment	Performance Model Output	SL	EUAC Model Output	EXP_{LCCA}
HMA/WMA	0.383	8	$ 4,000.00	-8.64
	0.358	10	$ 3,500.00	-7.96
	0.334	12	$ 3,000.00	-7.30
Chip Seal	0.432	4	$ 4,500.00	-10.02
	0.419	5	$ 3,700.00	-9.46
	0.407	6	$ 3,100.00	-8.95
PFC	0.383	8	$ 4,500.00	-8.77
	0.358	10	$ 3,800.00	-8.04
	0.334	12	$ 3,400.00	-7.42
UTBWC	0.383	8	$ 4,900.00	-8.85

Pavement Treatment	Performance Model Output	SL	EUAC Model Output	EXP_{LCCA}
	0.371	9	$ 4,400.00	-8.47
	0.358	10	$ 4,000.00	-8.09
HFST	0.395	7	$ 22,900.00	-10.82
	0.364	9.5	$ 17,700.00	-9.70
	0.334	12	$ 14,700.00	-8.76
Microsurfacing	0.395	7	$ 3,500.00	-8.79
	0.377	8.5	$ 3,100.00	-8.25
	0.358	10	$ 2,700.00	-7.70

Traffic and treatment age have the most influence on treatment life cycle cost. Table 6.7 shows the results for the hot mix/warm mix asphalt treatments based upon level of traffic (AADT) and expected service life. Although EUAC values were determined stochastically in the LCCA process, the sensitivity analysis is conducted with static mean EUAC values for the given service life values, meaning that the only variable changed within the model for this analysis is AADT. This methodology provides relative change to EUAC based upon friction performance. Table 6.7 provides EUAC results for the HMA/WMA treatment given the impact of traffic for three service life length scenarios. The “base case” for traffic in the friction model is 4,410 AADT. The “base case” for each service life’s EUAC in LCCA is its mean. If a segment of road is expected to have less traffic of 2,500 AADT, then the cost of the HMA could be estimated to be about 9% less. Alternatively, for 10,000 AADT, the segment would cost approximately 23% more. Due to the linearity of costs within a service life group in the sensitivity model, the same percentages apply to all HMA/WMA EUACs given this specific LCCA scenario (service life length and EUAC) for the given traffic level.

Table 6.7 HMA/WMA EUAC Sensitivity Analysis: Traffic (AADT)

AADT	EUAC, 8-yr SL (per lane-mile)	EUAC, 10-yr SL (per lane-mile)	EUAC, 12-yr SL (per lane-mile)	Change in EUAC
2,500	$ 3,668.02	$ 3,259.45	$ 2,749.17	-9%
4,410 (mean)	$ 4,000.00 (mean)	$ 3,500.00 (mean)	$ 3,000.00 (mean)	0
10,000	$ 5,180.51	$ 4,580.85	$ 3,842.27	+23%

Table 6.8 also shows the impact of service life length on (mean) EUAC, as calculated in the LCCA model. The lowest EUAC of $2,749.17 is attributed to the longest service life (12 years) and lowest AADT (2,500). The highest EUAC is attributed to the shortest service life (8 years) and the highest AADT (10,000). These results are intuitive; it is known that higher AADTs and shorter service lives have faster deterioration of friction and therefore, more frequent (costly) maintenance interventions. This methodology demonstrates that the impact of various performance parameters can be quantified and evaluated in terms of cost.

Since the performance-based sensitivity model adjusts EUAC as a function of cost, the analyst can evaluate sensitivity based upon an “estimated base case”. Table 6.8 demonstrates traffic and age impact on EUAC from a given “expected” base case scenario for HMA (i.e., 4410 AADT and 10-year service life EUAC from the OLS/ performance model and LCCA model, respectively). As expected, the shorter service life of 8 years will result in added costs: 4.4% more cost in the 2500 AADT scenario and 32.3% more cost when AADT is 10,000. If the HMA treatment gets an additional two years of service life at a lower traffic level (when compared to the 10-year EUAC), then the EUAC can be expected to be 27.3% less.

Performance-based LCCA and sensitivity analysis for other treatment EUACs being evaluated in this study are shown in Table 6.9 to Table 6.13. Given the nature of the sensitivity analysis, scenarios yield similar trends among the treatments.

Table 6.8 Traffic Sensitivity Scenarios for HMA/WMA

Scenario	AADT	Age	EUAC Output from LCCA	Sensitivity (change from base EUAC)
Base Case	4410	10	$ 3,500.03	0.0%
Lower AADT: 8-yr SL	2500	8	$ 3,661.11	+4.4%
Higher AADT: 8-yr SL	10000	8	$ 5,170.35	+32.3%
Lower AADT: 10-yr SL	2500	10	$ 3,259.45	-7.4%
Higher AADT: 10-yr SL	10000	10	$ 4,580.85	+23.6%
Lower AADT: 12-yr SL	2500	12	$ 2,749.17	-27.3%
Higher AADT: 12-yr SL	10000	12	$ 3,842.27	+8.9%

Table 6.9 Traffic Sensitivity Scenarios for Chip Seal

Scenario	AADT	Age	EUAC Output from LCCA	Sensitivity (change from base EUAC)
Base Case	4410	5	$ 3,700.03	0.0%
Lower AADT: 4-yr SL	2500	4	$ 4,115.78	+10.1%
Higher AADT: 4-yr SL	10000	4	$ 5,867.24	+36.9%
Lower AADT: 5-yr SL	2500	5	$ 3,393.00	-9.0%
Higher AADT: 5-yr SL	10000	5	$ 4,789.44	+22.7%
Lower AADT: 6-yr SL	2500	6	$ 2,848.69	-29.9%
Higher AADT: 6-yr SL	10000	6	$ 3,986.46	+7.2%

Table 6.10 Traffic Sensitivity Scenarios for PFC

Scenario	AADT	Age	EUAC Output from LCCA	Sensitivity (change from base EUAC)
Base Case	4410.59	10	$ 3,800.03	0.0%
Lower AADT: 8-yr SL	2500	8	$ 4,120.70	+7.8%
Higher AADT: 8-yr SL	10000	8	$ 5,848.42	+35.0%
Lower AADT: 10-yr SL	2500	10	$ 3,486.75	-9.0%
Higher AADT: 10-yr SL	10000	10	$ 4,914.22	+22.7%
Lower AADT: 12-yr SL	2500	12	$ 3,122.21	-21.7%
Higher AADT: 12-yr SL	10000	12	$ 4,387.17	+13.4%

Table 6.11 Traffic Sensitivity Scenarios for UTBWC

Scenario	AADT	Age	EUAC Output from LCCA	Sensitivity (change from base EUAC)
Base Case	4410.59	9	$ 4,400.04	0.0%
Lower AADT: 8-yr SL	2500	8	$ 4,485.60	+1.9%
Higher AADT: 8-yr SL	10000	8	$ 6,389.08	+31.1%
Lower AADT: 9-yr SL	2500	9	$ 4,089.95	-7.6%
Higher AADT: 9-yr SL	10000	9	$ 5,801.93	+24.2%
Lower AADT: 10-yr SL	2500	10	$ 3,670.10	-19.9%
Higher AADT: 10-yr SL	10000	10	$ 5,183.79	+15.1%

Table 6.12 Traffic Sensitivity Scenarios for HFST

Scenario	AADT	Age	EUAC Output from LCCA	Sensitivity (change from base EUAC)
Base Case	4410.59	9.5	$ 17,700.19	0.0%
Lower AADT: 7-yr SL	2500	7	$ 20,609.11	+14.1%
Higher AADT: 7-yr SL	10000	7	$ 31,320.10	+43.5%
Lower AADT: 9.5-yr SL	2500	9.5	$ 15,982.52	-10.7%
Higher AADT: 9.5-yr SL	10000	9.5	$ 24,011.34	+26.3%
Lower AADT: 12-yr SL	2500	12	$ 13,287.00	-33.2%
Higher AADT: 12-yr SL	10000	12	$ 19,848.94	+10.8%

Table 6.13 Traffic Sensitivity Scenarios for Microsurfacing

Scenario	AADT	Age	EUAC Output from LCCA	Sensitivity (change from base EUAC)
Base Case	4410.59	8.5	$ 3,100.03	0.0%
Lower AADT: 7-yr SL	2500	7	$ 3,212.98	+3.5%
Higher AADT: 7-yr SL	10000	7	$ 4,515.06	+31.3%
Lower AADT: 8.5-yr SL	2500	8.5	$ 2,873.60	-7.9%
Higher AADT: 8.5-yr SL	10000	8.5	$ 4,016.54	+22.8%
Lower AADT: 10-yr SL	2500	10	$ 2,486.22	-24.7%
Higher AADT: 10-yr SL	10000	10	$ 3,454.57	+10.3%

Literature shows that temperature effects on pavement performance are inconsistent, highly localized and temperature-extremes dependent (Choi et al., 2016). Therefore, having local performance data and models are critical to evaluating treatment costs. When effect of temperature is considered for the HMA treatment, EUAC decreases when temperature decreases and increases when temperature increases (shown in Table 6.14). The same trend exists for the other treatments, as shown in the calculation tables in Appendix B.

Table 6.14 Temperature Sensitivity Scenarios for HMA/WMA

Scenario	Temp	EUAC Output from LCCA	Change from base EUAC
Base Case	73.15	$ 3,500.03	0.0%
Sensitivity - Lower Temp	72.15	$ 3,278.58	-6.8%
Sensitivity - Higher Temp	74.15	$ 3,738.05	6.4%

Aggregate properties have significant effect on pavement friction. As shown in Table 6.15, lower Micro Deval loss and NMAS can be expected to result in lower EUACs in the instant case. The same trend exists for the other treatments, as shown in the calculation tables in Appendix B.

Table 6.15 Aggregate Characteristics Sensitivity Scenarios for HMA/WMA

Scenario	MD	NMAS	EUAC Output from LCCA	Change from base EUAC
Base Case	8.73	11.21	$ 3,500.03	0.0%
Lower MD Loss	5.73	-	$ 2,591.07	-35.1%
Higher MD Loss	11.73	-	$ 4,772.17	26.7%
Smaller NMAS	-	11.00	$ 2,962.60	-18.1%
Larger NMAS	-	11.42	$ 4,146.66	15.6%

LCCA Step 6: Reevaluate the Results

Lastly, the cost results should be reevaluated. Given field data, expertise and the LCCA results, a pavement manager would have enough information to make decisions about which treatment to employ. This information should be coupled with other decision-support factors such as “risk, available budgets, and political and environmental concerns” (FHWA, 2002). The output from an LCCA should not be considered the answer, but merely an indication of the relative cost effectiveness of alternatives (FHWA, 1998) and a rough measure of each treatment’s economic performance when compared to the other options.

6.4 Summary

This chapter has demonstrated that economic and engineering technical data gathered from the pavement preservation field trials can be quantified and correlated to produce meaningful, standardized economic and life cycle cost analysis (LCCA) information. The sensitivity insight from this study would assist pavement managers in selecting an alternative to extend service lives of Oklahoma pavements.

Specifically, life cycle cost analysis was conducted for field study pavement treatments. Additionally, a performance-based cost sensitivity model was created and demonstrated to analyze the sensitivity (relative differences) of annualized cost output for pavement treatments based upon specific friction performance parameters. This methodology can be correlated with engineering field data to assist Oklahoma Department of Transportation (ODOT) pavement managers in determining the “right treatment” component of the “right treatment for the right road at the right time” (Galehouse et al., 2003) pavement preservation strategy and increase the effectiveness of budget expenditure resulting in decision making validation and justification and enhanced stewardship.

CHAPTER 7 CONCLUSIONS

Skid resistance of pavements plays a significant role in road safety for the reduction of potential crashes. Various preventive maintenance treatments have been employed in the State of Oklahoma to restore pavement condition (skid resistance herein) and retard future deterioration. Aggregate is the primary component of pavement treatments, however, its properties in terms of shape, texture, angularity and abrasion resistance have not been integrated into the decision making process for optimal skid resistance.

The recent technological innovations have made it possible to measure aggregate properties in terms of shape, texture and angularity with higher precision than conventional methods, but also to collect pavement performance condition data, including cracking, profiling (transverse and longitudinal) and surface texture at highway speed with high resolution. In the laboratory, the project used the Aggregate Imaging System (AIMS) to collect high quality aggregate morphological characteristics data, including shape, angularity, and surface texture related index properties. In the field, multiple rounds of pavement surface condition data collection were performed during 2015 to 2017 for the selected testing sites with various preventive maintenance treatments. The most recent developments in 3D laser imaging technology was used to collect 3D pavement surface texture data at highway speed at 1 mm accuracy without interfering with the traveling public.

Pavement skid resistance data were collected in the field using a grip tester during the same time frame.

Working closely with ODOT, the most commonly used aggregate sources (7 types) and preventive maintenance treatments (8 types) in Oklahoma were identified. A systematic field experimental design was developed. It included 45 roadway segments constructed with these preventive treatments and aggregate sources. A wide range of physical characteristics of aggregates (shape, texture, angularity), mix gradation, durability, and polish resistance (under dry and wet conditions) were tested and analyzed for each aggregate source using conventional methods and AIMS. Meanwhile in the field, four to seven rounds of pavement performance data in terms of cracking, rutting, IRI, texture, and friction number were collected and analyzed. Statistical analyses were performed to evaluate the effects of various factors, such as the preventive treatment type, aggregate properties, surface age and traffic level, on pavement surface skid resistance performance. It is found that aggregate properties have more significant effects on pavement friction than the PM treatment types. Multiple regression models were developed with the most significant influencing variables. Subsequently, life cycle cost analysis and performance based sensitivity analysis were performed based on the developed friction deterioration model. The developed model is expected to assist pavement managers in selecting an alternative to extend service lives of Oklahoma pavements.

This report presents a detailed analysis of aggregate characteristics and its relationship to skid resistance of pavements. An understanding of the relationships

among and between the physical properties of aggregate can result in improvements in pavement performance for preventive maintenance treatments, especially for pavement safety resulting from enhanced pavement friction. The results of this study can be correlated with engineering field data to assist ODOT pavement managers in determining the “right treatment” component of the “right treatment for the right road at the right time” pavement preservation strategy. Such preservation strategy is expected to increase the effectiveness of budget expenditure and enhanced stewardship of financial resources.

REFERENCES

AASHTO. 2008. AASHTO T 304-08 Standard Method of Test for Uncompacted Void Content of Fine Aggregate, American Association of State Highway and Transportation Officials, Washington D.C.

AASHTO. 2009. Standard Specifications for Transportation Materials and Methods of Sampling and Testing, Twenty-ninth Edition. American Association of State Highway and Transportation Officials, Washington D.C.

Adams A. and Warren M. 2017. SAFE-T User Manual. ODOT Traffic Engineering Collision Analysis & Safety Branch, Oklahoma City, OK.

Ahammed M.A. and Tighe S.L. 2008. Concrete Pavement Surface Textures and Multivariables Frictional Performance Analysis: a North American Case Study. Canadian Journal of Civil Engineering, Vol. 35, No. 7, 727-738.

Ahammed M.A. and Tighe S.L. 2010. Pavement surface friction and noise: integration into the pavement management system. Canadian Journal of Civil Engineering, Vol. 37, 1331-1340.

Ahammed M.A. and Tighe S.L. 2012. Asphalt Pavements Surface Texture and Skid Resistance – Exploring the Reality. Canadian Journal of Civil Engineering, Vol. 39, 1-9.

Ahmed, A.A. 2010. Ultra-thin Bonded Wearing Course Performance Update. Minnesota Department of Transportation, Office of Materials, Research Services Section, St. Paul, Minnesota.

Al-Rousan Sarsam S.I. and Ali A.M. 2015. Assessing Pavement Surface Macrotexture Using Sand Patch Test and Close Range Photogrammetric Approaches. International Journal of Materials Chemistry and Physics, Vol. 1, No. 2, 124-131.

Al-Rousan, T., E. A. Masad, L. Myers, and C. Speigelman. 2005. New Methodology for Shape Classification of Aggregates. In Transportation Research Record:

Journal of the Transportation Research Board, No. 1913, Transportation Research Board of the National Academies, Washington, D.C., pp. 11–23.

Al-Rousan, T., E. Masad, E. Tutumluer, and T. Pan, N. Little, J. Button.2007. Test Methods for Characterizing Aggregate Shape, Texture, and Angularity. NCHRP 4-30A Final Report. Transportation Research Board of the National Academies, Washington, D. C.

Al-Rousan, T.M. 2004. Characterization of Aggregate Shape Properties Using a Computer Automated System. Ph.D. Dissertation, Texas A&M University, College Station, Texas.

Al-Rousan, T.M. et al. 2007. Evaluation of Image Analysis Techniques for Quantifying Aggregate Shape Characteristics. Construction and Building Materials, Vol. 21, 978-990.

Amirkhanian, S., D. Kaczmarek, and J. Burati., 1991. Effects of Los Angeles Abrasion Test Values on the Strengths of Laboratory-Prepared Marshall Specimens, Transportation Research Record, No. 1301, pp. 77-86.

Anupam, K., Srirangam, S. K., Scarpas, A., and Kasbergen, C. 2013. Influence of temperature on tire–pavement friction: analyses. Transportation Research Record: Journal of the Transportation Research Board, No. 2369, Transportation Research Board of the National Academies, Washington, D.C., pp. 114–124.

Arambula E. et al. 2013. Performance and Cost Effectiveness of Permeable Friction Course (PFC) Pavements. FHWA/TX-12/0-5836-2. FHWA, U.S. Department of Transportation.

Arampamoorthy H. and Patrick J. 2011. Potential of the Wehner-Schulze Test to Predict the On-Road Friction Performance of Aggregate. NZ Transport Agency Research Report 443. NZ Transport Agency, Wellington, New Zealand.

Asi I.M. 2007. Evaluating Skid Resistance of Different Asphalt Concrete Mixes. Building and Environment, Vol. 42, 325-329.

ASTM C88-13, 2013. Standard Test Method for Soundness of Aggregate by Use of Sodium Sulfate or Magnesium Sulfate. ASTM International, West Conshohocken, PA, DOI: 10.1520/C0088-13.

ASTM C131/C131M-14. 2006. Standard Test Method for Resistance to Degradation of Small-Size Coarse Aggregate by Abrasion and Impact in the Los Angeles Machine, ASTM International, West Conshohocken, PA. https://doi.org/10.1520/C0131_C0131M-14.

ASTM D3319-11, 2011. Standard Practice for the Accelerated Polishing of Aggregates Using the British Wheel. ASTM International, West Conshohocken, PA, DOI: 10.1520 / D3319-11.

ASTM D3744/D3744M-11a, 2013. Standard Test Method for Aggregate Durability Index. ASTM International, West Conshohocken, PA, DOI: 10.1520 /D3744_D3744_D3744M–11A.

ASTM D6928-10. 2017. Standard Test Method for Resistance of Coarse Aggregate to Degradation by Abrasion in the Micro-Deval Apparatus, ASTM International, West Conshohocken, PA.

ASTM D6928-10, 2010. Standard Test Method for Resistance of Coarse Aggregate to Degradation by Abrasion in the Micro-Deval Apparatus. ASTM International, West Conshohocken, PA, DOI: 10.1520/D6928-10. https://doi.org/10.1520/D6928-10.

ASTM D7428-15, 2015. Standard Test Method for Resistance of Fine Aggregate to Degradation by Abrasion in the Micro-Deval Apparatus. ASTM International, West Conshohocken, PA, 2015, DOI: 10.1520/D7428-15.

ASTM E274/E274M-11, 2011. Standard Test Method for Skid Resistance of Paved Surfaces Using a Full-Scale Tire. ASTM International, West Conshohocken, PA, 2008, DOI: 10.1520/E0274_E0274M-11.

ASTM E303-93, 2013. Standard Test Method for Measuring Surface Friction Properties Using the British Pendulum Tester. ASTM International, West Conshohocken, PA, 2013, DOI: 10.1520/E0303-93R13.

ASTM E670-09, 2009. Standard Test Method for Testing Side Force Friction on Paved Surfaces Using the Mu-Meter. ASTM International, West Conshohocken, PA, 2008, DOI: 10.1520/E0670- 09.

ASTM E965-15, 2015. Standard Test Method for Measuring Pavement Macrotexture Using a Volumetric Technique. ASTM International, West Conshohocken, PA, 2015, DOI: 10.1520/E0965-15.

ASTM E1844-08 (2015) Standard Specification for A Size 10 × 4–5 Smooth-Tread Friction Test Tire, ASTM International, West Conshohocken, PA. https://doi.org/10.1520/E1844-08R15.

ASTM E1845-15. 2015. Standard Practice for Calculating Pavement Macrotexture Mean Profile Depth. ASTM International, West Conshohocken, PA, DOI: 10.1520/E1845-15.

ASTM E1911-09a, 2009. Standard Test Method for Measuring Paved Surface Frictional Properties Using the Dynamic Friction Tester. ASTM International, West Conshohocken, PA, 2009, DOI: 10.1520/E1911-09AE01.

ASTM E1926-08. 2015. Standard Practice for Computing International Roughness Index of Roads from Longitudinal Profile Measurements. ASTM International, West Conshohocken, PA, DOI: 10.1520/E1926-08R15.

ASTM E1960-07, 2015. Standard Practice for Calculating International Friction Index of a Pavement Surface. ASTM International, West Conshohocken, PA, 2015, DOI: 10.1520/E1960-07R15.

ASTM E2157-15, 2015. Standard Test Method for Measuring Pavement Macrotexture Properties Using the Circular Track Meter. ASTM International, West Conshohocken, PA, 2015, DOI: 10.1520/E2157-15.

ASTM E2340/E2340M-11. 2015. Standard Test Method for Measuring the Skid Resistance of Pavements and Other Trafficked Surfaces Using a Continuous Reading, Fixed-Slip Technique. ASTM International, West Conshohocken, PA, DOI: 10.1520/E2340_E2340-11R15.

ATSSA. 2013. Safety Opportunities in High Friction Surfacing. American Traffic Safety Services Association. Fredericksburg, VA.

Bathina, M. 2005. Quality analysis of the aggregate imaging system (AIMS) measurements (M.Sc. thesis). Texas A&M University, College Station, TX.

Bausano, J.P., K. Chatti and R.C. Williams. 2004. Determining Life Expectancy of Preventive Maintenance Fixes for Asphalt-Surfaced Pavements,

Transportation Research Record: Journal of the Transportation Research Board, No. 1866, TRB, National Research Council, pp. 1-8. Washington D.C.

Beg M.A., Zhang Z., and Hudson W.R. 1998. A Rational Pavement Type Selection Procedure. Report No:FHWA/TX-04/0-1734-S, Austin, TX

Bessa, I. S., Branco, V. T., & Soares, J. B. 2014. Evaluation of polishing and degradation resistance of natural aggregates and steel slag using the aggregate image measurement system. Road Materials and Pavement Design, 15(2), 385-405. doi:10.1080/14680629.2014.883323

Bilal, M.K., M. Irfan and S. Labi. 2009. Comparing the Methods for Evaluating Pavement Interventions – A Discussion and Case Study, Transportation Research Board, TRB Paper No. 09-2661. Washington, D.C.

Bischoff D. 2008. Investigative Study of the Italgrip TM System. WI-04-08. Wisconsin Department of Transportation, Madison, WI.

Bledsoe J. 2015. Missouri Demonstration Project: The Use of High-Friction Surface Treatments on Missouri Highways. FHWA, U.S. Department of Transportation. Washingon D.C.

Bloem, D. 1971. Skid resistance – The role of aggregates and other factors (pp. 1–30). Silver Spring, MD: National Sand and Gravel Association Circular 109.

Brandes, H.G., and C.E. Robinson. 2006. Correlation of Aggregate Test Parameters to Hot Mix Asphalt Pavement Performance in Hawaii. Journal of Transportation Engineering, Vol 132, Issue 1.

Burchett, J. L. 1978. Seasonal variations in the skid resistance of pavements in Kentucky: Final report. Lexington, KY: Division of Research, Bureau of Highways, Dept. of Transportation.

California Department of Transportation (CalTrans). 2003. “Maintenance Resource Handbook.” Chapter 5 – Chip Seals. Division of Maintenance. Sacramento, CA.

California Department of Transportation (CalTrans). 2008. Maintenance Technical Advisory Guide Volume I – Flexible Pavement Preservation. Sacramento, CA.

Cambridge Systematics, Inc., PB Consult and System Metrics Group, Inc. 2005. Analytical Tools for Asset Management, National Cooperative Highway Research Program (NCHRP) Report 545, Washington, D.C.

Cenek, P. D. 2004. Prediction of Skid Resistance Performance of Chip Seal Roads in New Zealand. Wellington, N.Z.: Transfund New Zealand.

Chandan, C., 2002. Geometry Analysis Of Aggregate Particles Using Imaging Techniques, M.Sc Thesis, School of Electrical Engineering and Computer Science, Washington State University, Pullman, WA.

Chen D. et al. 2015. Exploring the Feasibility of Evaluating Asphalt Pavement Surface Macrotexture Using Image-based Texture Analysis Method. Road Materials and Pavement Design, 16:2, 405-420, DOI:10.1080/14680629.2015.1016547.

Chen X.H. and Wang D.W. 2011. Fractal and Spectral Analysis of Aggregate Surface Profile in Polishing Process. Wear, Vol. 271, 2746-2750.

Choi, K., Y. Kim, J. Bae and H. Lee. 2016. Determining Future Maintenance Costs of Low-Volume Highway Rehabilitation Projects for Incorporation into Life-Cycle Cost Analysis, Journal of Computing in Civil Engineering, Vol. 30(4). ASCE.

Chou, Eddie Y., D. Datta, and H. Pulugurta. 2008. Effectiveness of Thin Hot Mix Asphalt Overlay on Pavement Ride and Condition Performance. Report No. FHWA/OH-2008/4. Ohio Department of Transportation.

Cooley, L. Jr., and R. James, 2003. Micro-Deval Testing of Aggregates in the Southeast. Transportation Research Record 1837, Transportation Research Board, Washington, D.C., 73-79.

Csathy, T.I., W.C. Burnett, and M.D. Armstrong, 1968. State-of-the-Art of Skid Resistance Research, Highway Research Board Special Report 95, Highway Research Board, National Research Council, Washington, D.C.

Dan H. et al. 2015. Experimental Investigation on Skid Resistance of Asphalt Pavement under Various Slippery Conditions. International Journal of Pavement Engineering, DOI: 10.1080/10298436.2015.1095901.

Daniels G., Stockton W. R., and Hudley R. 2000. Estimating Road User Costs Associated with Highway Construction Projects-Simplified Method In Transportation Research Record: Journal of the Transportation Research Board, No. 1732, Washington DC, 2000, pp. 70-79.

Davis R. M. 2001 Comparison of surface characteristics of hot-mix asphalt pavement surfaces at the Virginia smart road. Thesis submitted to the Faculty of Virginia Polytechnic Institute and State University.

Do M. et al. 2007. Pavement Polishing-Development of a Dedicated Laboratory Test and its Correlation with Road Results. Wear, Vol. 263, 36-42.

Do M. et al. 2009. Evolution of Road-Surface Skid-Resistance and Texture Due to Polishing. Wear, Vol. 266, 574-577.

Do M. et al. 2009. Physical Model for the Prediction of Pavement Polishing. Wear, Vol. 267, 81-85.

Doty R.N. 1974. A Study of the Sand Patch and Outflow Meter Method of Pavement Surface Texture Measurement. Symposium on Surface Texture and Standard Surfaces. Washington, D.C.

Dunford A. 2013. Friction and the Texture of Aggregate Particles Used in the Road Surface Course. Ph.D. Dissertation, University of Nottingham, United Kingdom.

Dunford A.M. et al. 2012. Three-Dimensional Characterization of Surface Texture for Road Stones Undergoing Simulated Traffic Wear. Wear, Vol. 292-293, 188-196.

Dupont P., and Bauduin A. 2005. Pavement skid resistance: French national policy towards promoting road projects. Bulletin Des Laboratories Des Ponts Et Chaussees: Managing Road Pavement Skid Resistance, Ref. 4521, France, 159–168.

Erdogan S.T. et al. 2006. Three-Dimensional Shape Analysis of Coarse Aggregates: New Techniques for and Preliminary Result on Several Different Coarse Aggregates and Reference Rocks. Cement and Concrete Research, Vol. 36, 1619-1627.

Ergun M., Iyinam S., and Iyinam A.F. 2005. Prediction of Road Surface Friction Coefficient Using Only Macro- and Microtexture Measurements. Journal of Transportation Engineering, Vol. 131, 311-319.

Faheem A., B. Abboud, J. Coe, and M. Alsalihi. 2018. Effect of Warm Mix Asphalt (WMA) Low Mixing and Compaction Temperatures on Recycled Asphalt

Pavement (RAP) Binder Replacement. Pennsylvania Department of Transportation (PennDOT). Harrisburg, PA.

Falls, L.C. and Tighe, S. 2004. Analyzing Longitudinal Data to Demonstrate the Costs and Benefits of Pavement Management. Public Works Management & Policy, Vol. 8, No. 3, pp: 176-191.

Federal Aviation Administration (FAA). 1997. Measurement, Construction and Maintenance of Skid-resistant Airport Pavement Surfaces (Advisory Circular AC 150/5320-12C). Office of Airport Safety and Standards, FAA, Washington D.C.

Fernlund J.M.R. 1998. The Effect of Particle Form on Sieve Analysis: A Test by Image Analysis. Engineering Geology, Vol. 50, 111-124.

Fernlund J.M.R. 2005. 3D Image Analysis Size and Shape Method applied to the Evaluation of the Los Angeles Test. Engineering Geology, Vol. 77, 57-67.

Fowler, D. W., & Rached, M. M. 2012. Polish resistance of fine aggregates in Portland cement concrete pavements. Transportation Research Record: Journal of the Transportation Research Board, 2267(1), 29-36. doi:10.3141/2267-03

Federal Highway Administration (FHWA). 1998. Life Cycle Cost Analysis in Pavement Design, Interim Technical Bulletin. Washington, D.C.

Federal Highway Administration (FHWA). 2002. Life Cycle Cost Analysis Primer, Office of Asset Management Washington, D.C.

Federal Highway Administration (FHWA), 2003. Distress Identification Manual for The LTPP (Fourth Revised Edition), Office of Asset Management, Washington, D.C.

Federal Highway Administration (FHWA). 2005a. Transportation Asset Management Case Studies, Economics in Asset Management: The Hillsborough County, Florida Experience, Office of Asset Management, Washington D.C., 2005a.

Federal Highway Administration (FHWA). 2005b. Technical Advisory, “Surface Texture for Asphalt and Concrete Pavements,” T 5040.36, Office of Asset Management, Washington, D.C.

Federal Highway Administration (FHWA). 2007. Asset Management Overview, Office of Asset Management, Washington, D.C.

Federal Highway Administration (FHWA). 2011. Aggregate Image Measurement System 2 (AIMS2). Office of Asset Management, Washington, D.C.

Fletcher, T., C. Chandan, E. Masad, and K. Sivakumar, 2003. Aggregate Imaging System (AIMS) for Characterizing the Shape of Fine and Coarse Aggregates. Transportation Research Record, No.1832, Transportation Research Board, Washington, D.C., pp. 67–77.

Flintsch G.W. et al. 2012. The Little Book of Tire Pavement Friction. Pavement Surface Properties Consortium. Virginia Tech, Blacksburg, VA.

Flintsch G.W., Leon E.D., McGhee K.K., and Al-Qadi I.L. 2003. Pavement Surface Macrotexture Measurement and Application. In Transportation Research Board Annual Meeting CD-ROM, Transportation Research Board of the National Academies, Washington, D.C.

Fowler, D.W. and M. M. Rached, 2012. Polish Resistance of Fine Aggregates in Portland Cement Concrete Pavements, Transportation Research Record: Journal of the Transportation Research Board, No. 2267, Transportation Research Board of the National Academies, Washington, D.C., pp. 29–36.

Friel S. et al. 2013. Use of Wehner Schulze to Predict Skid Resistance of Irish Surfacing Materials. Airfield and Highway Pavement, France, 12 p.

Fuentes, L., Gunaratne, M., & Hess, D. 2010. Evaluation of the Effect of Pavement Roughness on Skid Resistance. Journal of Transportation Engineering J. Transp. Eng., 136(7), 640-653.

Fuents L.G. 2009. Investigation of the Factors Influencing Skid Resistance and the International Friction Index. Ph.D. Dissertation, University of South Florida, Tampa, FL.

Galehouse, L., J.S. Moulthrop, and R.G. Hicks. 2003. Principles for Pavement Preservation: Definitions, Benefits, Issues and Barriers. TR News, Transportation Research Board, pp. 4-9.

Garboczi E.J. 2002. Three-Dimensional Mathematical Analysis of Particle Shape Using X-ray Tomography and Spherical Harmonics: Application to Aggregates Used in Concrete. Cement and Concrete Research, Vol. 32, 1621-1638.

Garboczi E.J. et al. 2006. Using LADAR to Characterize the 3-D Shape of Aggregates: Preliminary Results. Cement and Concrete Research, Vol. 36, 1072-1075.

Gardiner M.S. et al. 2001. Influence of Hot Mix Asphalt Macrotexture on Skid Resistance. Auburn University, Alabama.

German Asphalt Pavement Association (GAPA). 2011. Asphalt Surface Courses Skid Resistance. Accessed 1 February 2016.

Gong H. et al. 2015. Effectiveness Analyses of Flexible Pavement Preventive Maintenance Treatments with LTPP SPS-3 Experiment Data. Journal of Transportation Engineering, 10.1061/(ASCE)TE.1943-5436.0000818, 04015045.

Gong, H., Dong, Q., Huang, B., & Jia, X. 2016. Effectiveness Analyses of Flexible Pavement Preventive Maintenance Treatments with LTPP SPS-3 Experiment Data. Journal of Transportation Engineering J. Transp. Eng., 142(2), 04015045. Doi: 10.1061/ (asce) te.1943-5436.0000818

Goodman, S.N. 2009. Quantification of Pavement Textural and Frictional Characteristics Using Digital Image. Ph.D. Dissertation, Carleton University, Ottawa, Canada.

Gransberg, D.D., and E. Scheepbouwer. 2010. Infrastructure Asset Life Cycle Cost Analysis Issues. Transactions, AACE, International, Atlanta, Georgia, pp. CSC.03.01- CSC.03.8.

Gransberg, N.J., 2012. Correlating Geologic Strata to Polished Stone Values: A Nationwide Analysis, Master's Report, Missouri School of Science and Technology, Rolla, Missouri.

Gudimettla, J., L.A. Myers and C. Paugh, 2006. AIMS: The Future in Rapid, Automated Aggregate Shape and Texture Measurement, US Department of Transportation, Federal Highway Administration, Washington, DC.

Hall J.W. et al. 2009. NCHRP Web Document 108: Guide for Pavement Friction. Transportation Research Board, National Research Council, Washington, D.C.

Hall, K. T., Correa, C. E., & Simpson, A. L. 200). LTPP data analysis: Effectiveness of pavement maintenance and rehabilitation options. Washington, D.C.: National Academy Press.

Hansen K.R. and Copeland A. 2014. Asphalt Pavement Industry Survey on Recycled Materials and Warm-Mix Asphalt Usage: 2014. Information Series 138 (5th edition). NAPA – National Asphalt Pavement Association. Lanham, MD.

Harmon T., Bahar G. and Gross F. 2018. Crash Costs for Highway Safety Analysis. Publication FHWA-AK-17-071. VHB, Vienna, VA.

Heitzman M. and Vrtis M. 2015. Development of Alternative High Friction Surfaces for Oklahoma. FHWA-OK-15-10. ODOT, Oklahoma City, OK.

Heitzman, M., 2011. NCAT Study Validates Procedure to Predict Friction. Asphalt Technology News. National Center for Asphalt Technology (NCAT), Vol. 23, No. 1.

Henry, J.J. 2000. NCHRP Synthesis 291: Evaluation of Pavement Friction Characteristics. Transportation Research Board, National Research Council, Washington, D.C.

Hossain M. et al. 2010. Extending Pavement Life Using Thin Surfacing to Counter the Effect of Increased Truck Traffic Due to Freight Movements on Highways. University of Nebraska, Mid America Transportation Center, Lincoln, Nebraska.

Ioannidis, J. P. 2007. Why most published research findings are false: authors reply to Goodman and Greenland. PLoS Medicine, 4(6). doi: 10.1371/journal.pmed.0040215

Izeppi E., Flintsch G. and McGhee K. 2010. Field Performance of High Friction Surfaces. Publication FHWA/VTRC 10-CR6. FHWA, U.S. Department of Transportation.

Jahn D. 2000. Evaluation of Aggregate Particle Shapes through Multiple Ratio Analysis. Proceedings of the 8th Annual Symposium of the International Center for Aggregate Research (ICAR), Denver, CO.

Jahromi S.G. et al. 2011. Evaluation of Pavement Temperature on Skid Frictional of Asphalt Concrete Surface. International Journal of Pavement Engineering, 12:1, 47-58, DOI: 10.1080/10298436.2010.501864.

Jayawickrama, P., & Thomas, B. 1998. Correction of Field Skid Measurements for Seasonal Variations in Texas. Transportation Research Record: Journal of the Transportation Research Board, 1639, 147-154. doi:10.3141/1639-16

Kanafi M.M. et al. 2015. Macro- and Microtexture Evolution of Road Pavements and Correlation with Friction. International Journal of Pavement Engineering, 16:2, 168-179, DOI: 10.1080/10298436.2014.937715.

Kanafi, M. M., Kuosmanen, A., Pellinen, T. K., & Tuononen, A. J. 2014. Macro- and Microtexture Evolution of Road Pavements and Correlation with Friction. International Journal of Pavement Engineering, 16(2), 168-179. Doi:10.1080/10298436.2014.937715

Kandhal, P. S., and F. Jr. Parker, 1998. Aggregate Tests Related to Asphalt Concrete Performance in Pavements, NCHRP Report 405, National Cooperative Highway Research Program, National Academy Press, Washington, D.C.

Kane M., Do M.T. and Piau J.M. 2010. On the Study of Polishing of Road Surface under Traffic Load. Journal of Transportation Engineering, Vol. 136, No. 1, 45-51.

Kane M., Rado Z. and Timmons A. 2015. Exploring the Texture-Friction Relationship: from Texture Empirical Decomposition to Pavement Friction. International Journal of Pavement Engineering, 16:10, 919-918, DOI:10.1080/10298436.2014.972956.

Kane, M., Rado, Z., & Timmons, A. 2014. Exploring the Texture–Friction Relationship: From Texture Empirical Decomposition to Pavement friction. International Journal of Pavement Engineering, 16(10), 919-928. Doi:10.1080/10298436.2014.972956

Kangkhajitre C, Kanitpong K. 2011 Effect of aggregate characteristics on texture and skid resistance of asphalt pavement surface. Eastern Asia Soc Transp Stud 8: 247.

Kassem, E., A. Ahwed, E.A. Masad, and D.N Little, 2013. Development of Predictive Model for Skid Loss of Asphalt Pavements, Transportation Research Record, Journal of the Transportation Research Board, No 2372, Transportation Research Board of the National Academies, pp: 83-96.

Kim H., Haas C.T., Rauch A.F. and Browne C. 2001. Development of a Laser-Based System for Testing Construction Aggregate. Accessed 28 Jan 2016.

Kim, H., C. Haas, A. Rauch and C. Browne, 2001. A Prototype Laser Scanner for Characterizing Size and Shape Properties in Aggregates, A Paper Presented at the 9th Annual International Center for Aggregate Research (ICAR) Symposium, Austin, Texas.

Kline, S.W., W. Phiukhao, M.L. Griffin, and J.W. Miller. 2007. Evaluation of the sodium sulfate soundness test for qualifying dolomites of northern Arkansas for construction aggregate. In Shaffer, N.R., and DeChurch, D.A., eds, Proceedings of the 40th Forum on the Geology of Industrial Minerals, Indiana Geological Survey Occasional Paper 67.

Knaub, J.R., Jr. 1987. Practical Interpretation of Hypothesis Tests. Vol. 41, No. 3 (August), letter, The American Statistician, American Statistical Association, pp. 246- 247

Kokkalis, A. G., & Panagouli, O. K. 1998. Fractal Evaluation of Pavement Skid Resistance Variations. I: Surface Wetting. Chaos, Solitons & Fractals, 9(11), 1875-1890. doi:10.1016/s0960-0779(97)00138-0

Komas, T., 2011. Advanced Surface Preparation and Preservation Treatments for Concrete Pavements, CP2 Center News, Newsletter of the California Pavement Preservation Center, No. 20, December.

Kotek P. and Florkova Z. 2014. Comparison of the Skid Resistance at Different Asphalt Pavement Surfaces over Time. Procedia Engineering, Vol. 91, 459-463.

Kotek P. and Kovac M. 2015. Comparison of valuation of Skid Resistance of Pavements by Two Device with Standard Methods. Procedia Engineering, Vol. 111, 436-443.

Kowalski K.J. et al. 2009. Long-Term Monitoring of Noise and Frictional Properties of Three Pavements: Dense-Graded Asphalt, Stone Matrix Asphalt, and Porous Friction Course. In Transportation Research Record: Journal of the Transportation Research Board, N0. 2127, Transportation Research Board of the National Academies, Washington, D.C., 12-19.

Kumar B. and Wilson D.J. 2010. Prediction of Pavement Surface Skid Resistance and the Effect of Smaller Chip Size. Accessed 17 Feb 2016.

Kwan A.K.H. et al. 1999. Particle Shape Analysis of Coarse Aggregate Using Digital Image Processing. Cement and Concrete Research, Vol. 29, 1403-1410.

Labbate A. et al. 2001. A Classification of Asphalt Surfacing Textures Based on 3D Imagery. Master Dissertation, University of Bologna, Italy.

Lamptey, G., M. Z. Ahmad, S. Labi, and K. C. Sinha. 2005. Life Cycle Cost Analysis for INDOT Pavement Design Procedures. Publication FHWA/IN/JTRP-2004/28. Joint Transportation Research Program, Indiana Department of Transportation and Purdue University, West Lafayette, Indiana.

Lancieri, F., M. Losa and A. Marradi, 2005. Polishing resistance and mechanical properties of aggregates for asphalt concrete wearing courses. SIIV - Società Italiana Infrastrutture Viarie, Archivio della Ricerca - Università di Pisa.

Lane, B., C. Rogers, and S. Senior, 2000. The Micro-Deval Test for Aggregates in Asphalt Pavement, Presented at the 8th Annual Symposium of International Center for Aggregate Research, Denver, Colorado.

Lee, Jr. Douglass B. 2002. Fundamentals of Life-Cycle Cost Analysis. Transportation Research Record 1812, Paper No. 02-3121, Transportation Research Board (TRB), Washington, D.C.

Lee J.R.J. et al. 2007. A New Approach to the Three-Dimensional Quantification of Angularity Using Image Analysis of the Size and Form of Coarse Aggregates. Engineering Geology, Vol. 91, 254-264.

Li S. et al. 2011. Evaluation of Pavement Surface Friction Treatments. FHWA/IN/JTRP-2012/04. FHWA, U.S. Department of Transportation.

Li S. et al. 2012. Pavement Surface Microtexture: Testing, Characterization and Frictional Interpretation. in Pavement Performance: Current Trends, Advances, and Challenges. West Conshohocken, PA. 59-76. https://doi.org/10.1520/STP104426.

Li S., Zhu K. and Noureldin S. 2007. Evaluation of Friction Performance of Coarse Aggregates and Hot-Mix Asphalt Pavements. Journal of Testing and Evaluation, Vol. 35, No. 6, 1-7.

Li, Q. J., Yang, G., Wang, K. C., Zhan, Y., Merritt, D., & Wang, C. 2016. Effectiveness and Performance of High Friction Surface Treatments at A National Scale.

Canadian Journal of Civil Engineering, 43(9), 812-821. doi:10.1139/cjce-2016-0132

Li, S., Noureldin, S., Jiang, Y., Sun, Y. 2012. Evaluation of Pavement Surface Friction Treatments. Publication FHWA/IN/JTRP- 2012/04. Joint Transportation Research Program, Indiana Department of Transportation and Purdue University, West Lafayette, Indiana. DOI: 10.5703/1288284314663

Lomax, R. 2007. An Introduction to Statistical Concepts, Second Edition. Lawrence Erlbaum Associates, Publishers. Mahwah, New Jersey.

Lu Q. and Steven B. 2006. Friction Testing of Pavement Preservation Treatments: Literature Review. UCPRC-TM-2006-10.

Lu, Q. and B. Steven, 2006. Friction Testing of Pavement Preservation Treatments: Literature Review, Technical Memorandum UCPRC-TM-2006-10, California Department of Transportation (Caltrans) Division of Research and Innovation and Division of Maintenance, University of California Pavement Research Center, UC Davis and Berkeley.

Luo Y. 2003. Effect of Pavement Temperature on Frictional Properties of Hot-Mix-Asphalt Pavement Surfaces at the Virginia Smart Road. Master Dissertation, Virginia Polytechnic Institute and State University, Blacksburg, Va.

Madanat, S. M., Karlaftis, M. G., & Mccarthy, P. S. 1997. Probabilistic Infrastructure Deterioration Models with Panel Data. Journal of Infrastructure Systems, 3(1), 4-9. Doi: 10.1061/ (asce) 1076-0342(1997)3:1(4)

Maerz, N. H., and Lusher, M. 2001. Measurement of Flat and Elongation of Coarse Aggregate Using Digital Image Processing. Transportation Research Board Proceedings, 80th Annual Meeting, Washington D.C., Paper No. 01-0177.

Mahmoud, E. 2005. Development of experimental methods for the evaluation of aggregate resistance to polishing, abrasion, and breakage (M.Sc. thesis). Texas A&M University, College Station, TX.

Mahmoud, E. and E. Ortiz, 2014. Implementation of AIMS in Measuring Aggregate Resistance to Polishing, Abrasion, and Breakage, Research Report No. FHWA-ICT-14-014, Illinois Center for Transportation, Urbana, IL.

Mahmoud, E., and E. Masad, 2007. Experimental Methods for the Evaluation of Aggregate Resistance to Polishing, Abrasion and Breakage, Journal of Materials in Civil Engineering, ASCE, Vol. 19, No. 11, pp. 977-985.

Masad E. 2003. Final Report for Highway-IDEA Project 77: The Development of a Computer Controlled Image Analysis System for Measuring Aggregate Shape Properties. Transportation Research Board, National Research Council, Washington, D.C.

Masad E. 2007. Relationship of Aggregate Texture to Asphalt Pavement Skid Resistance Using Image Analysis of Aggregate Shape. Final Report for Highway IDEA Project 114.

Masad E. et al. 2005. Computations of Particle Surface Characteristics Using Optical and X-ray CT Images. Computational Materials Science, Vol. 34, 406-424.

Masad E., Al-Rousan T., Button J. and Little D. 2007. NCHRP Report 555: Test Methods for Characterizing Aggregate Shape, Texture, and Angularity. Transportation Research Board, National Research Council, Washington, D.C.

Masad E., Rezaei A. and Chowdhury A. 2011. Field Evaluation of Asphalt Mixture Skid Resistance and Its Relationship to Aggregate Characteristics. FHWA/TX-11/0-5627-3.

Masad E., Rezaei A., Chowdhury A. and Chowdhury A. 2010. Field Evaluation of Asphalt Mixture Skid Resistance and Its Relationship to Aggregate Characteristics. FHWA/TX-10/0-5627-2.

Masad E., Rezaei A., Chowdhury A. and Harris P. 2009. Predicting Asphalt Mixture Skid Resistance Based on Aggregate Characteristics. FHWA/TX-09/0-5627-1.

Masad, E. (2005). "Aggregate Imaging Systems: Basics and Applications" Texas Department of Transportation. Report 5-1707-01-1.

Masad, E., 2003. The development of a Computer Controlled Image Analysis System for Measuring Aggregate Shape Properties, Final Report for Highway-IDEA Project 77, Transportation Research Board, Washington, D.C.

Masad, E., 2005. Aggregate Imaging System (AIMS) basics and applications, Report no. FHWA/TX-05/5-1707-01-1, Texas Department of Transportation and Federal Highway Administration, Washington, D.C.

Masad, E., Button, J., and Papagiannakis, T. 2000. Fine Aggregate Angularity: Automated Image Analysis Approach. Transportation Research Record 1721, Transportation Research Board, Washington D.C., pp. 66–72.

Masad, E., Muhunthan, B., Shashidhar, N., & Harman, T. 1999. Internal Structure Characterization of Asphalt Concrete Using Image Analysis. Journal of Computing in Civil Engineering, 13(2), 88-95. doi:10.1061/(asce)0887-3801(1999)13:2(88)

McGhee K.K. and Flintsch G.W. 2003. High-Speed Texture Measurement of Pavements. VTRC 03-R9. Charlottesville, Virginia.

Meegoda, J.N., and S. Gao, 2015. Evaluation of pavement skid resistance using high speed texture measurement. Journal of Traffic and Transportation Engineering. pp. 382-390.

Merritt D. and Moravec M. 2014. An Update on HFST for Horizontal Curves. Proceeding of Pavement Evaluation 2014, Blacksburg, Virginia. Accessed 14 Mar., 2016.

Millar P. et al. 2009. Use of Close Range Terrestrial Photogrammetry to Assess Accelerated Wear of Asphalt Concrete Surface Course Mixes. In: Sixth International Conference on Maintenance and Rehabilitation of Pavements and Technological Control, Politechnico di Torino, Italy. Politechnico di Torino. Vol 27 pp.

Miller et al. 2012. Characterization of Asphalt Pavement Surface Texture. In Transportation Research Record: Journal of the Transportation Research Board, N0. 2295, Transportation Research Board of the National Academies, Washington, D.C., 19-26.

MnDOT, 2000. Resistance of Fine Aggregate to Degradation by Abrasion in the Micro-Deval Apparatus. Lab Manual, Minnesota Department of Transportation.

MnDOT 2014. Cost-Effective Pavement Preservation Solutions for the Real World, Final Report, MN/RC 2014-33, Minnesota Department of Transportation, St. Paul, MN.

MnDOT 2017. Life-Cycle Cost Analyses. Minnesota Dept. of Transportation. St. Paul, MN.

Moaveni, M., E. Mahmoud, E. M. Ortiz, E. Tutumluer and S. Beshears 2014. Evaluation of Aggregate Resistance to Breakage, Abrasion, and Polishing Using Advanced Aggregate Imaging Systems, Transportation Research Record: Transportation Research Board, Washington, D.C.

Monsere, C.M., L. Diercksen, K. Dixon, and M. Liebler. 2009. Evaluating the Effectiveness of the Safety Investment Program (SIP) Policies for Oregon, SPR 651, Final Report, Oregon Department of Transportation Research Section., Portland, Oregon.

Montgomery, Douglas C., 2009. Introduction to Statistical Quality Control, 6th Edition. John Wiley and Sons, Inc. Hoboken, New Jersey.

Mora C.F. and Kwan A.K.H. 2000. Sphericity, Shape Factor, and Convexity Measurement of Coarse Aggregate for Concrete Using Digital Image Processing. Cement and Concrete Research, Vol. 30, 351-358.

Moravec M. 2013. High Friction Surface Treatments at High-Crash Horizontal Curves. Arizona Pavements/Materials Conference, Phoenix, AZ.

Najafi S. et al. 2015. Linking Roadway Crashes and Tire-Pavement Friction: A Case Study. International Journal of Pavement Engineering, DOI: 10.1080/10298436.2015.1039005.

NCAT 2017. Evaluation of the AIMS2 and Micro-Deval to Characterize Aggregate Friction Properties. NCAT Report 17-02, Auburn, AL.

NCHRP 2009a. NCHRP 41 Web-Only Document 108: Guide for Pavement Friction, National Cooperative 42 Highway Research Program (NCHRP) Project 01-43 Contractor's Final Report. 43 Transportation Research Board. Washington, D.C.

Neaylon, K., 2009. The PAFV Test and Road Friction. AAPA 13th International Flexible Pavements Conference. Brisbane Australia.

Newcomb D.E. 2009. Thin Asphalt Overlays for Pavement Preservation. Information Series 135, National Asphalt Pavement Association, Lanham, MD.

Noyce, D., A. 2005. Incorporating road safety into pavement management: maximizing asphalt pavement surface friction for road safety improvements.

Midwest Regional University Transportation Center Traffic Operations and Safety (TOPS) Laboratory.

NSP. 2010. Aggregate Classification Map of the United States, accessed July 16, 2014.

Oklahoma Department of Transportation (ODOT). 2010. SFY-2010 through SFY-2013 Asset Preservation Plan, Oklahoma City, Oklahoma.

Oklahoma Department of Transportation (ODOT). 2015. Development of Alternative High Friction Surfaces for Oklahoma, Final Report ~ FHWA-OK-15-10, ODOT SP&R Item Number 2269. Oklahoma City, Oklahoma.

Oklahoma Department of Transportation (ODOT). 2015. Maps AADT - Annual Average Daily Traffic. Oklahoma AADT Maps. Oklahoma City, OK.

Palisade Corporation, 2011. Palisade: Maker of the world's leading risk and decision analysis software, @RISK and the DecisionTools Suite. Palisade Corporation. Accessed January 4, 2011.

Park, Hun Myoung. 2011. Practical Guides to Panel Data Modeling: A Step-by-step Analysis Using Stata. Tutorial Working Paper. Graduate School of International Relations, International University of Japan.

Pavement Interactive. 2011. Los Angeles Abrasion.

Peshkin D.G., Hoerner T.E. and Zimmerman K.A. 2004. NCHRP Report 523: Optimal Timing of Pavement Preventive Maintenance Treatment Applications. Transportation Research Board, National Research Council, Washington, D.C.

Pidwerbesky et al. 2006. Road Surface Texture Measurement Using Digital Image Processing and Information Theory. Land Transport New Zealand Research Report 290. 65pp.

Pierce L.M. and Kebede N. 2015. Chip Seal Performance Measures – Best Practices. WA-RD 841.1. FHWA, U.S. Department of Transportation.

Pittenger, D.M., D. D. Gransberg, M. Zaman and C. Riemer. 2011. Life-Cycle Cost-Based Pavement Preservation Treatment Design. Transportation Research Record, Vol 2235, Issue 1, pp. 28 – 35.

Pittenger, D.M., D. D. Gransberg, M. Zaman and C. Riemer. 2012. Stochastic Life-Cycle Cost Analysis for Pavement Preservation Treatments. Transportation Research Record, Vol 2292, Issue 1, pp. 45 – 51.

Prapaitrakul, N., Freeman, T., and Glover, C. J. 2005. Analyze Existing Fog Seal Asphalts and Additives: Literature Review. Texas Transportation Institute, Research and Technology Implementation Office, Report No. FHWA/TX-06/0-5091-1.

Prowell B.D. and Hanson D.I. 2005. Evaluation of Circular Texture Meter for Measuring Surface Texture of Pavements. In Transportation Research Record: Journal of the Transportation Research Board, N0. 1929, Transportation Research Board of the National Academies, Washington, D.C., 88-96.

Prowell B.D., Hurley G.C., and Frank B. 2012. Warm-Mix Asphalt: Best Practices. 3rd Edition. NAPA – National Asphalt Pavement Association. Lanham, MD.

Prowell B.D., Zhang J. and Brown E.R. 2005. NCHRP Report 539: Aggregate Properties and the Performance of Superpave-Designed Hot Mix Asphalt. TRB, National Research Council, Washington, D.C.

Rado Z. and Kane M. 2014. An Initial Attempt to Develop an Empirical Relation between Texture and Pavement Friction Using the HHT Approach. Wear, Vol. 309, 233-236.

Ranstam, J. 2012. Why the P-value culture is bad and confidence intervals a better alternative. Osteoarthritis and Cartilage, 20(8), 805-808. doi: 10.1016/j.joca.2012.04.001

Rao C. 2002. Quantification of Coarse Aggregate Angularity Based on Image Analysis. In Transportation Research Record: Journal of the Transportation Research Board, No. 1787, Transportation Research Board of the National Academies, Washington, D.C., 117–124.

Reigle, J.A. and J. P. Zaniewski, 2002. Risk-Based Life-Cycle Cost Analysis for Project-Level Pavement Management, Transportation Research Record 1816, Paper No. 02-2579.

Rezaei A. and Masad E. 2013. Experimental-based Model for Predicting the Skid Resistance of Asphalt Pavements. International Journal of Pavement Engineering, Vol. 14, No. 1, 24-35.

Rezaei A., Masad E., Chowdhury A. and Harris P. 2009. Predicting Asphalt Mixture Skid Resistance by Aggregate Characteristics and Gradation. In Transportation Research Record: Journal of the Transportation Research Board, No. 2104, Transportation Research Board of the National Academies, Washington, D.C., 24–33. doi:10.3141/2104-03

Rezaei, A., E. Masad, A. Chowdhury and P. Harris, 2009. Predicting Asphalt Mixture Skid Resistance by Aggregate Characteristics and Gradation, Transportation Research Record: Journal of the Transportation Research Board, No. 2104, Transportation Research Board of the National Academies, Washington, D.C., pp. 24–33.

Rezaei, A., Masad, E., and Chowdhury, A. 2011. Development of a model for asphalt pavement skid resistance based on aggregate characteristics and gradation. Journal of Transportation Engineering, 137(12): 863–873. doi:10. 1061/(ASCE)TE.1943-5436.0000280.

Riemer, C., D.D. Gransberg, M. Zaman, and D. Pittenger. 2010. Comparative Field Testing of Asphalt and Concrete Pavement Preservation Treatments in Oklahoma. Proceedings, 1st International Conference on Pavement Preservation, Transportation Research Board, Newport Beach, California, pp.447-460.

Roberts, F.L. P.S. Kandhal, E.R. Brown, D.Y. Lee, and T.W. Kennedy, 1996. Hot Mix Asphalt Materials, Mixture Design, and Construction, National Asphalt Pavement Association Education Foundation, Lanham, MD.

Roe P.G. and Hartshorne S.A. 1998. The Polished Stone Value of Aggregates and In-Service Skidding Resistance. TRL Report 322, Transport Research Laboratory, Crowthorne, Berkshire.

Roe P.G., Webster D.C. and West G. 1991. The Relation between the Surface Texture of Roads and Accidents. Research Report 296, Transport and Road Research Laboratory, Crowthorne, Berkshire.

Rogers, C. 1998. Canadian Experience with the Micro-Deval Test for Aggregates, Advances in Aggregates and Armourstone Evaluation 13, 139-147.

Rogers C. A., M. L. Bailey, and B. Price. 1991. Micro-Deval Test for Evaluating the Quality of Fine Aggregate for Concrete and Asphalt. Transportation Research Record 1301, Transportation Research Record, Vol 1301, Issue 1, pp. 68-76.

Ronald L. Wasserstein & Nicole A. Lazar. 2016 The ASA's statement on p-values: context, process, and purpose. The American Statistician, 70:2, 129-133, doi: 10.1080/00031305.2016.1154108

SCDOT 2016. Ranking of Pavement Preservation Practices and Methods, Report No. FHWA-SC-16-05, South Carolina Department of Transportation. Columbia, SC.

Sengoz B, Onsori A, Topal A. 2014. Effect of aggregate shape on the surface properties of flexible pavement. KSCE J Civil Eng 18: 1364-1371.

Sengoz, B., Onsori, A., & Topal, A. 2014. Effect of aggregate shape on the surface properties of flexible pavement. KSCE Journal of Civil Engineering KSCE J Civ Eng, 18(5), 1364-1371. Doi: 10.1007/s12205-014-0516-0.

Serigos P.A. 2013. The Contribution of Micro- and Macrotexture to the Skid Resistance of Pavements. Southwest Region University Transportation Center, College Station TX.

Shah SMR, Abdullah M. E. 2010. Effect of aggregate shape on skid resistance of compacted Hot Mix Asphalt (HMA). 2nd International Conference on Computer and Network Technology, ICCNT 2010, 421-425.

Sinha, Kumares C., and S. Labi. 2007. Transportation Decision Making: Principles of Project Evaluation and Programming, pp. 199-211. John Wiley & Sons, Inc., Hoboken, New Jersey.

Smith, K.L., J.W. Hall and P. Littleton, 2009. NCHRP Report 634: Texturing of Concrete Pavements. Transportation Research Board, National Cooperative Highway Research Program, Washington DC.

Stanard et al. 2007. State of the Practice: Permeable Friction Course. FHWA/TX-08/0-5220-1. Center for Transportation Research, The University of Texas at Austin,

Austin, TX. Texas Department of Transportation, Research and Technology Implementation Office. Austin TX.

Stroup-Gardiner, M. and S. Shatnawi. 2008. The Economics of Flexible Pavement Preservation, TRB 2009 Annual Meeting Paper, Transportation Research Board, Washington D.C.

Steven B.D. 2009. Friction Testing of Pavement Preservation Treatments: Temperature Correlations and Operator/Machine Variability. CA11-1200 C. State of California Department of Transportation.

Susanna, A., Crispino, M., Giustozzi, F., & Toraldo, E. 2017. Deterioration trends of asphalt pavement friction and roughness from medium-term surveys on major Italian roads. International Journal of Pavement Research and Technology, 10(5), 421-433. doi: 10.1016/j.ijprt.2017.07.002

Tarefder, R.A., M. Zaman, and K. Hobson. 2003. Micro-Deval Test for Evaluating Properties of Roadway Aggregate. International Journal of Pavements: maintenance and rehabilitation of pavements and technological control, Vol. 2, Issue 1-2.

Thoreson, T., T. Martin, R. Hassain, M. Byrne, W. Hore-Lacy and G. Jameson, 2012. Preliminary Methodology for Estimating Cost Implications of Incremental Loads on Road Pavements. Austroads Research Report, Publication No. AP–R402-12, Sydney, Australia.

Tighe, S. 2001. Guidelines for Probabilistic Pavement Life Cycle Cost Analysis. Transportation Research Record: Journal of the Transportation Research Board, No. 1769, TRB, National Research Council, pp. 28-38. Washington, D.C.

Tutumluer, E., C. Rao, and J. Stefanski, 2000. Video Image Analysis of Aggregates, Final Project Report, FHWA-IL-UI-278, Civil Engineering Studies UILU-ENG-2000-2015, University of Illinois Urbana-Champaign, Urbana, IL.

Ueckermann et al. 2015. A Contribution to Non-contact Skid Resistance Measurement. International Journal of Pavement Engineering, Vol. 16, No. 7, 646-659.

Ueckermann et al. 2015. Calculation of Skid Resistance from Texture Measurements. Journal of Traffic and Transportation Engineering, Vol. 2, No. 1, 3-16.

Viner H. et al. 2006. Surface Texture Measurement on Local Roads. TRL Limited PPR148.

Volovski, M., J. Murillo-Hoyos, T. Saeed and S. Labi, 2017. Estimation of Routine Maintenance Expenditures for Highway Pavement Segments: Accounting for Heterogeneity Using Random-Effects Models, Journal of Transportation Engineering, May 2017, Vol.143(5), p.1.

Wang Kelvin C. P. 2011. Elements of Automated Survey of Pavements and a 3D Methodology. Journal of Modern Transportation, Volume 19, Number 1, pp: 51-57.

Wang K. C. P., Q. J. Li. 2017. Safety Analysis Opportunities Using Pavement Surface Characterization Based on 3D Laser Imaging. Federal Highway Administration, Washington, D.C.

Wang L., Sun W., et al. 2012. NCHRP Report 724: Application of LADAR in the Analysis of Aggregate Characteristics. Transportation Research Board, National Research Council, Washington, D.C.

Wang Z. 2013. Analysis of Effectiveness of Pavement Preservation Using Long-Term Pavement Performance Data. Master Dissertation, Rutgers, The State University of New Jersey, New Jersey.

Wang, H., and Wang, Z. 2013. Evaluation of pavement surface friction subject to various pavement preservation treatments. Construction and Building Materials, 48: 194–202. doi: 10.1016/j.conbuildmat.2013.06.048.

Wang, L., W. Sun, E. M. Lally, A. Wang, and E. Tutumluer. 2011. Application of LADAR in the Analysis of Aggregate Characteristics. NCHRP 4-34 Final Report. Transportation Research Board of the National Academies, Washington, D. C.

Watson M. et al. 2011. Hot Mixed Asphalt Pavement Surface Characteristics Related to: Ride, Texture, Friction, Noise and Durability. Minnesota Department of Transportation, Maplewood, MN.

White, J., K. Case, and D. Pratt. 2010. Principles of Engineering Economic Analysis, Fifth Edition, John Wiley & Sons, Inc., Hoboken, New Jersey.

White, T.D., Haddock, J.E., and Rismantojo, E. 2006. Aggregate Tests for Hot-Mix Asphalt Mixtures Used in Pavements. NCHRP Report No. 557, Transportation Research Board, Washington, D.C.

Wilson D.J. 2006. An Analysis of the Seasonal and Short-Term Variation of Road Pavement Skid Resistance. Ph.D. Dissertation, The University of Auckland, New Zealand.

Wu, Y. F. Parker, and K. Kandhal, 1998. Aggregate Toughness/Abrasion Resistance and Durability/Soundness Tests Related to Asphalt Concrete Performance in Pavements. NCAT Report 98-4. National Center for Asphalt Technology. Auburn, AL.

Yager T.J. 2013. How Best to Determine Runway/Highway Pavement Surface Friction Performance. Tenth ALACPA Airport Pavement Seminar, Mexico City, Mexico. Accessed 12 Jan, 2016 from

Zaman, M., D. D. Gransberg, C. Riemer, D. Pittenger, B. Aktas, 2012. Quantifying the Costs and Benefits of Pavement Preservation – Phases 1 & 2, Final Report, OTCREOS9.1-21-F, Oklahoma Transportation Center.

Zaman M., D. Pittenger, D. Gransberg, R. Bulut, S. Commuri. 2014. Develop Draft Chip Seal Cover Aggregate Specification based on Aggregate Imaging System (AIMS) Angularity, Shape, and Texture Test Results. Final Report. Oklahoma Department of Transportation, Oklahoma City, OK.

Zaniewski J.P. and Mamlouk M.S. 1996. Preventive Maintenance Effectiveness – Preventive Maintenance Treatments. FHWA-SA-96-027. FHWA, U.S. Department of Transportation.

Zelelew H.M. et al. 2013. Pavement Macrotexture Analysis Using Wavelets. International Journal of Pavement Engineering, 14:8, 725-735, DOI: 10.1080/10298436.2012.705004.

Zelelew H.M. et al. 2014. Wavelet-based Characterization of Asphalt Pavement Surface Macrotexture. Road Materials and Pavement Design, 15:3, 622-641, DOI:10.1080/14680629.

APPENDIX A AIMS LABORATORY TESTING DATA AND RESULTS

This appendix contains AIMS results for each aggregate type and size consistent with the nominal maximum aggregate size contained in this study's field pavement treatments. Pre- and Post- Micro Deval data are provided. Graphical data for the 12.5-NMAS aggregate are provided within the body of the report in the "Preliminary Results" section. Graphical data for other NMAS aggregate are found herein.

Table A1 AIMS Results for APAC Central 14 (Jenny Lind, Arkansas), 12.5mm

AIMS Property	**Pre MD Range**	**Pre MD %**	**Post MD Range**	**Post MD %**
Gradient Angularity	1500 - 9900	100	1000 - 8000	100
Rounded (< 2100)		9		38
Sub-Rounded (2100 - 4000)		71		57
Sub-Angular (4000 - 5400)		24		0
Angular (> 5400)		4		5
Sphericity	0.50 – 0.91	100	0.45 – 0.90	100
Flat/Elongated (< 0.6)		20		38
Low Sphericity (0.6 – 0.7)		32		22
Moderate Sphericity (0.7 – 0.8)		33		33
High Sphericity (> 0.8)		15		7
AIMS Property: Texture				
Texture	100 - 400	100	40 - 400	100
Polished Faces (< 165)		23		10
Smooth Faces (165 – 275)		73		70
Low Roughness (275 – 350)		4		16
Mod. Roughness (350 - 460)		0		4
High Roughness (> 460)		0		0

Table A2 AIMS Results for APAC Pawhuska, 12.5mm

AIMS Property	**Pre MD Range**	**Pre MD %**	**Post MD Range**	**Post MD %**
Gradient Angularity	900 - 5500	100	250 - 5700	100
Rounded (< 2100)		31		65
Sub-Rounded (2100 - 4000)		63		30
Sub-Angular (4000 - 5400)		4		4
Angular (> 5400)		2		1
Sphericity	0.55 – 0.80	100	0.33 – 0.88	100
Flat/Elongated (< 0.6)		20		37
Low Sphericity (0.6 – 0.7)		43		43
Moderate Sphericity (0.7 – 0.8)		37		15
High Sphericity (> 0.8)		0		5
AIMS Property: Texture				
Texture	40 - 570	100	30 - 400	100
Polished Faces (< 165)		16		57
Smooth Faces (165 – 275)		34		31
Low Roughness (275 – 350)		23		10
Mod. Roughness (350 - 460)		17		2
High Roughness (> 460)		10		0

Table A3 AIMS Results for APAC Spiro, 9.5mm

AIMS Property	**Pre MD Range**	**Pre MD %**	**Post MD Range**	**Post MD %**
Gradient Angularity	1100 - 7100	100	300 - 7300	100
Rounded (< 2100)		37		70
Sub-Rounded (2100 - 4000)		48		27
Sub-Angular (4000 - 5400)		2		0
Angular (> 5400)		13		3
Sphericity	0.18 – 0.82	100	0.30 – 0.75	100
Flat/Elongated (< 0.6)		50		65
Low Sphericity (0.6 – 0.7)		30		29
Moderate Sphericity (0.7 – 0.8)		17		6
High Sphericity (> 0.8)		3		0
AIMS Property: Texture				
Texture	85 - 300	100	70 - 220	100
Polished Faces (< 165)		70		73
Smooth Faces (165 – 275)		29		27
Low Roughness (275 – 350)		1		0
Mod. Roughness (350 - 460)		0		0
High Roughness (> 460)		0		0

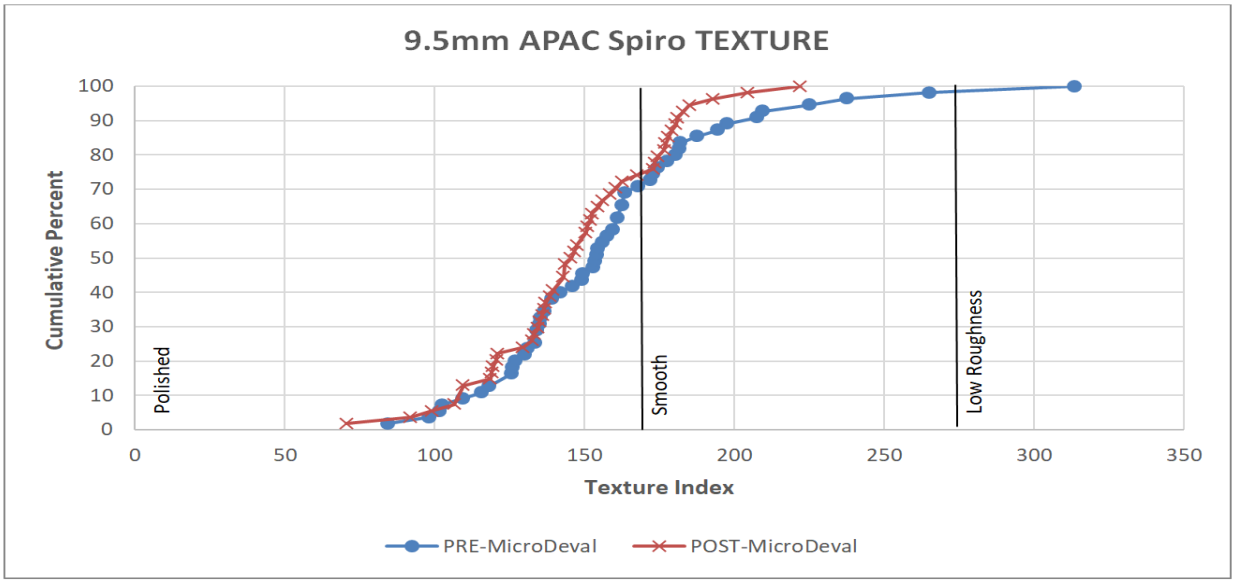

Figure A1 AIMS Texture Results for APAC Spiro, 9.5mm

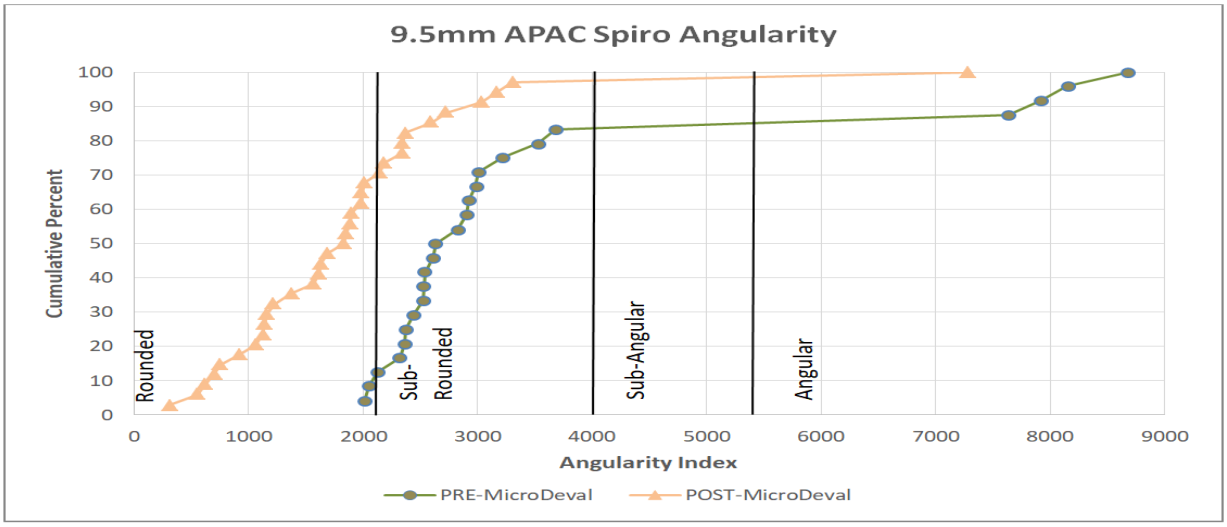

Figure A2 AIMS Angularity Results for APAC Spiro, 9.5mm

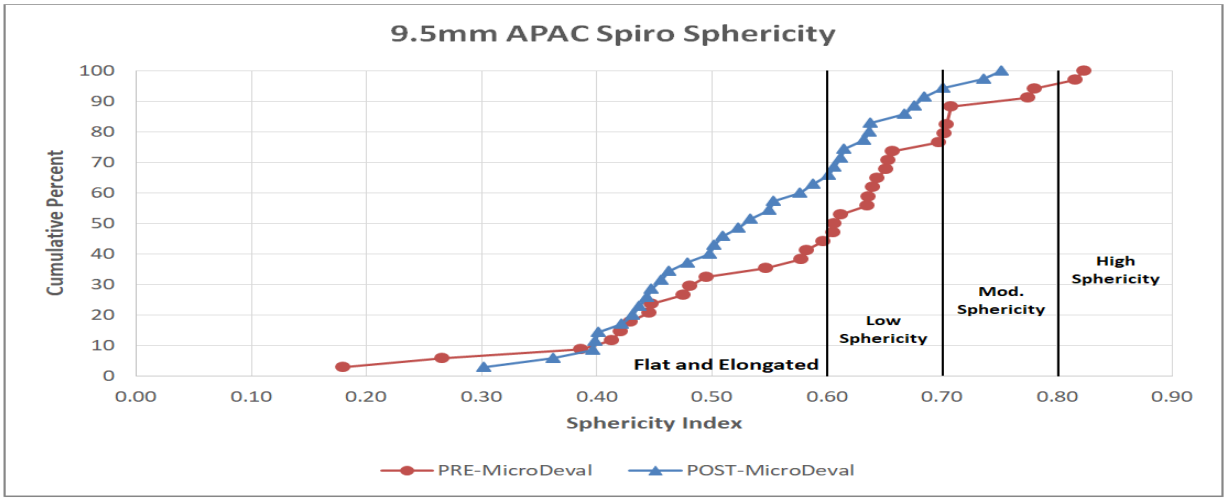

Figure A3 AIMS Sphericity Results for APAC Spiro, 9.5mm

Table A4 AIMS Results for Bauxite, No.8

AIMS Property	Pre MD Range	Pre MD %	Post MD Range	Post MD %
Gradient Angularity	230 - 7000	100	220 - 7200	100
Rounded (< 2100)		27		34
Sub-Rounded (2100 - 4000)		68		63
Sub-Angular (4000 - 5400)		4		2
Angular (> 5400)		1		1
Sphericity				
	N/A – Too small for procedure		N/A – Too small for procedure	
Texture				
	N/A – Too small for procedure		N/A – Too small for procedure	

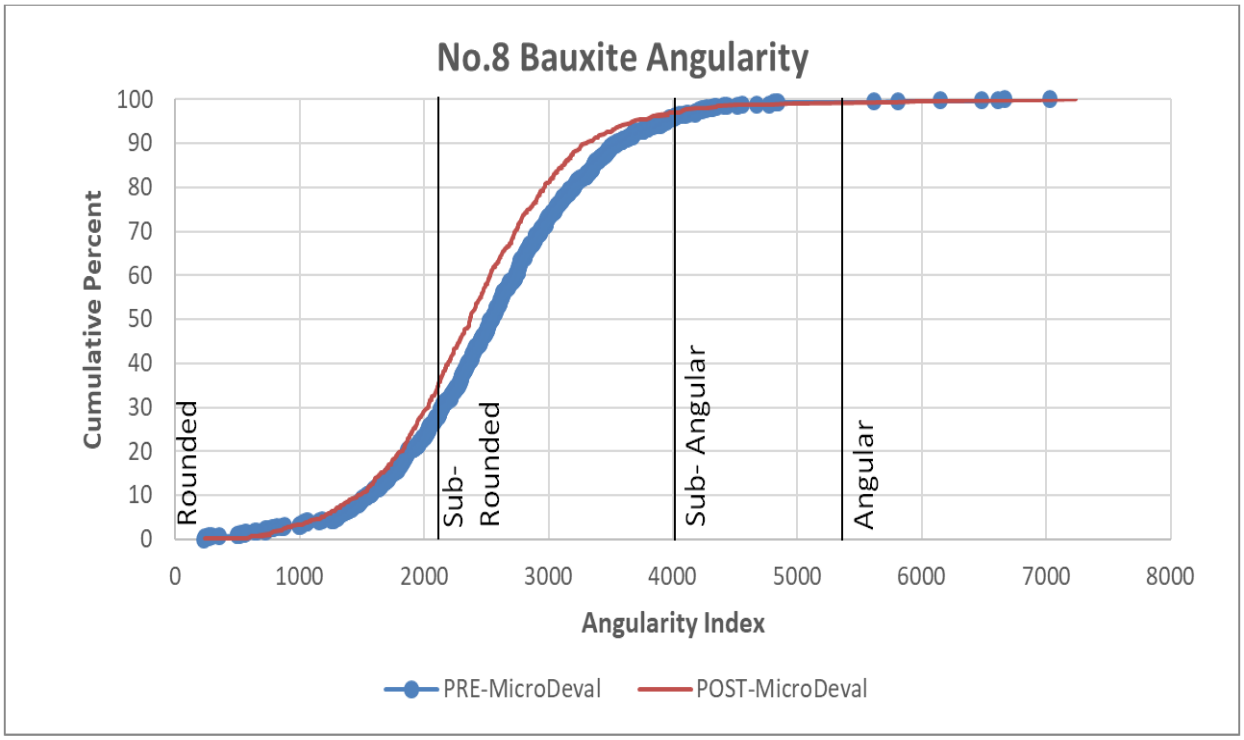

Figure A4 AIMS Angularity Results for Bauxite, No.8

Table A5 AIMS Results for Dolese Davis, 12.5mm

AIMS Property	**Pre MD Range**	**Pre MD %**	**Post MD Range**	**Post MD %**
Gradient Angularity	1000 - 9700	100	500 - 8000	100
Rounded (< 2100)		15		47
Sub-Rounded (2100 - 4000)		63		38
Sub-Angular (4000 - 5400)		10		7
Angular (> 5400)		12		8
Sphericity	0.30 – 0.90	100	0.30 – 0.90	100
Flat/Elongated (< 0.6)		20		20
Low Sphericity (0.6 – 0.7)		30		36
Moderate Sphericity (0.7 – 0.8)		32		31
High Sphericity (> 0.8)		18		13
AIMS Property: Texture				
Texture	100 - 400	100	30 - 300	100
Polished Faces (< 165)		21		70
Smooth Faces (165 – 275)		50		28
Low Roughness (275 – 350)		25		2
Mod. Roughness (350 - 460)		4		0
High Roughness (> 460)		0		0

Table A6 AIMS Results for Dolese Hartshorne, 12.5mm

AIMS Property	Pre MD Range	Pre MD %	Post MD Range	Post MD %
Gradient Angularity	1500 - 6000	100	500 - 8000	100
Rounded (< 2100)		8		33
Sub-Rounded (2100 - 4000)		78		53
Sub-Angular (4000 - 5400)		12		7
Angular (> 5400)		2		7
Sphericity	0.30 – 0.90	100	0.40 – 0.97	100
Flat/Elongated (< 0.6)		13		5
Low Sphericity (0.6 – 0.7)		22		15
Moderate Sphericity (0.7 – 0.8)		36		29
High Sphericity (> 0.8)		29		51
AIMS Property: Texture				
Texture	70 - 450	100	20 - 400	100
Polished Faces (< 165)		19		29
Smooth Faces (165 – 275)		43		60
Low Roughness (275 – 350)		26		8
Mod. Roughness (350 - 460)		12		3
High Roughness (> 460)		0		0

Table A7 AIMS Results for Dolese Richard Spur, 12.5mm

AIMS Property	Pre MD Range	Pre MD %	Post MD Range	Post MD %
Gradient Angularity	1600 - 5700	100	300 - 6300	100
Rounded (< 2100)		7		49
Sub-Rounded (2100 - 4000)		73		44
Sub-Angular (4000 - 5400)		18		4
Angular (> 5400)		2		3
Sphericity	0.30 – 0.82	100	0.30 – 0.80	100
Flat/Elongated (< 0.6)		45		55
Low Sphericity (0.6 – 0.7)		35		30
Moderate Sphericity (0.7 – 0.8)		18		15
High Sphericity (> 0.8)		2		0
AIMS Property: Texture				
Texture	50 - 650	100	20 - 300	100
Polished Faces (< 165)		20		64
Smooth Faces (165 – 275)		38		32
Low Roughness (275 – 350)		22		4
Mod. Roughness (350 - 460)		13		0
High Roughness (> 460)		7		0

Table A8 AIMS Results for Flint Rock Mine Chat, 6.3mm

AIMS Property	**Pre MD Range**	**Pre MD %**	**Post MD Range**	**Post MD %**
Gradient Angularity	1700 - 6300	100	900 - 7000	100
Rounded (< 2100)		5		10
Sub-Rounded (2100 - 4000)		75		72
Sub-Angular (4000 - 5400)		17		13
Angular (> 5400)		3		5
Sphericity	0.40 – 0.93	100	0.40 – 0.97	100
Flat/Elongated (< 0.6)		27		32
Low Sphericity (0.6 – 0.7)		17		10
Moderate Sphericity (0.7 – 0.8)		32		26
High Sphericity (> 0.8)		24		32
AIMS Property: Texture				
Texture	15 - 300	100	15 - 200	100
Polished Faces (< 165)		85		97
Smooth Faces (165 – 275)		13		3
Low Roughness (275 – 350)		2		0
Mod. Roughness (350 - 460)		0		0
High Roughness (> 460)		0		0

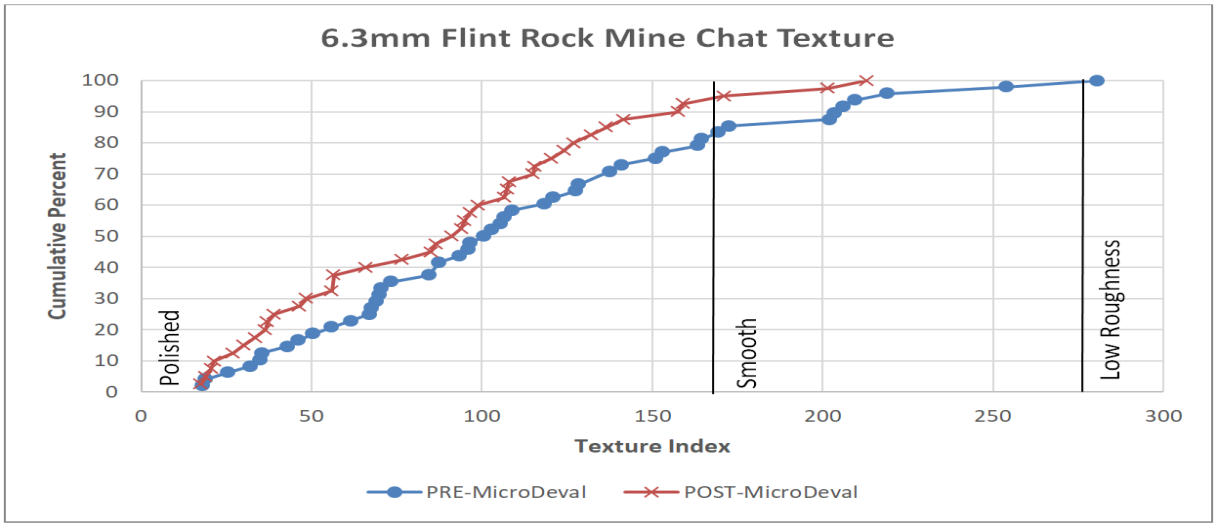

Figure A5 AIMS Texture Results for Flint Rock Mine Chat, 6.3mm

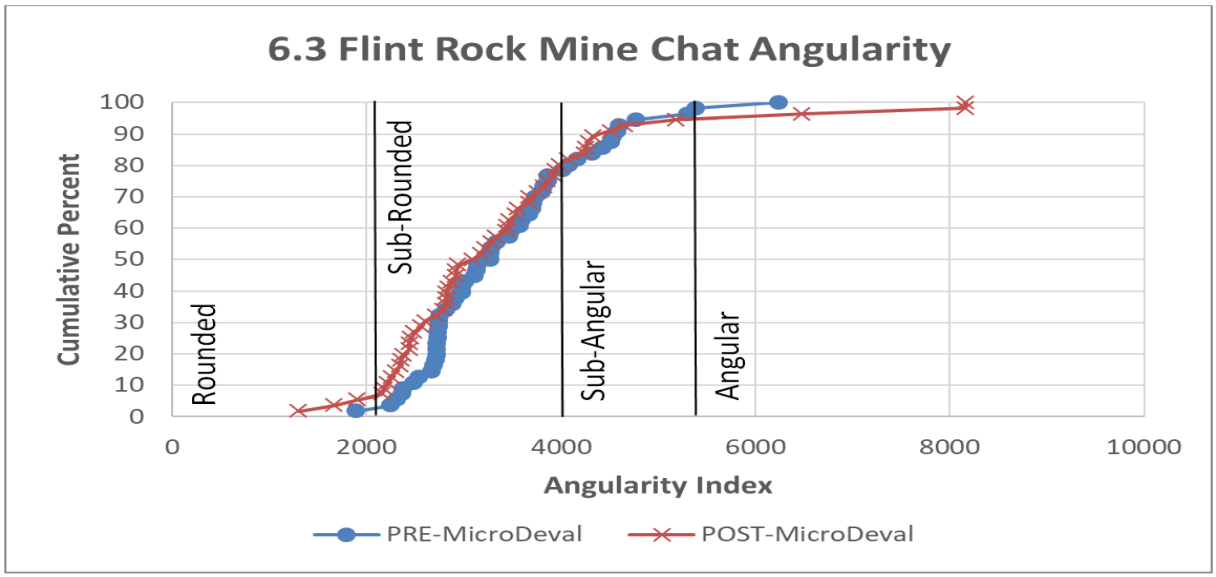

Figure A6 AIMS Angularity Results for Flint Rock Mine Chat, 6.3mm

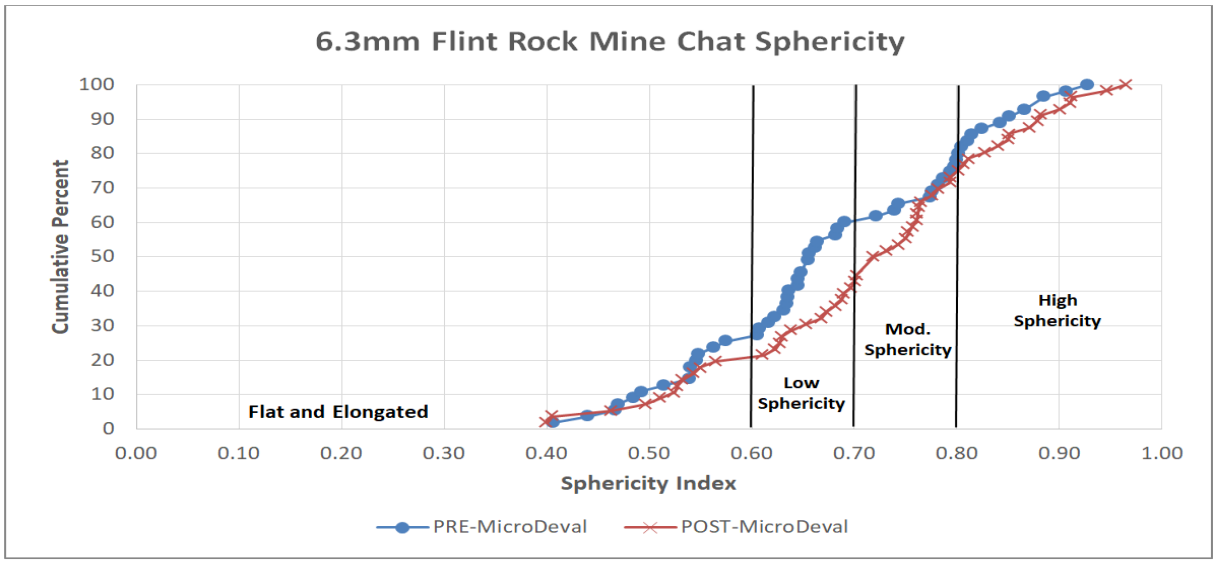

Figure A7 AIMS Sphericity Results for Flint Rock Mine Chat, 6.3mm

Table A9 AIMS Results for Hanson Davis, 12.5mm

AIMS Property	**Pre MD Range**	**Pre MD %**	**Post MD Range**	**Post MD %**
Gradient Angularity	1300 - 9500	100	1100 - 8100	100
Rounded (< 2100)		8		25
Sub-Rounded (2100 - 4000)		75		65
Sub-Angular (4000 - 5400)		12		3
Angular (> 5400)		5		7
Sphericity	0.40 – 0.83	100	0.30 – 0.84	100
Flat/Elongated (< 0.6)		37		43
Low Sphericity (0.6 – 0.7)		49		41
Moderate Sphericity (0.7 – 0.8)		11		14
High Sphericity (> 0.8)		3		2
AIMS Property: Texture				
Texture	40 - 350	100	90 - 330	100
Polished Faces (< 165)		26		24
Smooth Faces (165 – 275)		58		65
Low Roughness (275 – 350)		16		11
Mod. Roughness (350 - 460)		0		0
High Roughness (> 460)		0		0

Table A10 AIMS Results for Martin Marietta Mill Creek, No.4

AIMS Property	Pre MD Range	Pre MD %	Post MD Range	Post MD %
Gradient Angularity	1800 - 7000	100	1300 - 9400	100
Rounded (< 2100)		3		14
Sub-Rounded (2100 - 4000)		65		64
Sub-Angular (4000 - 5400)		26		9
Angular (> 5400)		6		13
Sphericity	0.30 – 0.90	100	0.40 – 0.85	100
Flat/Elongated (< 0.6)		39		11
Low Sphericity (0.6 – 0.7)		35		33
Moderate Sphericity (0.7 – 0.8)		22		43
High Sphericity (> 0.8)		4		13
AIMS Property: Texture				
Texture	30 - 430	100	25 - 200	100
Polished Faces (< 165)		65		90
Smooth Faces (165 – 275)		25		10
Low Roughness (275 – 350)		6		0
Mod. Roughness (350 - 460)		4		0
High Roughness (> 460)		0		0

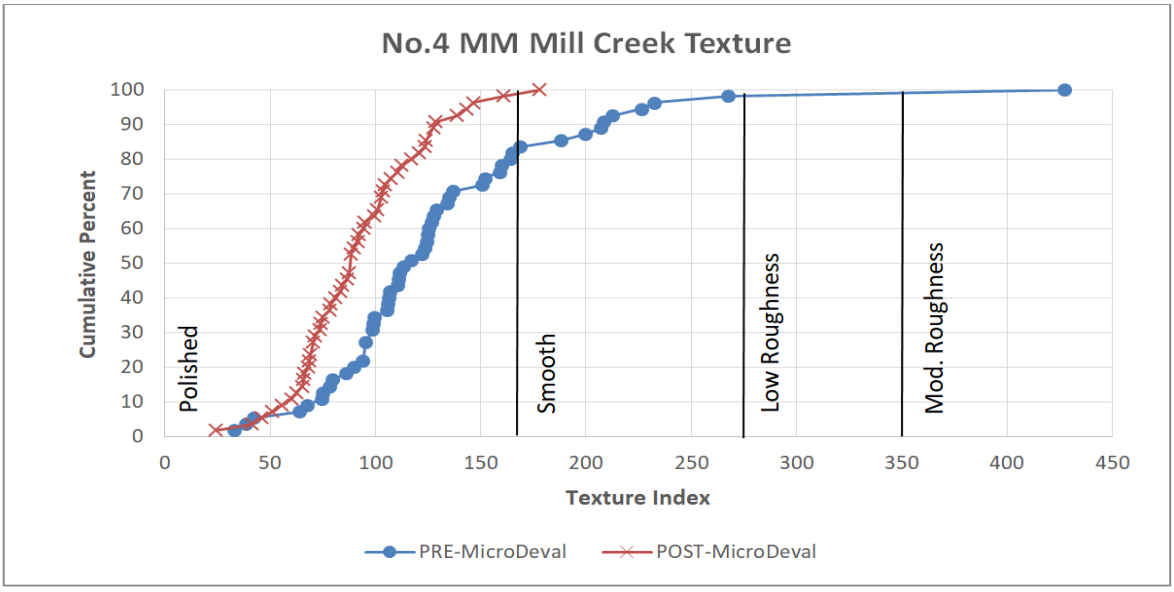

Figure A8 AIMS Texture Results for Martin Marietta Mill Creek, No.4

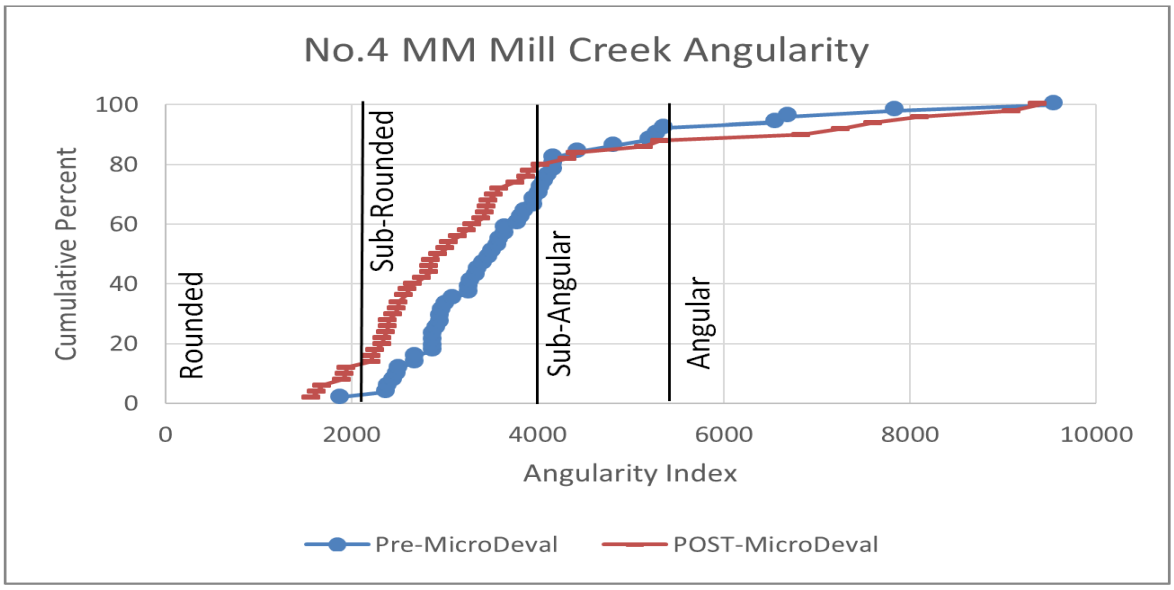

Figure A9 AIMS Angularity Results for Martin Marietta Mill Creek, No.4

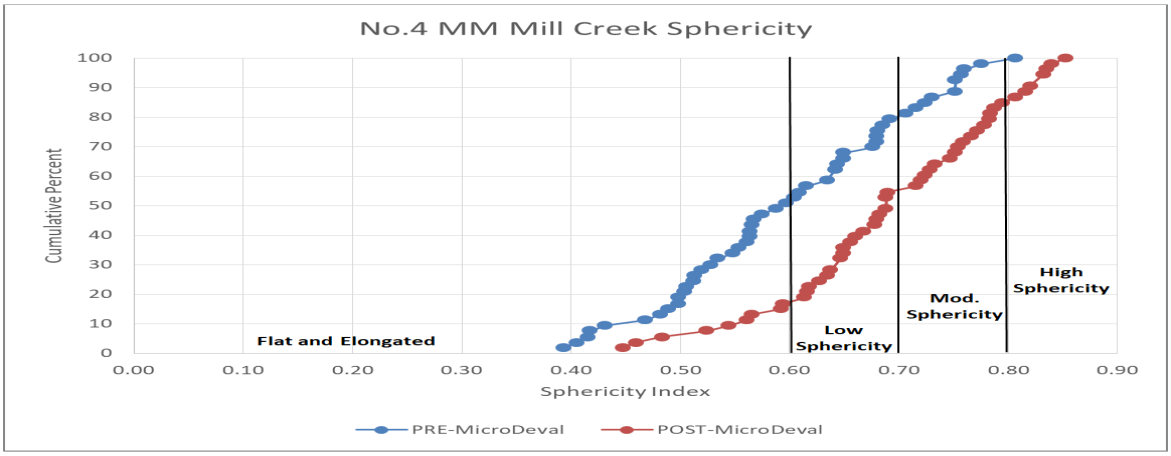

Figure A10 AIMS Sphericity Results for Martin Marietta Mill Creek, No.4

Table A11 AIMS Results for Martin Marietta Sawyer, 12.5mm

AIMS Property	**Pre MD Range**	**Pre MD %**	**Post MD Range**	**Post MD %**
Gradient Angularity	1800 - 8000	100	900 - 8000	100
Rounded (< 2100)		13		42
Sub-Rounded (2100 - 4000)		70		53
Sub-Angular (4000 - 5400)		13		3
Angular (> 5400)		4		2
Sphericity	0.30 – 0.73	100	0.30 – 0.82	100
Flat/Elongated (< 0.6)		65		51
Low Sphericity (0.6 – 0.7)		31		35
Moderate Sphericity (0.7 – 0.8)		4		12
High Sphericity (> 0.8)		0		2
AIMS Property: Texture				
Texture	40 - 300	100	40 - 250	100
Polished Faces (< 165)		60		83
Smooth Faces (165 – 275)		37		17
Low Roughness (275 – 350)		3		0
Mod. Roughness (350 - 460)		0		0
High Roughness (> 460)		0		0

Table A12 AIMS Results for Martin Marietta Snyder, 12.5mm

AIMS Property	Pre MD Range	Pre MD %	Post MD Range	Post MD %
Gradient Angularity	1200 - 7400	100	1000 - 9000	100
Rounded (< 2100)		10		15
Sub-Rounded (2100 - 4000)		75		65
Sub-Angular (4000 - 5400)		10		10
Angular (> 5400)		5		10
Sphericity	0.30 – 0.85	100	0.40 – 0.90	100
Flat/Elongated (< 0.6)		40		49
Low Sphericity (0.6 – 0.7)		39		24
Moderate Sphericity (0.7 – 0.8)		19		25
High Sphericity (> 0.8)		2		2
AIMS Property: Texture				
Texture	200 - 670	100	150 - 400	100
Polished Faces (< 165)		0		2
Smooth Faces (165 – 275)		2		66
Low Roughness (275 – 350)		16		30
Mod. Roughness (350 - 460)		29		2
High Roughness (> 460)		53		0

Table A13 AIMS Results for Quapaw Drumright, 12.5mm

AIMS Property	**Pre MD Range**	**Pre MD %**	**Post MD Range**	**Post MD %**
Gradient Angularity	1100 - 8500	100	500 - 3000	100
Rounded (< 2100)		20		60
Sub-Rounded (2100 - 4000)		66		40
Sub-Angular (4000 - 5400)		9		0
Angular (> 5400)		5		0
Sphericity	0.20 – 0.90	100	0.30 – 0.84	100
Flat/Elongated (< 0.6)		19		51
Low Sphericity (0.6 – 0.7)		31		35
Moderate Sphericity (0.7 – 0.8)		32		11
High Sphericity (> 0.8)		18		3
AIMS Property: Texture				
Texture	100 - 450	100	80 - 300	100
Polished Faces (< 165)		20		40
Smooth Faces (165 – 275)		64		57
Low Roughness (275 – 350)		14		3
Mod. Roughness (350 - 460)		2		0
High Roughness (> 460)		0		0

APPENDIX B PERFORMANCE BASED LCCA RESULTS

The application of the EUAC LCCA model used in this research is informed by the OLS friction prediction model created for this project. Input values are based upon field trial, vendor and ODOT survey data, literature review results and bid tabulations. The LCCA procedures, as excerpted from the FHWA Life Cycle Cost Analysis Primer (FHWA 2002) and the Interim Technical Bulletin (FHWA 1998), serve as the basis for the EUAC model. This Appendix provides the detailed performance based LCCA results.

Table B1 Performance (Friction) Based Cost Analysis Results for HMA/WMA Scenario

Parameter	Intercept	AADT LR	AADT Mean	Age LR	Age Mean	Temp LR	Temp Mean	MD LR	MD Mean	NMAS LR	NMAS Mean	AB LR	AB Mean	TC LR	TC Mean	SC LR	SC Mean	Perf Output	EXP LCCA	EUAC Output
TRAFFIC	2.41	-0.00000202	4411	-0.0122	3.19	-0.0029	73.15	-0.0045	8.73	-0.0354	11.21	-0.0004	2970	0.005	-12.13	0.011	-2.14	0.442	-9.993	$3,500
HMA BASE	2.41	-0.00000202	4411	-0.0122	8	-0.0029	73.15	-0.0045	8.73	-0.0354	11.21	-0.0004	2970	0.005	-12.13	0.011	-2.14	0.383	-8.646	$3,992
Sensitivity	2.41	-0.00000202	10000	-0.0122	8	-0.0029	73.15	-0.0045	8.73	-0.0354	11.21	-0.0004	2970	0.005	-12.13	0.011	-2.14	0.372	-8.646	$5,170
Sensitivity	2.41	-0.00000202	2500	-0.0122	8	-0.0029	73.15	-0.0045	8.73	-0.0354	11.21	-0.0004	2970	0.005	-12.13	0.011	-2.14	0.387	-8.646	$3,661
HMA BASE	2.41	-0.00000202	4411	-0.0122	10	-0.0029	73.15	-0.0045	8.73	-0.0354	11.21	-0.0004	2970	0.005	-12.13	0.011	-2.14	0.359	-7.976	$3,550
Sensitivity	2.41	-0.00000202	10000	-0.0122	10	-0.0029	73.15	-0.0045	8.73	-0.0354	11.21	-0.0004	2970	0.005	-12.13	0.011	-2.14	0.348	-7.976	$4,581
Sensitivity	2.41	-0.00000202	2500	-0.0122	10	-0.0029	73.15	-0.0045	8.73	-0.0354	11.21	-0.0004	2970	0.005	-12.13	0.011	-2.14	0.363	-7.976	$3,259
HMA BASE	2.41	-0.00000202	4411	-0.0122	12	-0.0029	73.15	-0.0045	8.73	-0.0354	11.21	-0.0004	2970	0.005	-12.13	0.011	-2.14	0.334	-7.306	$2,990
Sensitivity	2.41	-0.00000202	10000	-0.0122	12	-0.0029	73.15	-0.0045	8.73	-0.0354	11.21	-0.0004	2970	0.005	-12.13	0.011	-2.14	0.323	-7.306	$3,842
Sensitivity	2.41	-0.00000202	2500	-0.0122	12	-0.0029	73.15	-0.0045	8.73	-0.0354	11.21	-0.0004	2970	0.005	-12.13	0.011	-2.14	0.338	-7.306	$2,749
TEMP																				
Sensitivity	2.41	-0.00000202	4411	-0.0122	3.19	-0.0029	72.15	-0.0045	8.73	-0.0354	11.21	-0.0004	2970	0.005	-12.13	0.011	-2.14	0.445	-9.993	$3,279
HMA BASE	2.41	-0.00000202	4411	-0.0122	3.19	-0.0029	73.15	-0.0045	8.73	-0.0354	11.21	-0.0004	2970	0.005	-12.13	0.011	-2.14	0.442	-9.993	$3,500
Sensitivity	2.41	-0.00000202	4411	-0.0122	3.19	-0.0029	74.15	-0.0045	8.73	-0.0354	11.21	-0.0004	2970	0.005	-12.13	0.011	-2.14	0.439	-9.993	$3,738
MD																				
Sensitivity	2.41	-0.00000202	4411	-0.0122	3.19	-0.0029	73.15	-0.0045	5.73	-0.0354	11.21	-0.0004	2970	0.005	-12.13	0.011	-2.14	0.455	-9.993	$2,591
HMA BASE	2.41	-0.00000202	4411	-0.0122	3.19	-0.0029	73.15	-0.0045	8.73	-0.0354	11.21	-0.0004	2970	0.005	-12.13	0.011	-2.14	0.442	-9.993	$3,500
Sensitivity	2.41	-0.00000202	4411	-0.0122	3.19	-0.0029	73.15	-0.0045	11.73	-0.0354	11.21	-0.0004	2970	0.005	-12.13	0.011	-2.14	0.428	-9.993	$4,772
NMAS																				
Sensitivity	2.41	-0.00000202	4411	-0.0122	3.19	-0.0029	73.15	-0.0045	8.73	-0.0354	11	-0.0004	2970	0.005	-12.13	0.011	-2.14	0.449	-9.993	$2,963
HMA BASE	2.41	-0.00000202	4411	-0.0122	3.19	-0.0029	73.15	-0.0045	8.73	-0.0354	11.21	-0.0004	2970	0.005	-12.13	0.011	-2.14	0.442	-9.993	$3,500
Sensitivity	2.41	-0.00000202	4411	-0.0122	3.19	-0.0029	73.15	-0.0045	8.73	-0.0354	11.42	-0.0004	2970	0.005	-12.13	0.011	-2.14	0.434	-9.993	$4,147
AB																				
Sensitivity	2.41	-0.00000202	4411	-0.0122	3.19	-0.0029	73.15	-0.0045	8.73	-0.0354	11.21	-0.0004	2900	0.005	-12.13	0.011	-2.14	0.470	-9.993	$1,902
HMA BASE	2.41	-0.00000202	4411	-0.0122	3.19	-0.0029	73.15	-0.0045	8.73	-0.0354	11.21	-0.0004	2970	0.005	-12.13	0.011	-2.14	0.442	-9.993	$3,500
Sensitivity	2.41	-0.00000202	4411	-0.0122	3.19	-0.0029	73.15	-0.0045	8.73	-0.0354	11.21	-0.0004	3000	0.005	-12.13	0.011	-2.14	0.430	-9.993	$4,628
TC																				
Sensitivity	2.41	-0.00000202	4411	-0.0122	3.19	-0.0029	73.15	-0.0045	8.73	-0.0354	11.21	-0.0004	2970	0.005	-10	0.011	-2.14	0.453	-9.993	$2,759
HMA BASE	2.41	-0.00000202	4411	-0.0122	3.19	-0.0029	73.15	-0.0045	8.73	-0.0354	11.21	-0.0004	2970	0.005	-12.13	0.011	-2.14	0.442	-9.993	$3,500
Sensitivity	2.41	-0.00000202	4411	-0.0122	3.19	-0.0029	73.15	-0.0045	8.73	-0.0354	11.21	-0.0004	2970	0.005	-14	0.011	-2.14	0.433	-9.993	$4,334

Parameter	Intercept	AADT LR	AADT Mean	Age LR	Age Mean	Temp LR	Temp Mean	MD LR	MD Mean	NMAS LR	NMAS Mean	AB LR	AB Mean	TC LR	TC Mean	SC LR	SC Mean	Perf Output	EXP LCCA	EUAC Output
SC																				
Sensitivity	2.41	-0.00000202	4411	-0.0122	3.19	-0.0029	73.15	-0.0045	8.73	-0.0354	11.21	-0.0004	2970	0.005	-12.13	0.011	-1.14	0.453	-9.993	$2,738
HMA BASE	2.41	-0.00000202	4411	-0.0122	3.19	-0.0029	73.15	-0.0045	8.73	-0.0354	11.21	-0.0004	2970	0.005	-12.13	0.011	-2.14	0.442	-9.993	$3,500
Sensitivity	2.41	-0.00000202	4411	-0.0122	3.19	-0.0029	73.15	-0.0045	8.73	-0.0354	11.21	-0.0004	2970	0.005	-12.13	0.011	-3.14	0.431	-9.993	$4,503

Table B2 Performance (Friction) -Based Cost Analysis Results for Chip Seal Scenario

Parameter	Intercept	AADT LR	AADT Mean	Age LR	Age Mean	Temp LR	Temp Mean	MD LR	MD Mean	NMAS LR	NMAS Mean	AB LR	AB Mean	TC LR	TC Mean	SC LR	SC Mean	Perf Output	EXP LCCA	EUAC Output
TRAFFIC	2.41	-0.00000202	4411	-0.0122	3.19	-0.0029	73.15	-0.0045	8.73	-0.0354	11.21	-0.0004	2970	0.005	-12.13	0.011	-2.14	0.442	-10.061	$3,700
Chip BASE	2.41	-0.00000202	4411	-0.0122	4	-0.0029	73.15	-0.0045	8.73	-0.0354	11.21	-0.0004	2970	0.005	-12.13	0.011	-2.14	0.432	-10.023	$4,500
Sensitivity	2.41	-0.00000202	10000	-0.0122	4	-0.0029	73.15	-0.0045	8.73	-0.0354	11.21	-0.0004	2970	0.005	-12.13	0.011	-2.14	0.421	-10.023	$5,867
Sensitivity	2.41	-0.00000202	2500	-0.0122	4	-0.0029	73.15	-0.0045	8.73	-0.0354	11.21	-0.0004	2970	0.005	-12.13	0.011	-2.14	0.436	-10.023	$4,116
Chip BASE	2.41	-0.00000202	4411	-0.0122	5	-0.0029	73.15	-0.0045	8.73	-0.0354	11.21	-0.0004	2970	0.005	-12.13	0.011	-2.14	0.420	-9.467	$3,700
Sensitivity	2.41	-0.00000202	10000	-0.0122	5	-0.0029	73.15	-0.0045	8.73	-0.0354	11.21	-0.0004	2970	0.005	-12.13	0.011	-2.14	0.409	-9.467	$4,789
Sensitivity	2.41	-0.00000202	2500	-0.0122	5	-0.0029	73.15	-0.0045	8.73	-0.0354	11.21	-0.0004	2970	0.005	-12.13	0.011	-2.14	0.424	-9.467	$3,393
Chip BASE	2.41	-0.00000202	4411	-0.0122	6	-0.0029	73.15	-0.0045	8.73	-0.0354	11.21	-0.0004	2970	0.005	-12.13	0.011	-2.14	0.408	-8.958	$3,100
Sensitivity	2.41	-0.00000202	10000	-0.0122	6	-0.0029	73.15	-0.0045	8.73	-0.0354	11.21	-0.0004	2970	0.005	-12.13	0.011	-2.14	0.396	-8.958	$3,986
Sensitivity	2.41	-0.00000202	2500	-0.0122	6	-0.0029	73.15	-0.0045	8.73	-0.0354	11.21	-0.0004	2970	0.005	-12.13	0.011	-2.14	0.411	-8.958	$2,849
TEMP																				
Sensitivity	2.41	-0.00000202	4411	-0.0122	3.19	-0.0029	72.15	-0.0045	8.73	-0.0354	11.21	-0.0004	2970	0.005	-12.13	0.011	-2.14	0.445	-10.061	$3,464
Chip BASE	2.41	-0.00000202	4411	-0.0122	3.19	-0.0029	73.15	-0.0045	8.73	-0.0354	11.21	-0.0004	2970	0.005	-12.13	0.011	-2.14	0.442	-10.061	$3,700
Sensitivity	2.41	-0.00000202	4411	-0.0122	3.19	-0.0029	74.15	-0.0045	8.73	-0.0354	11.21	-0.0004	2970	0.005	-12.13	0.011	-2.14	0.439	-10.061	$3,953
MD																				
Sensitivity	2.41	-0.00000202	4411	-0.0122	3.19	-0.0029	73.15	-0.0045	5.73	-0.0354	11.21	-0.0004	2970	0.005	-12.13	0.011	-2.14	0.455	-10.061	$2,734
Chip BASE	2.41	-0.00000202	4411	-0.0122	3.19	-0.0029	73.15	-0.0045	8.73	-0.0354	11.21	-0.0004	2970	0.005	-12.13	0.011	-2.14	0.442	-10.061	$3,700
Sensitivity	2.41	-0.00000202	4411	-0.0122	3.19	-0.0029	73.15	-0.0045	11.73	-0.0354	11.21	-0.0004	2970	0.005	-12.13	0.011	-2.14	0.428	-10.061	$5,056
NMAS																				
Sensitivity	2.41	-0.00000202	4411	-0.0122	3.19	-0.0029	73.15	-0.0045	8.73	-0.0354	11	-0.0004	2970	0.005	-12.13	0.011	-2.14	0.449	-10.061	$3,128
Chip BASE	2.41	-0.00000202	4411	-0.0122	3.19	-0.0029	73.15	-0.0045	8.73	-0.0354	11.21	-0.0004	2970	0.005	-12.13	0.011	-2.14	0.442	-10.061	$3,700
Sensitivity	2.41	-0.00000202	4411	-0.0122	3.19	-0.0029	73.15	-0.0045	8.73	-0.0354	11.42	-0.0004	2970	0.005	-12.13	0.011	-2.14	0.434	-10.061	$4,389
AB																				
Sensitivity	2.41	-0.00000202	4411	-0.0122	3.19	-0.0029	73.15	-0.0045	8.73	-0.0354	11.21	-0.0004	2900	0.005	-12.13	0.011	-2.14	0.470	-10.061	$2,002
Chip BASE	2.41	-0.00000202	4411	-0.0122	3.19	-0.0029	73.15	-0.0045	8.73	-0.0354	11.21	-0.0004	2970	0.005	-12.13	0.011	-2.14	0.442	-10.061	$3,700
Sensitivity	2.41	-0.00000202	4411	-0.0122	3.19	-0.0029	73.15	-0.0045	8.73	-0.0354	11.21	-0.0004	3000	0.005	-12.13	0.011	-2.14	0.430	-10.061	$4,902
TC																				
Sensitivity	2.41	-0.00000202	4411	-0.0122	3.19	-0.0029	73.15	-0.0045	8.73	-0.0354	11.21	-0.0004	2970	0.005	-10	0.011	-2.14	0.453	-10.061	$2,912
Chip BASE	2.41	-0.00000202	4411	-0.0122	3.19	-0.0029	73.15	-0.0045	8.73	-0.0354	11.21	-0.0004	2970	0.005	-12.13	0.011	-2.14	0.442	-10.061	$3,700
Sensitivity	2.41	-0.00000202	4411	-0.0122	3.19	-0.0029	73.15	-0.0045	8.73	-0.0354	11.21	-0.0004	2970	0.005	-14	0.011	-2.14	0.433	-10.061	$4,588

Parameter	Intercept	AADT LR	AADT Mean	Age LR	Age Mean	Temp LR	Temp Mean	MD LR	MD Mean	NMAS LR	NMAS Mean	AB LR	AB Mean	TC LR	TC Mean	SC LR	SC Mean	Perf Output	EXP LCCA	EUAC Output
SC																				
Sensitivity	2.41	-0.00000202	4411	-0.0122	3.19	-0.0029	73.15	-0.0045	8.73	-0.0354	11.21	-0.0004	2970	0.005	-12.13	0.011	-1.14	0.453	-10.061	$2,889
Chip BASE	2.41	-0.00000202	4411	-0.0122	3.19	-0.0029	73.15	-0.0045	8.73	-0.0354	11.21	-0.0004	2970	0.005	-12.13	0.011	-2.14	0.442	-10.061	$3,700
Sensitivity	2.41	-0.00000202	4411	-0.0122	3.19	-0.0029	73.15	-0.0045	8.73	-0.0354	11.21	-0.0004	2970	0.005	-12.13	0.011	-3.14	0.431	-10.061	$4,768

Table B3 Performance (Friction) -Based Cost Analysis Results for PFC Scenario

Parameter	Intercept	AADT LR	AADT Mean	Age LR	Age Mean	Temp LR	Temp Mean	MD LR	MD Mean	NMAS LR	NMAS Mean	AB LR	AB Mean	TC LR	TC Mean	SC LR	SC Mean	Perf Output	EXP LCCA	EUAC Output
TRAFFIC	2.41	-0.00000202	4411	-0.0122	3.19	-0.0029	73.15	-0.0045	8.73	-0.0354	11.21	-0.0004	2970	0.005	-12.13	0.011	-2.14	0.442	-10.093	$3,800
PFC BASE	2.41	-0.00000202	4411	-0.0122	8	-0.0029	73.15	-0.0045	8.73	-0.0354	11.21	-0.0004	2970	0.005	-12.13	0.011	-2.14	0.383	-8.770	$4,499
Sensitivity	2.41	-0.00000202	10000	-0.0122	8	-0.0029	73.15	-0.0045	8.73	-0.0354	11.21	-0.0004	2970	0.005	-12.13	0.011	-2.14	0.372	-8.770	$5,848
Sensitivity	2.41	-0.00000202	2500	-0.0122	8	-0.0029	73.15	-0.0045	8.73	-0.0354	11.21	-0.0004	2970	0.005	-12.13	0.011	-2.14	0.387	-8.770	$4,121
PFC BASE	2.41	-0.00000202	4411	-0.0122	10	-0.0029	73.15	-0.0045	8.73	-0.0354	11.21	-0.0004	2970	0.005	-12.13	0.011	-2.14	0.359	-8.042	$3,800
Sensitivity	2.41	-0.00000202	10000	-0.0122	10	-0.0029	73.15	-0.0045	8.73	-0.0354	11.21	-0.0004	2970	0.005	-12.13	0.011	-2.14	0.348	-8.042	$4,914
Sensitivity	2.41	-0.00000202	2500	-0.0122	10	-0.0029	73.15	-0.0045	8.73	-0.0354	11.21	-0.0004	2970	0.005	-12.13	0.011	-2.14	0.363	-8.042	$3,487
PFC BASE	2.41	-0.00000202	4411	-0.0122	12	-0.0029	73.15	-0.0045	8.73	-0.0354	11.21	-0.0004	2970	0.005	-12.13	0.011	-2.14	0.334	-7.424	$3,400
Sensitivity	2.41	-0.00000202	10000	-0.0122	12	-0.0029	73.15	-0.0045	8.73	-0.0354	11.21	-0.0004	2970	0.005	-12.13	0.011	-2.14	0.323	-7.424	$4,387
Sensitivity	2.41	-0.00000202	2500	-0.0122	12	-0.0029	73.15	-0.0045	8.73	-0.0354	11.21	-0.0004	2970	0.005	-12.13	0.011	-2.14	0.338	-7.424	$3,122
TEMP																				
Sensitivity	2.41	-0.00000202	4411	-0.0122	3.19	-0.0029	72.15	-0.0045	8.73	-0.0354	11.21	-0.0004	2970	0.005	-12.13	0.011	-2.14	0.445	-10.093	$3,557
PFC BASE	2.41	-0.00000202	4411	-0.0122	3.19	-0.0029	73.15	-0.0045	8.73	-0.0354	11.21	-0.0004	2970	0.005	-12.13	0.011	-2.14	0.442	-10.093	$3,800
Sensitivity	2.41	-0.00000202	4411	-0.0122	3.19	-0.0029	74.15	-0.0045	8.73	-0.0354	11.21	-0.0004	2970	0.005	-12.13	0.011	-2.14	0.439	-10.093	$4,061
MD																				
Sensitivity	2.41	-0.00000202	4411	-0.0122	3.19	-0.0029	73.15	-0.0045	5.73	-0.0354	11.21	-0.0004	2970	0.005	-12.13	0.011	-2.14	0.455	-10.093	$2,805
PFC BASE	2.41	-0.00000202	4411	-0.0122	3.19	-0.0029	73.15	-0.0045	8.73	-0.0354	11.21	-0.0004	2970	0.005	-12.13	0.011	-2.14	0.442	-10.093	$3,800
Sensitivity	2.41	-0.00000202	4411	-0.0122	3.19	-0.0029	73.15	-0.0045	11.73	-0.0354	11.21	-0.0004	2970	0.005	-12.13	0.011	-2.14	0.428	-10.093	$5,197
NMAS																				
Sensitivity	2.41	-0.00000202	4411	-0.0122	3.19	-0.0029	73.15	-0.0045	8.73	-0.0354	11	-0.0004	2970	0.005	-12.13	0.011	-2.14	0.449	-10.093	$3,211
PFC BASE	2.41	-0.00000202	4411	-0.0122	3.19	-0.0029	73.15	-0.0045	8.73	-0.0354	11.21	-0.0004	2970	0.005	-12.13	0.011	-2.14	0.442	-10.093	$3,800
Sensitivity	2.41	-0.00000202	4411	-0.0122	3.19	-0.0029	73.15	-0.0045	8.73	-0.0354	11.42	-0.0004	2970	0.005	-12.13	0.011	-2.14	0.434	-10.093	$4,510
AB																				
Sensitivity	2.41	-0.00000202	4411	-0.0122	3.19	-0.0029	73.15	-0.0045	8.73	-0.0354	11.21	-0.0004	2900	0.005	-12.13	0.011	-2.14	0.470	-10.093	$2,052
PFC BASE	2.41	-0.00000202	4411	-0.0122	3.19	-0.0029	73.15	-0.0045	8.73	-0.0354	11.21	-0.0004	2970	0.005	-12.13	0.011	-2.14	0.442	-10.093	$3,800
Sensitivity	2.41	-0.00000202	4411	-0.0122	3.19	-0.0029	73.15	-0.0045	8.73	-0.0354	11.21	-0.0004	3000	0.005	-12.13	0.011	-2.14	0.430	-10.093	$5,039
TC																				
Sensitivity	2.41	-0.00000202	4411	-0.0122	3.19	-0.0029	73.15	-0.0045	8.73	-0.0354	11.21	-0.0004	2970	0.005	-10	0.011	-2.14	0.453	-10.093	$2,988
PFC BASE	2.41	-0.00000202	4411	-0.0122	3.19	-0.0029	73.15	-0.0045	8.73	-0.0354	11.21	-0.0004	2970	0.005	-12.13	0.011	-2.14	0.442	-10.093	$3,800
Sensitivity	2.41	-0.00000202	4411	-0.0122	3.19	-0.0029	73.15	-0.0045	8.73	-0.0354	11.21	-0.0004	2970	0.005	-14	0.011	-2.14	0.433	-10.093	$4,716

Parameter	Intercept	AADT LR	AADT Mean	Age LR	Age Mean	Temp LR	Temp Mean	MD LR	MD Mean	NMAS LR	NMAS Mean	AB LR	AB Mean	TC LR	TC Mean	SC LR	SC Mean	Perf Output	EXP LCCA	EUAC Output
SC																				
Sensitivity	2.41	-0.00000202	4411	-0.0122	3.19	-0.0029	73.15	-0.0045	8.73	-0.0354	11.21	-0.0004	2970	0.005	-12.13	0.011	-1.14	0.453	-10.093	$2,965
PFC BASE	2.41	-0.00000202	4411	-0.0122	3.19	-0.0029	73.15	-0.0045	8.73	-0.0354	11.21	-0.0004	2970	0.005	-12.13	0.011	-2.14	0.442	-10.093	$3,800
Sensitivity	2.41	-0.00000202	4411	-0.0122	3.19	-0.0029	73.15	-0.0045	8.73	-0.0354	11.21	-0.0004	2970	0.005	-12.13	0.011	-3.14	0.431	-10.093	$4,901

Table B4 Performance (Friction) -Based Cost Analysis Results for UTBWC Scenario

Parameter	Intercept	AADT LR	AADT Mean	Age LR	Age Mean	Temp LR	Temp Mean	MD LR	MD Mean	NMAS LR	NMAS Mean	AB LR	AB Mean	TC LR	TC Mean	SC LR	SC Mean	Perf Output	EXP LCCA	EUAC Output
TRAFFIC	2.41	-0.00000202	4411	-0.0122	3.19	-0.0029	73.15	-0.0045	8.73	-0.0354	11.21	-0.0004	2970	0.005	-12.13	0.011	-2.14	0.442	-10.273	$4,400
UTBWC BASE	2.41	-0.00000202	4411	-0.0122	8	-0.0029	73.15	-0.0045	8.73	-0.0354	11.21	-0.0004	2970	0.005	-12.13	0.011	-2.14	0.383	-8.860	$4,902
Sensitivity	2.41	-0.00000202	10000	-0.0122	8	-0.0029	73.15	-0.0045	8.73	-0.0354	11.21	-0.0004	2970	0.005	-12.13	0.011	-2.14	0.372	-8.860	$6,389
Sensitivity	2.41	-0.00000202	2500	-0.0122	8	-0.0029	73.15	-0.0045	8.73	-0.0354	11.21	-0.0004	2970	0.005	-12.13	0.011	-2.14	0.387	-8.860	$4,486
UTBWC BASE	2.41	-0.00000202	4411	-0.0122	9	-0.0029	73.15	-0.0045	8.73	-0.0354	11.21	-0.0004	2970	0.005	-12.13	0.011	-2.14	0.371	-8.476	$4,465
Sensitivity	2.41	-0.00000202	10000	-0.0122	9	-0.0029	73.15	-0.0045	8.73	-0.0354	11.21	-0.0004	2970	0.005	-12.13	0.011	-2.14	0.360	-8.476	$5,802
Sensitivity	2.41	-0.00000202	2500	-0.0122	9	-0.0029	73.15	-0.0045	8.73	-0.0354	11.21	-0.0004	2970	0.005	-12.13	0.011	-2.14	0.375	-8.476	$4,090
UTBWC BASE	2.41	-0.00000202	4411	-0.0122	10	-0.0029	73.15	-0.0045	8.73	-0.0354	11.21	-0.0004	2970	0.005	-12.13	0.011	-2.14	0.359	-8.093	$4,002
Sensitivity	2.41	-0.00000202	10000	-0.0122	10	-0.0029	73.15	-0.0045	8.73	-0.0354	11.21	-0.0004	2970	0.005	-12.13	0.011	-2.14	0.348	-8.093	$5,184
Sensitivity	2.41	-0.00000202	2500	-0.0122	10	-0.0029	73.15	-0.0045	8.73	-0.0354	11.21	-0.0004	2970	0.005	-12.13	0.011	-2.14	0.363	-8.093	$3,670
TEMP																				
Sensitivity	2.41	-0.00000202	4411	-0.0122	3.19	-0.0029	72.15	-0.0045	8.73	-0.0354	11.21	-0.0004	2970	0.005	-12.13	0.011	-2.14	0.445	-10.273	$4,114
UTBWC BASE	2.41	-0.00000202	4411	-0.0122	3.19	-0.0029	73.15	-0.0045	8.73	-0.0354	11.21	-0.0004	2970	0.005	-12.13	0.011	-2.14	0.442	-10.273	$4,400
Sensitivity	2.41	-0.00000202	4411	-0.0122	3.19	-0.0029	74.15	-0.0045	8.73	-0.0354	11.21	-0.0004	2970	0.005	-12.13	0.011	-2.14	0.439	-10.273	$4,708
MD																				
Sensitivity	2.41	-0.00000202	4411	-0.0122	3.19	-0.0029	73.15	-0.0045	5.73	-0.0354	11.21	-0.0004	2970	0.005	-12.13	0.011	-2.14	0.455	-10.273	$3,230
UTBWC BASE	2.41	-0.00000202	4411	-0.0122	3.19	-0.0029	73.15	-0.0045	8.73	-0.0354	11.21	-0.0004	2970	0.005	-12.13	0.011	-2.14	0.442	-10.273	$4,400
Sensitivity	2.41	-0.00000202	4411	-0.0122	3.19	-0.0029	73.15	-0.0045	11.73	-0.0354	11.21	-0.0004	2970	0.005	-12.13	0.011	-2.14	0.428	-10.273	$6,052
NMAS																				
Sensitivity	2.41	-0.00000202	4411	-0.0122	3.19	-0.0029	73.15	-0.0045	8.73	-0.0354	11	-0.0004	2970	0.005	-12.13	0.011	-2.14	0.449	-10.273	$3,707
UTBWC BASE	2.41	-0.00000202	4411	-0.0122	3.19	-0.0029	73.15	-0.0045	8.73	-0.0354	11.21	-0.0004	2970	0.005	-12.13	0.011	-2.14	0.442	-10.273	$4,400
Sensitivity	2.41	-0.00000202	4411	-0.0122	3.19	-0.0029	73.15	-0.0045	8.73	-0.0354	11.42	-0.0004	2970	0.005	-12.13	0.011	-2.14	0.434	-10.273	$5,238
AB																				
Sensitivity	2.41	-0.00000202	4411	-0.0122	3.19	-0.0029	73.15	-0.0045	8.73	-0.0354	11.21	-0.0004	2900	0.005	-12.13	0.011	-2.14	0.470	-10.273	$2,350
UTBWC BASE	2.41	-0.00000202	4411	-0.0122	3.19	-0.0029	73.15	-0.0045	8.73	-0.0354	11.21	-0.0004	2970	0.005	-12.13	0.011	-2.14	0.442	-10.273	$4,400
Sensitivity	2.41	-0.00000202	4411	-0.0122	3.19	-0.0029	73.15	-0.0045	8.73	-0.0354	11.21	-0.0004	3000	0.005	-12.13	0.011	-2.14	0.430	-10.273	$5,864
TC																				
Sensitivity	2.41	-0.00000202	4411	-0.0122	3.19	-0.0029	73.15	-0.0045	8.73	-0.0354	11.21	-0.0004	2970	0.005	-10	0.011	-2.14	0.453	-10.273	$3,445
UTBWC BASE	2.41	-0.00000202	4411	-0.0122	3.19	-0.0029	73.15	-0.0045	8.73	-0.0354	11.21	-0.0004	2970	0.005	-12.13	0.011	-2.14	0.442	-10.273	$4,400
Sensitivity	2.41	-0.00000202	4411	-0.0122	3.19	-0.0029	73.15	-0.0045	8.73	-0.0354	11.21	-0.0004	2970	0.005	-14	0.011	-2.14	0.433	-10.273	$5,481

Parameter	Intercept	AADT LR	AADT Mean	Age LR	Age Mean	Temp LR	Temp Mean	MD LR	MD Mean	NMAS LR	NMAS Mean	AB LR	AB Mean	TC LR	TC Mean	SC LR	SC Mean	Perf Output	EXP LCCA	EUAC Output
SC																				
Sensitivity	2.41	-0.00000202	4411	-0.0122	3.19	-0.0029	73.15	-0.0045	8.73	-0.0354	11.21	-0.0004	2970	0.005	-12.13	0.011	-1.14	0.453	-10.273	$3,418
UTBWC BASE	2.41	-0.00000202	4411	-0.0122	3.19	-0.0029	73.15	-0.0045	8.73	-0.0354	11.21	-0.0004	2970	0.005	-12.13	0.011	-2.14	0.442	-10.273	$4,400
Sensitivity	2.41	-0.00000202	4411	-0.0122	3.19	-0.0029	73.15	-0.0045	8.73	-0.0354	11.21	-0.0004	2970	0.005	-12.13	0.011	-3.14	0.431	-10.273	$5,701

Table B5 Performance (Friction) -Based Cost Analysis Results for HFST Scenario

Parameter	Intercept	AADT LR	AADT Mean	Age LR	Age Mean	Temp LR	Temp Mean	MD LR	MD Mean	NMAS LR	NMAS Mean	AB LR	AB Mean	TC LR	TC Mean	SC LR	SC Mean	Perf Output	EXP LCCA	EUAC Output
TRAFFIC	2.41	-0.00000202	4411	2.41	3.19	-0.003	73.15	-0.005	8.73	-0.035	11.21	-4.00E-04	2970	0.005	-12.13	0.011	-2.14	0.442	-11.977	$17,700
HFST BASE	2.41	-0.00000202	4411	2.41	7	-0.003	73.15	-0.005	8.73	-0.035	11.21	-4.00E-04	2970	0.005	-12.13	0.011	-2.14	0.395	-10.82	$22,893
Sensitivity	2.41	-0.00000202	10000	2.41	7	-0.003	73.15	-0.005	8.73	-0.035	11.21	-4.00E-04	2970	0.005	-12.13	0.011	-2.14	0.384	-10.82	$31,320
Sensitivity	2.41	-0.00000202	2500	2.41	7	-0.003	73.15	-0.005	8.73	-0.035	11.21	-4.00E-04	2970	0.005	-12.13	0.011	-2.14	0.399	-10.82	$20,609
HFST BASE	2.41	-0.00000202	4411	2.41	9.5	-0.003	73.15	-0.005	8.73	-0.035	11.21	-4.00E-04	2970	0.005	-12.13	0.011	-2.14	0.365	-9.703	$17,700
Sensitivity	2.41	-0.00000202	10000	2.41	9.5	-0.003	73.15	-0.005	8.73	-0.035	11.21	-4.00E-04	2970	0.005	-12.13	0.011	-2.14	0.354	-9.703	$24,011
Sensitivity	2.41	-0.00000202	2500	2.41	9.5	-0.003	73.15	-0.005	8.73	-0.035	11.21	-4.00E-04	2970	0.005	-12.13	0.011	-2.14	0.369	-9.703	$15,983
HFST BASE	2.41	-0.00000202	4411	2.41	12	-0.003	73.15	-0.005	8.73	-0.035	11.21	-4.00E-04	2970	0.005	-12.13	0.011	-2.14	0.334	-8.76	$14,692
Sensitivity	2.41	-0.00000202	10000	2.41	12	-0.003	73.15	-0.005	8.73	-0.035	11.21	-4.00E-04	2970	0.005	-12.13	0.011	-2.14	0.323	-8.76	$19,849
Sensitivity	2.41	-0.00000202	2500	2.41	12	-0.003	73.15	-0.005	8.73	-0.035	11.21	-4.00E-04	2970	0.005	-12.13	0.011	-2.14	0.338	-8.76	$13,287
TEMP																				
Sensitivity	2.41	-0.00000202	4411	2.41	3.19	-0.003	72.15	-0.005	8.73	-0.035	11.21	-4.00E-04	2970	0.005	-12.13	0.011	-2.14	0.445	-11.977	$16,366
HFST BASE	2.41	-0.00000202	4411	2.41	3.19	-0.003	73.15	-0.005	8.73	-0.035	11.21	-4.00E-04	2970	0.005	-12.13	0.011	-2.14	0.442	-11.977	$17,700
Sensitivity	2.41	-0.00000202	4411	2.41	3.19	-0.003	74.15	-0.005	8.73	-0.035	11.21	-4.00E-04	2970	0.005	-12.13	0.011	-2.14	0.439	-11.977	$19,153
MD																				
Sensitivity	2.41	-0.00000202	4411	2.41	3.19	-0.003	73.15	-0.005	5.73	-0.035	11.21	-4.00E-04	2970	0.005	-12.13	0.011	-2.14	0.455	-11.977	$12,344
HFST BASE	2.41	-0.00000202	4411	2.41	3.19	-0.003	73.15	-0.005	8.73	-0.035	11.21	-4.00E-04	2970	0.005	-12.13	0.011	-2.14	0.442	-11.977	$17,700
Sensitivity	2.41	-0.00000202	4411	2.41	3.19	-0.003	73.15	-0.005	11.73	-0.035	11.21	-4.00E-04	2970	0.005	-12.13	0.011	-2.14	0.428	-11.977	$25,666
NMAS																				
Sensitivity	2.41	-0.00000202	4411	2.41	3.19	-0.003	73.15	-0.005	8.73	-0.035	11	-4.00E-04	2970	0.005	-12.13	0.011	-2.14	0.449	-11.977	$14,494
HFST BASE	2.41	-0.00000202	4411	2.41	3.19	-0.003	73.15	-0.005	8.73	-0.035	11.21	-4.00E-04	2970	0.005	-12.13	0.011	-2.14	0.442	-11.977	$17,700
Sensitivity	2.41	-0.00000202	4411	2.41	3.19	-0.003	73.15	-0.005	8.73	-0.035	11.42	-4.00E-04	2970	0.005	-12.13	0.011	-2.14	0.434	-11.977	$21,688
AB																				
Sensitivity	2.41	-0.00000202	4411	2.41	3.19	-0.003	73.15	-0.005	8.73	-0.035	11.21	-4.00E-04	2900	0.005	-12.13	0.011	-2.14	0.470	-11.977	$8,520
HFST BASE	2.41	-0.00000202	4411	2.41	3.19	-0.003	73.15	-0.005	8.73	-0.035	11.21	-4.00E-04	2970	0.005	-12.13	0.011	-2.14	0.442	-11.977	$17,700
Sensitivity	2.41	-0.00000202	4411	2.41	3.19	-0.003	73.15	-0.005	8.73	-0.035	11.21	-4.00E-04	3000	0.005	-12.13	0.011	-2.14	0.430	-11.977	$24,741
TC																				
Sensitivity	2.41	-0.00000202	4411	2.41	3.19	-0.003	73.15	-0.005	8.73	-0.035	11.21	-4.00E-04	2970	0.005	-10	0.011	-2.14	0.453	-11.977	$13,308
HFST BASE	2.41	-0.00000202	4411	2.41	3.19	-0.003	73.15	-0.005	8.73	-0.035	11.21	-4.00E-04	2970	0.005	-12.13	0.011	-2.14	0.442	-11.977	$17,700
Sensitivity	2.41	-0.00000202	4411	2.41	3.19	-0.003	73.15	-0.005	8.73	-0.035	11.21	-4.00E-04	2970	0.005	-14	0.011	-2.14	0.433	-11.977	$22,867

Parameter	Intercept	AADT LR	AADT Mean	Age LR	Age Mean	Temp LR	Temp Mean	MD LR	MD Mean	NMAS LR	NMAS Mean	AB LR	AB Mean	TC LR	TC Mean	SC LR	SC Mean	Perf Output	EXP LCCA	EUAC Output
SC																				
Sensitivity	2.41	-0.00000202	4411	2.41	3.19	-0.003	73.15	-0.005	8.73	-0.035	11.21	-4.00E-04	2970	0.005	-12.13	0.011	-1.14	0.453	-11.977	$13,185
HFST BASE	2.41	-0.00000202	4411	2.41	3.19	-0.003	73.15	-0.005	8.73	-0.035	11.21	-4.00E-04	2970	0.005	-12.13	0.011	-2.14	0.442	-11.977	$17,700
Sensitivity	2.41	-0.00000202	4411	2.41	3.19	-0.003	73.15	-0.005	8.73	-0.035	11.21	-4.00E-04	2970	0.005	-12.13	0.011	-3.14	0.431	-11.977	$23,939

Table B6 Performance (Friction) -Based Cost Analysis Results for Microsurfacing Scenario

Parameter	Intercept	AADT LR	AADT Mean	Age LR	Age Mean	Temp LR	Temp Mean	MD LR	MD Mean	NMAS LR	NMAS Mean	AB LR	AB Mean	TC LR	TC Mean	SC LR	SC Mean	Perf Output	EXP LCCA	EUAC Output
TRAFFIC	2.41	-0.00000202	4411	-0.0122	3.19	-0.0029	73.15	-0.0045	8.73	-0.0354	11.21	-0.0004	2970	0.005	-12.13	0.011	-2.14	0.442	-9.844	$3,100
Micro BASE	2.41	-0.00000202	4411	-0.0122	7	-0.0029	73.15	-0.0045	8.73	-0.0354	11.21	-0.0004	2970	0.005	-12.13	0.011	-2.14	0.395	-8.796	$3,500
Sensitivity	2.41	-0.00000202	10000	-0.0122	7	-0.0029	73.15	-0.0045	8.73	-0.0354	11.21	-0.0004	2970	0.005	-12.13	0.011	-2.14	0.384	-8.796	$4,515
Sensitivity	2.41	-0.00000202	2500	-0.0122	7	-0.0029	73.15	-0.0045	8.73	-0.0354	11.21	-0.0004	2970	0.005	-12.13	0.011	-2.14	0.399	-8.796	$3,213
Micro BASE	2.41	-0.00000202	4411	-0.0122	8.5	-0.0029	73.15	-0.0045	8.73	-0.0354	11.21	-0.0004	2970	0.005	-12.13	0.011	-2.14	0.377	-8.252	$3,125
Sensitivity	2.41	-0.00000202	10000	-0.0122	8.5	-0.0029	73.15	-0.0045	8.73	-0.0354	11.21	-0.0004	2970	0.005	-12.13	0.011	-2.14	0.366	-8.252	$4,017
Sensitivity	2.41	-0.00000202	2500	-0.0122	8.5	-0.0029	73.15	-0.0045	8.73	-0.0354	11.21	-0.0004	2970	0.005	-12.13	0.011	-2.14	0.381	-8.252	$2,874
Micro BASE	2.41	-0.00000202	4411	-0.0122	10	-0.0029	73.15	-0.0045	8.73	-0.0354	11.21	-0.0004	2970	0.005	-12.13	0.011	-2.14	0.359	-7.709	$2,700
Sensitivity	2.41	-0.00000202	10000	-0.0122	10	-0.0029	73.15	-0.0045	8.73	-0.0354	11.21	-0.0004	2970	0.005	-12.13	0.011	-2.14	0.348	-7.709	$3,455
Sensitivity	2.41	-0.00000202	2500	-0.0122	10	-0.0029	73.15	-0.0045	8.73	-0.0354	11.21	-0.0004	2970	0.005	-12.13	0.011	-2.14	0.363	-7.709	$2,486
TEMP																				
Sensitivity	2.41	-0.00000202	4411	-0.0122	3.19	-0.0029	72.15	-0.0045	8.73	-0.0354	11.21	-0.0004	2970	0.005	-12.13	0.011	-2.14	0.445	-9.844	$2,907
Micro BASE	2.41	-0.00000202	4411	-0.0122	3.19	-0.0029	73.15	-0.0045	8.73	-0.0354	11.21	-0.0004	2970	0.005	-12.13	0.011	-2.14	0.442	-9.844	$3,100
Sensitivity	2.41	-0.00000202	4411	-0.0122	3.19	-0.0029	74.15	-0.0045	8.73	-0.0354	11.21	-0.0004	2970	0.005	-12.13	0.011	-2.14	0.439	-9.844	$3,308
MD																				
Sensitivity	2.41	-0.00000202	4411	-0.0122	3.19	-0.0029	73.15	-0.0045	5.73	-0.0354	11.21	-0.0004	2970	0.005	-12.13	0.011	-2.14	0.455	-9.844	$2,305
Micro BASE	2.41	-0.00000202	4411	-0.0122	3.19	-0.0029	73.15	-0.0045	8.73	-0.0354	11.21	-0.0004	2970	0.005	-12.13	0.011	-2.14	0.442	-9.844	$3,100
Sensitivity	2.41	-0.00000202	4411	-0.0122	3.19	-0.0029	73.15	-0.0045	11.73	-0.0354	11.21	-0.0004	2970	0.005	-12.13	0.011	-2.14	0.428	-9.844	$4,207
NMAS																				
Sensitivity	2.41	-0.00000202	4411	-0.0122	3.19	-0.0029	73.15	-0.0045	8.73	-0.0354	11	-0.0004	2970	0.005	-12.13	0.011	-2.14	0.449	-9.844	$2,631
Micro BASE	2.41	-0.00000202	4411	-0.0122	3.19	-0.0029	73.15	-0.0045	8.73	-0.0354	11.21	-0.0004	2970	0.005	-12.13	0.011	-2.14	0.442	-9.844	$3,100
Sensitivity	2.41	-0.00000202	4411	-0.0122	3.19	-0.0029	73.15	-0.0045	8.73	-0.0354	11.42	-0.0004	2970	0.005	-12.13	0.011	-2.14	0.434	-9.844	$3,664
AB																				
Sensitivity	2.41	-0.00000202	4411	-0.0122	3.19	-0.0029	73.15	-0.0045	8.73	-0.0354	11.21	-0.0004	2900	0.005	-12.13	0.011	-2.14	0.470	-9.844	$1,700
Micro BASE	2.41	-0.00000202	4411	-0.0122	3.19	-0.0029	73.15	-0.0045	8.73	-0.0354	11.21	-0.0004	2970	0.005	-12.13	0.011	-2.14	0.442	-9.844	$3,100
Sensitivity	2.41	-0.00000202	4411	-0.0122	3.19	-0.0029	73.15	-0.0045	8.73	-0.0354	11.21	-0.0004	3000	0.005	-12.13	0.011	-2.14	0.430	-9.844	$4,082
TC																				
Sensitivity	2.41	-0.00000202	4411	-0.0122	3.19	-0.0029	73.15	-0.0045	8.73	-0.0354	11.21	-0.0004	2970	0.005	-10	0.011	-2.14	0.453	-9.844	$2,452
Micro BASE	2.41	-0.00000202	4411	-0.0122	3.19	-0.0029	73.15	-0.0045	8.73	-0.0354	11.21	-0.0004	2970	0.005	-12.13	0.011	-2.14	0.442	-9.844	$3,100
Sensitivity	2.41	-0.00000202	4411	-0.0122	3.19	-0.0029	73.15	-0.0045	8.73	-0.0354	11.21	-0.0004	2970	0.005	-14	0.011	-2.14	0.433	-9.844	$3,826

Parameter	Intercept	AADT LR	AADT Mean	Age LR	Age Mean	Temp LR	Temp Mean	MD LR	MD Mean	NMAS LR	NMAS Mean	AB LR	AB Mean	TC LR	TC Mean	SC LR	SC Mean	Perf Output	EXP LCCA	EUAC Output
SC																				
Sensitivity	2.41	-0.00000202	4411	-0.0122	3.19	-0.0029	73.15	-0.0045	8.73	-0.0354	11.21	-0.0004	2970	0.005	-12.13	0.011	-1.14	0.453	-9.844	$2,434
Micro BASE	2.41	-0.00000202	4411	-0.0122	3.19	-0.0029	73.15	-0.0045	8.73	-0.0354	11.21	-0.0004	2970	0.005	-12.13	0.011	-2.14	0.442	-9.844	$3,100
Sensitivity	2.41	-0.00000202	4411	-0.0122	3.19	-0.0029	73.15	-0.0045	8.73	-0.0354	11.21	-0.0004	2970	0.005	-12.13	0.011	-3.14	0.431	-9.844	$3,973